

SEISMIC ANALYSIS OF CONCRETE GRAVITY DAMS INCLUDING DAM-
FOUNDATION-RESERVOIR INTERACTION

A THESIS SUBMITTED TO
THE GRADUATE SCHOOL OF NATURAL AND APPLIED SCIENCES
OF
MIDDLE EAST TECHNICAL UNIVERSITY

BY

ALİ RIZA YÜCEL

IN PARTIAL FULFILLMENT OF THE REQUIREMENTS
FOR
THE DEGREE OF MASTER OF SCIENCE
IN
CIVIL ENGINEERING

SEPTEMBER 2013

Approval of the thesis:

**SEISMIC ANALYSIS OF CONCRETE GRAVITY DAMS INCLUDING DAM-
FOUNDATION-RESERVOIR INTERACTION**

submitted by **ALİ RIZA YÜCEL** in partial fulfillment of the requirements for the degree of **Master of Science in Civil Engineering Department, Middle East Technical University** by,

Prof. Dr. Canan Özgen
Dean, Graduate School of **Natural and Applied Sciences**

Prof. Dr. Ahmet Cevdet Yalçın
Head of Department, **Civil Engineering**

Prof. Dr. Barış Binici
Supervisor, **Civil Engineering Dept., METU**

Examining Committee Members:

Prof. Dr. Ahmet Yakut
Civil Engineering Dept., METU

Prof. Dr. Barış Binici
Civil Engineering Dept., METU

Assoc. Prof. Dr. Erdem Canbay
Civil Engineering Dept., METU

Assoc. Prof. Dr. Özgür Kurç
Civil Engineering Dept., METU

Altuğ Akman, M. Sc.
ES Project Engineering and Consultancy

Date: 04.09.2013

I hereby declare that all information in this document has been obtained and presented in accordance with academic rules and ethical conduct. I also declare that, as required by these rules and conduct, I have fully cited and referenced all material and results that are not original to this work.

Name, Last name : ALI RIZA YÜCEL
Signature :

ABSTRACT

SEISMIC ANALYSIS OF CONCRETE GRAVITY DAMS INCLUDING DAM- FOUNDATION-RESERVOIR INTERACTION

Yücel, Ali Rıza

M.Sc., Department of Civil Engineering

Supervisor: Prof. Dr. Barış Binici

September 2013, 82 pages

The attractiveness of the hydroelectric power as a domestic, clean and renewable energy source increased with the rise of the energy demand within the last decade. In this context, concrete gravity dam construction gained a high momentum. Use of roller compacted concrete as a dam construction material became popular due to advantages such as reducing the construction duration and costs. Concrete gravity dams are special type of structures which requires an extensive care for their seismic analysis and design due to lack of any definite ductility providing mechanisms. Several methods are available for the dynamic analysis of concrete gravity dams. In this study seismic response of concrete gravity dams are investigated by utilizing the method of Fenves and Chopra (1984). This method considers the dam-reservoir-foundation rock interaction by taking the foundation rock flexibility effects, compressibility of the impounded water and the absorptive effect of the reservoir bottom materials into consideration. A user interface for the dynamic analysis of concrete gravity dams are developed for the engine originally developed by Fenves and Chopra (1984). The necessity of conducting response history analysis is demonstrated by the comparison of the parametric studies results with results obtained by pseudo-static analyses. Parametric studies and a deterministic sensitivity analysis were conducted to better understand the effects of parameters on the seismic response of concrete gravity dams. Fragility curves of a set of dams with typical sections and various properties were determined by damage assessments conducted with linear elastic analysis.

Keywords: two dimensional dynamic analysis, concrete gravity dam, roller compacted concrete dam, dam-reservoir-foundation interaction, fragility analyses of concrete gravity dams.

ÖZ

BETON AĞIRLIK BARAJLARIN BARAJ-TEMEL-REZERVUAR ETKİLEŞİMİNİ İÇEREN SİSMİK ANALİZİ

Yücel, Ali Rıza
Yüksek lisans, İnşaat Mühendisliği Bölümü
Tez Yöneticisi: Prof. Dr. Barış Binici

Eylül 2013, 82 sayfa

Hidroelektrik enerjinin yerli, temiz ve yenilenebilir bir enerji kaynağı olarak cazibesi son on yılda artmıştır. Bu bağlamda, beton ağırlık baraj inşaatı ivme kazanmıştır. Silindire sıkıştırılmış betonun baraj inşaat malzemesi olarak kullanılması süre ve maliyetleri azaltmaktadır. Beton ağırlık barajlar, sismik analiz ve tasarımlarında büyük özen gerektiren özel tip yapılardır. Beton ağırlık barajların dinamik analizleri için çeşitli metotlar mevcuttur. Bu çalışmada beton ağırlık barajların sismik tepkileri Fenves ve Chopra tarafından önerilen metot kullanılarak araştırılmıştır. Bu metot baraj-rezervuar-temel etkileşimini temel kayası rijitliğini, toplanan suyun sıkıştırılabilirliğini ve rezervuar taban malzemelerinin sönüm etkisini göz önüne alarak temsil etmektedir. Beton ağırlık barajların dinamik analizi için bir kullanıcı arayüzü geliştirilmiştir. Zaman tanım alanında yapılan analiz sonuçları stabilite analizlerinden elde edilen sonuçlarla kıyaslanmıştır. Değişkenlerin beton ağırlık barajların sismik tepkisi üzerindeki etkilerini daha iyi anlamak için parametrik çalışmalar ve deterministik duyarlılık analizi yapılmıştır. Tipik kesitlerde ve çeşitli özelliklerde bir dizi beton ağırlık barajının kırılma eğrileri doğrusal elastik analiz ile yapılmış hasar değerlendirmeleri aracılığı ile elde edilmiştir.

Anahtar Kelimeler: iki boyutlu dinamik analiz, beton ağırlık baraj, silindire sıkıştırılmış beton baraj, baraj-rezervuar-zemin kayası etkileşimi, beton ağırlık barajların kırılma eğrileri analizi

ACKNOWLEDGEMENTS

I would like to express my special thanks to my thesis supervisor Prof. Dr. Barış Binici for his invaluable guidance, encouragement and assistance throughout the research. I was glad to work with him.

I would like to thank Alper Aldemir and Sema Melek Yılmaztürk for their help and guidance whenever I asked for it.

I would like to thank all my friends that worked and are currently working with me in K7-Z01 for their friendship, help and support.

I would like express my gratitude to my sincere friends Sadun Tanışer, Serdar Söğüt, Seyit Alp Yılmaz and Ahmet Fatih Koç for sharing my feelings.

I am thankful to Alper Artaç, Çağrı Şahin and Atilla Özen for their friendship.

I would like to express my sincere gratitude to my mother Fatma and my father Sadi Yücel for their immeasurable love and support throughout my entire life.

I would like to express heartfelt gratitude to Canan Yüksel for her patience and support. Her constancy gave me endurance during this exhausting period.

To My Dear Family...

TABLE OF CONTENTS

ABSTRACT	v
ÖZ.....	vi
ACKNOWLEDGEMENTS.....	vii
TABLE OF CONTENTS.....	ix
LIST OF TABLES.....	xi
LIST OF FIGURES	xii
CHAPTERS	
1 INTRODUCTION	1
1.1 General.....	1
1.2 Literature Survey	2
1.3 Approach of Fenves and Chopra (1984): EAGD-84	7
1.3.1 General Information.....	7
1.3.2 General Analytical Procedure	8
1.4 Importance of Detailed Response History Analysis	16
1.5 Scope and Objective	19
2 A USER INTERFACE FOR DAM ANALYSIS.....	21
2.1 General.....	21
2.2 Input Parameters and Pre-Processing of Input Data for Analysis.....	22
2.2.1 Material Properties.....	23
2.2.2 Foundation Rock Properties.....	23
2.2.3 Geometric Properties of Dam	24
2.2.4 Dynamic Response Parameters.....	26
2.2.5 Analysis Output Parameters.....	29
2.2.6 Analysis Execution Parameters.....	30
2.2.7 Structural Performance Check Parameters	30
2.3 Analysis Results and Post-Processing of Raw Output Data	31
2.4 A Dam Analysis Example Conducted with EAGD ModPro	34
2.4.1 Modeling.....	34

2.4.2	Results	37
3	VULNERABILITY OF CONCRETE GRAVITY DAMS	43
3.1	Parametric Studies.....	43
3.2	Deterministic Sensitivity Analysis (Tornado Diagrams)	52
3.3	Fragility Curves.....	59
4	CONCLUSION	79
4.1	General	79
	REFERENCES.....	81

LIST OF TABLES

TABLES

Table 1.1 Properties of dam design alternatives and optimum downstream slopes.....	18
Table 3.1 Values of the parameters utilized in parametric study.....	45
Table 3.2 Values of the dam concrete properties and foundation rock properties utilized in parametric study.....	46
Table 3.3 Input parameters utilized in deterministic sensitivity analysis	53
Table 3.4 Values of the dam concrete properties and foundation rock properties utilized in deterministic sensitivity analysis	55
Table 3.5 Median model results for engineering demand parameters	55
Table 3.6 Maximum principal tensile stress results (in MPa).....	56
Table 3.7 Maximum crest displacement results (in meters)	56
Table 3.8 Maximum cumulative inelastic duration results (in sec)	57
Table 3.9 Values of the parameters utilized in fragility analysis.....	62
Table 3.10 Values of the dam concrete properties and foundation rock properties utilized in fragility analysis.....	63
Table 3.11 General information about the ground motions utilized in fragility analysis	64

LIST OF FIGURES

FIGURES

Figure 1.1 Cumulative installed capacities of hydroelectric power plants and total installed capacity in Turkey (World Energy Council Turkish National Committee, 2012)	1
Figure 1.2 Distribution of the added mass of virtual water body	3
Figure 1.3 The idealized dam-water-foundation rock system	7
Figure 1.4 Substructures of the dam-reservoir-foundation rock system	9
Figure 1.5 Analysis procedure of EAGD-84	16
Figure 1.6 Stress distribution through dam base of case 1	19
Figure 1.7 Stress distribution through dam base of case 2	19
Figure 1.8 Stress distribution through dam base of case 3	19
Figure 1.9 Stress distribution through dam base of case 4	19
Figure 2.1 A screen capture of graphical user interface of EAGD ModPro	22
Figure 2.2 A screen capture of material properties section from GUI of EAGD ModPro	23
Figure 2.3 A screen capture of foundation rock properties section from GUI of EAGD ModPro	24
Figure 2.4 The typical dam cross section and a screen capture of geometric properties of dam section from GUI of EAGD ModPro	25
Figure 2.5 A screen capture of dynamic response parameters section from GUI of EAGD ModPro	27
Figure 2.6 A screen capture of analysis output parameters section from GUI of EAGD ModPro	29
Figure 2.7 A screen capture of analysis execution parameters section from GUI of EAGD ModPro	30
Figure 2.8 A screen capture of structural performance check parameters section from GUI of EAGD ModPro	31
Figure 2.9 Screen captures of the push buttons that control execution of EAGD-84 and post-processing operations from GUI of EAGD ModPro	31
Figure 2.10 A screen capture of output options for analysis results section from GUI of EAGD ModPro	32
Figure 2.11 Computation of the cumulative inelastic durations for acceptable DCR levels	33
Figure 2.12 Structural performance check and damage criteria assesment curve	33
Figure 2.13 Input data entered under material properties section	34
Figure 2.14 Input data entered under foundation rock properties section	34

Figure 2.15 Input data entered under geometric properties of dam section and the typical dam cross section	35
Figure 2.16 Horizontal earthquake ground motion utilized for dam analysis example ..	35
Figure 2.17 Input data entered under dynamic response parameters section.....	35
Figure 2.18 Input data entered under analysis output parameters section	36
Figure 2.19 Selected analysis execution options under analysis execution parameters section	36
Figure 2.20 Input data entered under structural performance check parameters section	37
Figure 2.21 Selected output options for the dam analysis example.....	37
Figure 2.22 A screen capture from the text file which includes the details of the finite element meshing properties	38
Figure 2.23 The finite element meshing of the dam cross section	38
Figure 2.24 A screen capture from the text file which includes natural vibration frequencies and verification of selected NEXP and DT values	39
Figure 2.25 Maximum principal stress contour plot.....	40
Figure 2.26 Minimum principal stress contour plot.....	40
Figure 2.27 Maximum sigma-x envelope contour plot.....	40
Figure 2.28 Minimum sigma-x envelope contour plot	40
Figure 2.29 Maximum sigma-y envelope contour plot.....	40
Figure 2.30 Minimum sigma-y envelope contour plot	40
Figure 2.31 Maximum thao-xy envelope contour plot	41
Figure 2.32 Minimum thao-xy envelope contour plot	41
Figure 2.33 Time history of horizontal crest displacement	41
Figure 2.34 Maximum principal stress through dam base	41
Figure 2.35 Maximum principal stress time history of the thalweg element.....	42
Figure 2.36 Cumulative inelastic duration curve of the thalweg element.....	42
Figure 2.37 Message window which shows the ratio of the cracked area to the dam cross section	42
Figure 3.1 Maximum principal stress contourplots and structural performance curves of dams with the same E_c/E_f ratio (with different values of elastic moduli)	44
Figure 3.2 Acceleration time history and acceleration response spectrum of the proposed synthetic ground motion	45
Figure 3.3 Typical dam meshing utilized in the parametric study.....	47
Figure 3.4 Maximum principal stresses through dam base obtained by different finite element models	48
Figure 3.5 Schematic illustration of the exceeded area	48
Figure 3.6 The parametric study results for the thalweg elements of analyzed dams	49
Figure 3.7 Maximum horizontal crest displacements	51
Figure 3.8 Tornado diagram production process (Binici and Mosalam, 2007)	52
Figure 3.9 Acceleration time histories and elastic response spectra of the proposed synthetic ground motions.....	54
Figure 3.10 Tornado diagram for maximum principal tensile stress	58
Figure 3.11 Tornado diagram for maximum crest displacement	58
Figure 3.12 Tornado diagram for maximum cumulative inelastic duration	58

Figure 3.13 The procedure of the determination of a fragility curve	61
Figure 3.14 Acceleration response spectra of the ground motions utilized in fragility analyses	65
Figure 3.15 Fragility curves of dams with a height of 50 meters and a downstream slope of 0.70	66
Figure 3.16 Fragility curves of dams with a height of 50 meters and a downstream slope of 0.85	67
Figure 3.17 Fragility curves of dams with a height of 50 meters and a downstream slope of 1.00	67
Figure 3.18 Fragility curves of dams with a height of 75 meters and a downstream slope of 0.70	68
Figure 3.19 Fragility curves of dams with a height of 75 meters and a downstream slope of 0.85	68
Figure 3.20 Fragility curves of dams with a height of 75 meters and a downstream slope of 1.00	69
Figure 3.21 Fragility curves of dams with a height of 100 meters and a downstream slope of 0.70	69
Figure 3.22 Fragility curves of dams with a height of 100 meters and a downstream slope of 0.85	70
Figure 3.23 Fragility curves of dams with a height of 100 meters and a downstream slope of 1.00	70
Figure 3.24 Fragility curves of dams with a height of 125 meters and a downstream slope of 0.70	71
Figure 3.25 Fragility curves of dams with a height of 125 meters and a downstream slope of 0.85	71
Figure 3.26 Fragility curves of dams with a height of 125 meters and a downstream slope of 1.00	72
Figure 3.27 Fragility curves of dams with a height of 150 meters and a downstream slope of 0.70	72
Figure 3.28 Fragility curves of dams with a height of 150 meters and a downstream slope of 0.85	73
Figure 3.29 Fragility curves of dams with a height of 150 meters and a downstream slope of 1.00	73
Figure 3.30 Spectral acceleration demands for 50% probability of observing visible damage ($E_c/E_f = 0.02$)	74
Figure 3.31 Spectral acceleration demands for 50% probability of observing visible damage ($E_c/E_f = 1.00$)	75
Figure 3.32 Spectral acceleration demands for 50% probability of observing visible damage ($E_c/E_f = 2.00$)	75
Figure 3.33 Spectral acceleration demands for 90% probability of observing visible damage ($E_c/E_f = 0.02$)	76
Figure 3.34 Spectral acceleration demands for 90% probability of observing visible damage ($E_c/E_f = 1.00$)	76

Figure 3.35 Spectral acceleration demands for 90% probability of observing visible damage ($E_o/E_f = 2.00$) 77

CHAPTER 1

INTRODUCTION

1.1 General

The energy demand in Turkey has risen significantly as a result of the industrial developments and increase in population within the last decades. The sharp increase of the energy demand forces Turkey to utilize all available energy production options. In order to satisfy the supply demand equilibrium for energy, a large number of power plants are constructed and taken into operation. The majority of these power plants are natural gas power plants and natural gas combined cycle power plants. As a result of the increase in the number of power plants utilizing non-domestic natural resources, foreign resource dependent energy production becomes one of the most crucial problems of Turkey. This critical situation makes utilization of domestic sources for energy production important for Turkey.

The dramatic increase in energy demand and current dependence on the petroleum based energy production requires utilization of hydroelectric power an important option as a domestic, clean and reliable energy source. In addition to the increase in energy demand, irrigation and water demand also increase with the population growth. The aggregation of these factors results in a trend of dam construction in Turkey. This trend gained momentum, especially in the last decade, with the legislation which opened the doors of the energy production to private sector. The sharp increase of the cumulative installed capacities of hydroelectric power plants and at the total installed capacity is shown in Figure 1.1.

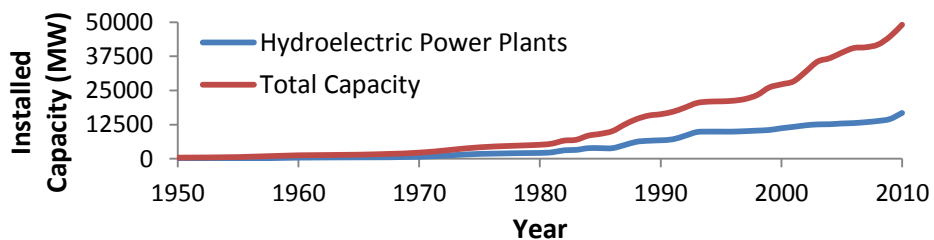


Figure 1.1 Cumulative installed capacities of hydroelectric power plants and total installed capacity in Turkey (World Energy Council Turkish National Committee, 2012)

The number of dams constructed by the private hydroelectricity companies is about 600. A significant number of dams are constructed or at the construction phase as a result of this. It is also planned to construct a large number of dams in the following years. Use of roller compacted concrete, as an alternative to conventionally vibrated concrete, increases the attractiveness of the concrete gravity dams by decreasing the construction duration and costs. Despite the recent advancements in the dam construction sector, the history of modern concrete gravity dam construction dates back to the first years of the Turkish Republic. Çubuk I Dam, which is the first concrete arch gravity dam of Turkey was taken into operation in 1936, interestingly at a similar date to that of Hoover Dam. Following the Çubuk I Dam a number of concrete gravity dams were constructed in the following approximately 20 years. Some of these dams with their construction dates are Porsuk I Dam (1948), Elmanlı II Dam (1955), Sarıyar Dam (1956) and Kemer Dam (1958) (Öziş, 1990).

Turkey lies at the intersection of a number of major and minor active faults, hence she is in a seismic prone region with severe earthquake risk. Dams are special and monumental type of structures requiring extensive care at their seismic design stage. Therefore modern analysis and design techniques must be utilized in today's computer age. In addition to the need of modern tools for seismic design of new dams, methods for the seismic damage assessment of old dams are also needed. A concrete step for the recommendation of modern seismic design and analysis principles is taken by the general directorate of state hydraulic works. Dams Congress is organized by the general directorate of state hydraulic works in 2012 and design guidelines were formed as a result of collaboration of the academicians and professionals. The procedures proposed by these guidelines (BK Guidelines, 2012) are taken as a basis for the conducted studies in this work.

1.2 Literature Survey

The seismic behavior of concrete gravity dams under strong ground motion is investigated by numerous researchers in the past. Various assumptions and simplifications were made to simulate the dynamic behavior of the dam-reservoir-foundation rock system. Although these assumptions may cause deviations from the actual seismic behavior of the dam, better estimations of the seismic response of the dams is achieved in time by the efforts of researchers. The most critical research available in the literature is the studies focused on the evaluation of hydrodynamic pressures, dam-reservoir-foundation rock interactions and reservoir bottom absorption.

The pioneer of the research on the response of the dams under earthquake acceleration dates back to study presented by Westergaard in 1933. In order to determine the hydrodynamic pressures resulting from a strong ground motion, a straight and rigid dam body with a vertical upstream face and an infinite reservoir was considered. Only the horizontal component of the ground motion was taken into account and the compressibility of the water was included. Resulting displacements were assumed to be small and the effects of the surface waves were ignored. The effects of hydrodynamic pressures was

simplified as an added mass of a virtual water body which results in inertial forces acting on the upstream face of the dam (Figure 1.2). This study made a worldwide impact and various researchers examined the validity of the proposed technique by reconsidering the problem with different approaches and through experimentation.

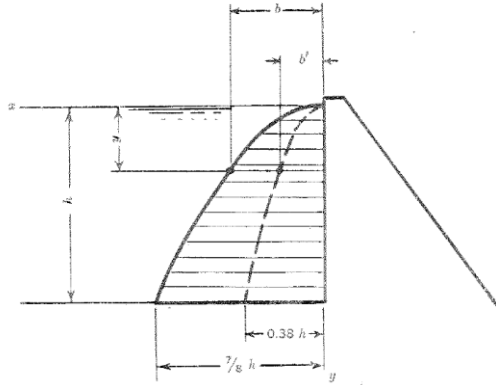


Figure 1.2 Distribution of the added mass of virtual water body

Chopra introduced his findings evaluation of the hydrodynamic pressures in 1966. His work could be considered as one of the most significant developments since the formulation proposed by Westergaard. An infinitely long channel and a rigid dam with a vertical upstream face were considered. Effects of surface waves were not taken into account. Complex valued frequency response functions were derived for both horizontal and vertical ground motions. The significance of the effect of water compressibility on the response was highlighted. Differently from the Westergaard's study, the proposed complex frequency response functions were capable of taking compressibility of water into account for entire frequency range. The importance of the consideration of vertical ground motion was also found in that study. However, amplified response was obtained for vertical ground motion since the response to vertical unit impulse demonstrated no decrease.

Following the major developments in the determination of the hydrodynamic effects on dams subjected to strong ground motion, another important development was made in the determination of the effects of soil-structure interaction on the seismic response. Dasgupta and Chopra (1977) presented a procedure to produce a complex valued, frequency dependent stiffness matrix for the surface of a dam base which is supporting the structure. The half space foundation was idealized as homogenous, isotropic, linear and viscoelastic. This idealization eliminated the misleading assumption of soil region limited with a horizontal rigid boundary. The dynamic stiffness matrix was determined by

utilizing the influence coefficients of the surface of a viscoelastic half space in plane stress or plane strain. The influence coefficients were obtained by solving two boundary value problems with prescribed harmonically time varying normal and shear stresses which are distributed uniformly over a surface element. It was shown that the introduced procedure increases the accuracy of the produced dynamic stiffness matrix. The compatibility of displacements at nodal points and equilibrium of stresses were also ensured with the proposed method.

Fenves and Chopra developed a semi analytical-numerical procedure to analyze the earthquake response of concrete gravity dams in 1984. The effects of dam-reservoir-foundation rock interaction and sediments accumulated at reservoir bottom were included with substructure method in this study. The effects of the reservoir bottom materials were discussed for a simplified system at first. The flexibility of foundation rock was neglected by rigid foundation assumption and only the fundamental vibration mode was taken into account in the first part of the work. Both the horizontal and vertical components of the ground motion were taken into consideration. The absorptive effect of the reservoir bottom materials was reflected by a boundary condition which dissipates a portion of the hydrodynamic pressure waves. The results of simplified system demonstrated that the absorptive reservoir bottom materials have a major effect on the earthquake response. A general analytical procedure which includes the dam-reservoir-foundation rock interaction and the reservoir bottom absorption effects was developed next by improving the considered simplified system. Effects of all significant modes and flexibility of the foundation rock were taken into account in the proposed procedure. Continuum solutions for the foundation and numerical evaluation methods for the dam body were discussed. The earthquake response of an idealized concrete gravity dam was investigated by utilizing the developed general procedure. The response of the dam subjected to a harmonic ground motion was found for a wide range of design parameters and the results were presented in the form of frequency response functions. The obtained frequency response functions proved that the effect of absorptive reservoir bottom was important. The tallest non-overflow monolith of Pine Flat concrete gravity dam was analyzed under the Taft ground motion. Several assumptions for the reservoir and foundation rock and various ratios of reservoir bottom absorption were considered. Horizontal and vertical components of the Taft ground motion was taken into account. The analyses results demonstrated that the dam-reservoir and dam-foundation rock interactions and the reservoir bottom absorption had a significant influence on the resulting stresses and displacements. The importance of considering the vertical component of the ground motion was also observed from the results. Finally a simplified method was developed for the preliminary design and safety assessment of concrete gravity dams. The proposed method considered an equivalent single degree of freedom system for approximate representation of the dam behavior. The results obtained by the simplified method were independent from the excitation frequency. Only the fundamental mode response to horizontal ground motion was taken into account.

A computer program named as EAGD-84 was prepared by Fenves and Chopra in 1984. EAGD-84 was developed for the numerical evaluation of the earthquake response of the dams by utilizing the proposed procedure. The dam cross section was idealized as a two dimensional finite element system. Stress and displacement response histories of dams were obtained as the fundamental result of the analyses. The details of the proposed analytical procedure and EAGD-84 are described in the following section.

Lotfi et al. presented an alternative study to Fenves and Chopra's work in 1987. The major difference of the developed technique was its approach to the reservoir water-flexible foundation interaction. The water-foundation interaction was considered by enforcing stress and displacement continuity normal to reservoir foundation interface. The developed hyper-element technique was capable of considering layered foundations. Analysis of an idealized dam-foundation-reservoir system with the proposed technique was presented. The results of the conducted analyses were discussed and the efficiency of the developed technique in the consideration of the reservoir-foundation interaction was introduced.

Effect of reservoir-foundation interaction was the subject of a study conducted by Dominguez et al (1990). A boundary integral technique was proposed for the investigation of the response of dam-reservoir-sediment-foundation systems subjected to ground acceleration. The boundary element method was utilized for the development of the proposed technique. The study took both the viscoelastic half plane and layered foundation assumptions into consideration. The effects of the foundation flexibility, full and empty reservoir cases and the existence of the sediment layer were investigated. The results were compared with the previous studies conducted by Fenves and Chopra (1984) and Lotfi et al (1987). The results of the majority of the cases were consistent with the previous studies. The most significant inconsistency was observed at the full reservoir with viscoelastic half space foundation case. This inconsistency was introduced as a result of the exaggerated damping arising from the boundary condition of absorptive reservoir bottom proposed by Fenves and Chopra.

Bougacha et al. introduced a technique based on the finite element method for the analysis of wave generation in a layered, fluid filled poroelastic media to consider the sediments in 1993. The wave motion was considered as the combination of the modes which are continuous in horizontal and vertical directions. The plane strain and antiplane shear deformations were taken into account. Deformations in both plane and axisymmetric regions were considered and consistent transmitting boundaries were formulated for these regions. The application of the developed technique was given in a companion study. The dynamic stiffness matrices of strip and circular foundations with a rigid surface were determined. In addition to the application of the developed technique a simplified method for the determination of the dynamic stiffness matrix was also presented. The simplified method assumed an equivalent solid for the representation of the two phase medium. It was demonstrated that the accuracy of the approximate method is satisfactory especially for the low frequency range.

The studies presented above concentrated on the evaluation of the dynamic response of dams by taking dam-reservoir-foundation rock interactions and the effects of reservoir bottom materials into consideration. The focus of the researchers has been shifted to the nonlinear analysis and assessment of dams towards the end of 20th century.

Bhattacharjee et al. conducted a study on the two dimensional static fracture behavior of dams in 1994. Smearred crack models were developed from a nonlinear fracture mechanics point of view that can simulate the tensile and shear softening of the plain concrete. A coaxial rotating crack model and a fixed crack model with a variable shear resistance factor were presented. The nonlinear analyses of a notched shear beam, a model and a full scale concrete gravity dams were conducted by the proposed crack models. The results were compared with the experimental and analytical results presented by the previous researchers. It was shown that the both models give satisfactory results for full scale concrete gravity dams.

The static fracture behavior of a dam subjected to an incremental increase of the reservoir water level was also investigated by Bhattacharjee et al. in 1995. A rotating smearred crack model was considered in the nonlinear finite element analyses. The uplift pressure occurring inside the smearred crack bands was taken into account by effective porosity concept. The analyses results obtained by finite element analyses and conventional no-tension gravity method were compared. The fracture analysis of dams was recommended for the safety evaluation of dams since it was observed that the usage of gravity method might give results on the unsafe side.

Ghanaat introduced a method for the seismic performance evaluation of dams in 2004. The proposed assessment approach utilized linear time history analyses. The potential failure mechanisms of concrete gravity, buttress and arch dams were discussed and taken into consideration at the introduced performance evaluation approach. The performance evaluation procedure took magnitudes of demand capacity ratios, cumulative duration of inelastic stresses and magnitude of the cracked area into account. The criteria for the sufficiency of linear elastic analyses were introduced. The effectiveness of the proposed performance evaluation approach was demonstrated with linear and nonlinear analyses.

Javanmardi et al. developed a theoretical method to determine the water pressure variations along a tensile crack during dynamic response in 2005. The results of the proposed model were compared with experimental test results. It was demonstrated that reservoir water enters the crack and a certain length of the crack become partially saturated. Finite element analyses of a 90 meters high gravity dam were conducted. The uplift pressure inside the crack was decreased with crack opening and increased with crack closing. It was noted that crack opening does not affect the downstream sliding safety factor. Since the excessive water pressure mainly occurs close the crack mouth crack closing mechanism also did not pose a serious threat to the sliding safety.

Lotfi et al. conducted a study on the natural vibration mechanisms due to damage at the dam foundation interface in 2008. Dynamic stress distribution resulting from the nonlinear response of a concrete gravity dam was investigated with a finite element program developed by the researchers. Local stress space of the interface elements were modeled by a plasticity based approach. It was demonstrated that a reasonable amount of base sliding decreased the tensile stresses occurring at the dam body especially at the base. The effects of uplifting, joint opening and flexible foundation idealizations were also discussed. It was underlined that tensile stresses observed especially at the upper parts of the dam body did not decrease enough to prevent nonlinear deformation of the dam.

1.3 Approach of Fenves and Chopra (1984): EAGD-84

This study is mainly based on the development of a graphical user interface for EAGD-84 and various analyses conducted using this interface. General information on EAGD-84 and the analytical procedure utilized for the evaluation of the dynamic response is introduced in this section.

1.3.1 General Information

The earthquake response of gravity dams under strong ground motion could be determined by considering the two dimensional independent vibration of the dam monoliths (Fenves and Chopra, 1984). The analytical procedure of EAGD-84 which is developed for the evaluation of the earthquake response is founded on this fundamental assumption. The two dimensional response of gravity dams to the strong ground motion is determined by taking an idealized dam-water-foundation rock system into account with several assumptions (Figure 1.3).

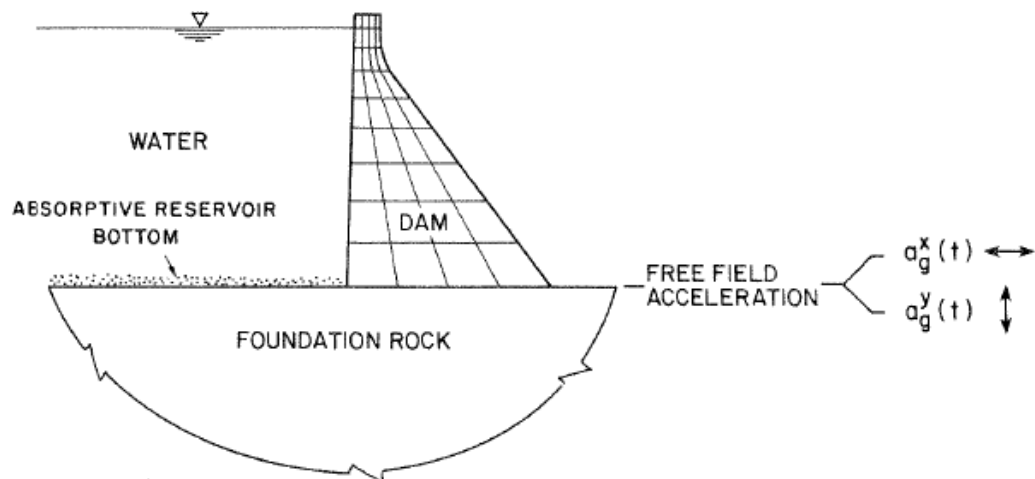


Figure 1.3 The idealized dam-water-foundation rock system

The bottom of the gravity dam cross section is idealized as a horizontal line. Except this limitation, the dam cross section could be an arbitrary shape with different upstream and downstream slopes and a crest region which has a different slope. The dam cross section is modeled as a two dimensional finite element system with plane stress or plane strain assumption. The effects of the static loads such as gravity of the dam and the hydrostatic pressure could be included in the dam response by the finite element system. The foundation rock beneath the dam body is modeled with a homogenous, isotropic, viscoelastic half space. The horizontal dam body base restriction is the result of the idealization of the foundation rock under the dam body.

The hydrodynamic effects are determined with the idealization of the impounded water as a fluid domain of a constant depth. The compressibility of water is taken into account. The length of the reservoir is assumed as infinite in the upstream direction. The upstream face of the dam body is assumed as vertical at the idealization of the impounded water. This is a realistic assumption for the majority of the existing gravity dams since the upstream faces of the existing dams are usually vertical or almost vertical. Moreover, the effect of a small slope at the upstream face of the dam on the determination of the hydrodynamic pressures is negligible.

The accumulated reservoir bottom materials partially absorb the hydrodynamic waves and reflect only a portion of them. In the analytical procedure the absorptive effect of the reservoir bottom materials is included by a boundary condition which considers a one dimensional wave absorption mechanism at the reservoir bottom. Since the materials deposited at the bottom of the reservoir are soft and almost fully saturated, the thickness of the reservoir bottom materials is neglected. Influence of the reservoir bottom materials on the dynamic properties of the dam is negligible and is not taken into account in the analytical procedure. Since the reservoir bottom materials are soft, small in thickness and located at the lower part of the dam; the pressure resulting from the reservoir bottom materials are also not taken into consideration at the static analyses.

It is assumed that the ground motion equally affects the entire base of the dam body. The earthquake excitation is composed of two components of the ground motion which are the horizontal and the vertical components. The horizontal component of the ground motion $a_g^x(t)$ is transverse to the dam axis and the vertical component of the ground motion $a_g^y(t)$ is perpendicular to the dam axis. The dam-water-foundation rock system is assumed to behave linearly. The concrete cracking due to hydration heat, opening of construction joints or water cavitation are not taken into consideration.

1.3.2 General Analytical Procedure

A general analytical procedure to evaluate the response of concrete gravity dams subjected to strong ground motion is developed by the substructure method approach. The response of dam-reservoir-foundation rock system is formulated by discretizing the sys-

tem into three substructures which are dam substructure, foundation rock substructure and fluid domain substructure (Figure 1.4).

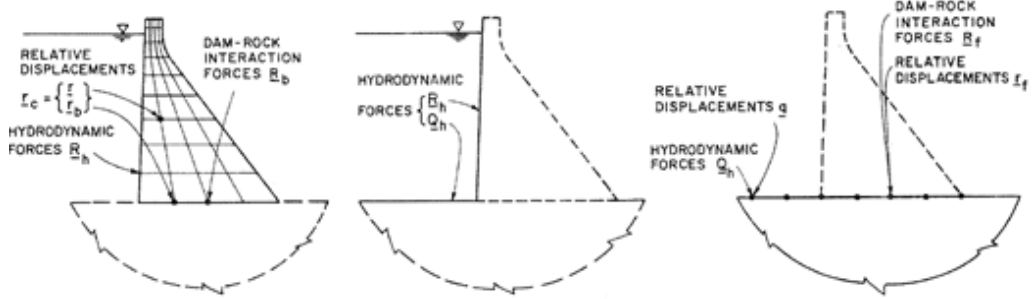


Figure 1.4 Substructures of the dam-reservoir-foundation rock system

The general equation of motion of a two dimensional finite element system of a dam is:

$$m_c \ddot{r}_c + c_c \dot{r}_c + k_c r_c = -m_c \underline{1}_c^x a_g^x(t) - m_c \underline{1}_c^y a_g^y(t) + R_c(t) \quad (1.1)$$

where m_c , c_c and k_c are the mass, damping and stiffness matrices of the dam, r_c is the vector of relative displacements of the nodes, $\underline{1}_c^x$ and $\underline{1}_c^y$ are directional unit vectors, a_g^x and a_g^y are horizontal and vertical ground accelerations respectively, R_c is the force vector which is composed of forces acting on the upstream face and the base of the dam.

The equation of motion of the dam-foundation rock system is obtained by the partitioning of nodal points into nodal points at the base and nodal points above the base. The equation of motion is written in the frequency domain by considering harmonic ground accelerations (Equation 1.2).

$$\left[-\omega^2 \begin{bmatrix} m & 0 \\ 0 & m_b \end{bmatrix} + (1 + i\eta_s) \begin{bmatrix} k & k_b \\ k_b^T & k_{bb} \end{bmatrix} \right] \begin{Bmatrix} \bar{r}^l(\omega) \\ \bar{r}_b^l(\omega) \end{Bmatrix} = - \begin{Bmatrix} m \underline{1}^l \\ m_b \underline{1}_b^l \end{Bmatrix} + \begin{Bmatrix} \bar{R}_h^l(\omega) \\ \bar{R}_b^l(\omega) \end{Bmatrix} \quad (1.2)$$

In Equation 1.2, \bar{r}^l and \bar{r}_b^l represent relative displacement of nodal points above the base and the nodal points on the base, \bar{R}_h^l and \bar{R}_b^l represent hydrodynamic forces on the upstream face and dam-foundation interaction forces on the base and η_s represents the constant hysteretic factor for the dam concrete.

The dynamic stiffness matrix of the foundation rock substructure is:

$$\begin{bmatrix} \underline{S}_{rr}(\omega) & \underline{S}_{rq}(\omega) \\ \underline{S}_{rq}^T(\omega) & \underline{S}_{qq}(\omega) \end{bmatrix} \begin{Bmatrix} \bar{r}_f(\omega) \\ \bar{q}(\omega) \end{Bmatrix} = \begin{Bmatrix} \bar{R}_f(\omega) \\ \bar{Q}_h(\omega) \end{Bmatrix} \quad (1.3)$$

where \bar{R}_f and \bar{r}_f are forces and displacements at the dam base, \bar{Q}_h and \bar{q} are forces and displacements at the reservoir bottom. By the substituting \bar{q} which is obtained by the second matrix equation the first matrix equation could be given as in Equation 1.4.

$$\underline{S}_f(\omega)\bar{r}_f(\omega) = \bar{R}_f(\omega) - \underline{S}_{rq}(\omega)\underline{S}_{qq}^{-1}(\omega)\bar{Q}_h(\omega) \quad (1.4)$$

The dynamic foundation stiffness matrix $\underline{S}_f(\omega)$ given Equation 1.5 is obtained by vis-coelastic half plane idealization proposed by Dasgupta and Chopra (1977).

$$\underline{S}_f(\omega) = \underline{S}_{rr}(\omega) - \underline{S}_{rq}(\omega)\underline{S}_{qq}^{-1}(\omega)\underline{S}_{rq}^T(\omega) \quad (1.5)$$

Forces acting on the dam base are derived in Equation 1.6 by utilizing the equilibrium of interaction forces and compatibility of displacements at the dam-foundation interface.

$$\bar{R}_b^l(\omega) = -\underline{S}_f(\omega)\bar{r}_b^l(\omega) - \underline{S}_{rq}(\omega)\underline{S}_{qq}^{-1}(\omega)\bar{Q}_h(\omega) \quad (1.6)$$

The equation of motion of the dam-foundation rock system could be expressed as:

$$\begin{aligned} & \left(-\omega^2 \begin{bmatrix} m & 0 \\ 0 & m_b \end{bmatrix} + (1 + i\eta_s) \begin{bmatrix} k & k_b \\ k_b^T & k_{bb} \end{bmatrix} + \begin{bmatrix} 0 & 0 \\ 0 & \underline{S}_f(\omega) \end{bmatrix} \right) \begin{Bmatrix} \bar{r}^l(\omega) \\ \bar{r}_b^l(\omega) \end{Bmatrix} = \\ & - \begin{Bmatrix} m\mathbf{1}^l \\ m_b\mathbf{1}_b^l \end{Bmatrix} + \begin{Bmatrix} \bar{R}_h^l(\omega) \\ -\underline{S}_{rq}\underline{S}_{qq}^{-1}\bar{Q}_h(\omega) \end{Bmatrix} \end{aligned} \quad (1.7)$$

Equation 1.7 includes a set of $2(N+N_b)$ frequency dependent complex valued equations where N and N_b are the number of nodal points above and on the base of the dam. Since the solution of these equations requires an excessive amount of computation power the number of degrees of freedom is decreased by Ritz method. The relative displacement frequency functions are formulated as linear combinations of J Ritz vectors.

$$\bar{r}_c^l(\omega) = \sum_{j=1}^J \bar{Z}_j^l(\omega)\psi_j \quad (1.8)$$

ψ_j is the j^{th} Ritz vector and \bar{Z}_j^l is the generalized coordinate of the corresponding Ritz vector. Ritz vectors ψ_j and vibration frequencies λ_j are determined by the solution of the following eigenvalue problem.

$$[k_c + \check{\underline{S}}_f(0)]\psi_j = \lambda_j^2 m_c \psi_j \quad (1.9)$$

where

$$\check{S}_f(\omega) = \begin{bmatrix} 0 & 0 \\ 0 & \underline{S}_f(\omega) \end{bmatrix} \quad (1.10)$$

In order to normalize the determined Ritz vectors the equation of $\psi_j^T m_c \psi_j = 1$ is satisfied. The following equation is obtained by introducing Equation 1.8 into Equation 1.7, multiplying the equation by ψ_j^T and utilizing the orthogonality properties of eigenvectors.

$$S(\omega)\bar{Z}^l(\omega) = L^l(\omega) \quad (1.11)$$

The elements of the matrix S and the vector L^l could be expressed as the following.

$$S_{nj}(\omega) = [-\omega^2 + (1 + i\eta_s)\lambda_n^2]\delta_{nj} + \psi_n^T [\check{S}_f(\omega) - (1 + i\eta_s)\check{S}_f(0)]\psi_j \quad (1.12a)$$

$$L_n^l = -\psi_n^T m_c \underline{1}_c^l + \{\psi_n^f\}^T \bar{R}_h^l(\omega) - \psi_{bn}^T \underline{S}_{rq}(\omega) \underline{S}_{q^l}^{-1}(\omega) \bar{Q}_h(\omega) \quad (1.12b)$$

The vector \bar{Z}^l includes J number of dynamic frequency response functions for the generalized coordinates \bar{Z}_j^l . A sub vector of Ritz vectors which corresponds to nodal points of the upstream face of dam is represented as ψ_j^f and the Kronecker delta function is represented as δ_{nj} .

The complex valued frequency response functions for the hydrodynamic pressures are obtained by the solution of the two dimensional Helmholtz equation (Equation 1.13).

$$\frac{\partial^2 \bar{p}}{\partial x^2} + \frac{\partial^2 \bar{p}}{\partial y^2} + \frac{\omega^2}{c^2} \bar{p} = 0 \quad (1.13)$$

In the Helmholtz equation \bar{p} represents the frequency response function for hydrodynamic pressure and C represents the velocity of the pressure waves in water. The Helmholtz equation is solved for the following boundary conditions:

$$\frac{\partial}{\partial x} \bar{p}(0, y, \omega) = -\rho \left[\delta_{xl} + \sum_{j=1}^J \psi_j(y) \bar{Z}_j^l(\omega) \right], \quad l = x, y \quad (1.14a)$$

$$\frac{\partial}{\partial y} \bar{p}(x, 0, \omega) - \rho \omega^2 \bar{q}_h(x, \omega) = -\rho \left[\delta_{yl} + \sum_{j=1}^J \chi_j(x) \bar{Z}_j^l(\omega) \right], \quad l = x, y \quad (1.14b)$$

$$\bar{p}(x, H, \omega) = 0 \quad (1.14c)$$

where

$$\chi_j = -\underline{S}_{\bar{q}q}^{-1}(0)\underline{S}_{rq}^T(0)\psi_{bj} \quad (1.15)$$

and ρ represents the density of the water. The effects of the absorptive reservoir bottom materials are taken into account as one dimensional wave absorption. For this purpose the frequency response function for the vertical displacement at the reservoir bottom is expressed as following.

$$\bar{q}_h(x, \omega) = -C(\omega)\bar{p}(x, 0, \omega) \quad (1.16)$$

The compliance function $C(\omega)$ which represents the absorptive reservoir bottom materials is obtained by the solution of the one dimensional Helmholtz equation:

$$C(\omega) = -i \left[\frac{1}{\rho_r C_r \omega} \right] \quad (1.17)$$

where $C_r = \sqrt{E_r/\rho_r}$, E_r and ρ_r are the elastic modulus and density of the reservoir bottom materials.

The boundary condition Equation 14.b could be expressed as the following by the substitution of Equation 1.16.

$$\left[\frac{\partial}{\partial y} - i\omega q \right] \bar{p}(x, 0, \omega) = -\rho \left[\delta_{yl} + \sum_{j=1}^J \chi_j(x) \bar{Z}_j^l(\omega) \right], \quad l = x, y \quad (1.18)$$

The damping coefficient is represented by q . The absorptive effect of the reservoir bottom materials is included by the damping coefficient which is obtained from the solution of equation of $q = \rho/\rho_r C_r$. In order to better represent the reservoir bottom absorption the wave reflection coefficient α is frequently utilized in analyses. The wave reflection coefficient is formulated as a function of the damping coefficient (Equation 1.19). The wave reflection coefficient could be defined as the ratio of the wave pressures which are reflected from the reservoir bottom.

$$\alpha = \frac{1-qC_r}{1+qC_r} \quad (1.19)$$

The complex valued frequency response function of the hydrodynamic pressures could be expressed in a linear form.

$$\bar{p}^l(x, y, \omega) = \bar{p}_0^l(x, y, \omega) + \sum_{j=1}^J \bar{Z}_j^l(\omega) \left[\bar{p}_j^f(x, y, \omega) + \bar{p}_j^b(x, y, \omega) \right] \quad (1.20)$$

The hydrodynamic pressure resulting from the horizontal acceleration of a rigid dam is determined by utilizing the following boundary conditions.

$$\frac{\partial}{\partial x} \bar{p}(0, y, \omega) = -\rho \quad (1.21a)$$

$$\left[\frac{\partial}{\partial y} - i\omega q \right] \bar{p}(x, 0, \omega) = 0 \quad (1.21b)$$

$$\bar{p}(x, H, \omega) = 0 \quad (1.21c)$$

The hydrodynamic pressure resulting from the vertical acceleration of a rigid dam is determined by utilizing the following boundary conditions.

$$\frac{\partial}{\partial x} \bar{p}(0, y, \omega) = 0 \quad (1.22a)$$

$$\left[\frac{\partial}{\partial y} - i\omega q \right] \bar{p}(x, 0, \omega) = -\rho \quad (1.22b)$$

$$\bar{p}(x, H, \omega) = 0 \quad (1.22c)$$

The hydrodynamic pressure resulting from the horizontal acceleration of the upstream face of the dam is determined by utilizing the following boundary conditions.

$$\frac{\partial}{\partial x} \bar{p}(0, y, \omega) = -\rho \psi_j(y) \quad (1.23a)$$

$$\left[\frac{\partial}{\partial y} - i\omega q \right] \bar{p}(x, 0, \omega) = 0 \quad (1.23b)$$

$$\bar{p}(x, H, \omega) = 0 \quad (1.23c)$$

The frequency response functions for the hydrodynamic pressures are obtained by the solution of the Helmholtz equation (Equation 1.13) subject to the boundary conditions given above. It should be noted that the effects of hydrodynamic pressures resulting from the vertical acceleration of the reservoir bottom is neglected. The frequency response functions for the hydrodynamic pressures acting on the upstream face of the dam are:

$$\bar{p}_0^x(0, y, \omega) = -2\rho H \sum_{n=1}^{\infty} \frac{\mu_n^2(\omega)}{H[\mu_n^2(\omega) - (\omega q)^2] + i(\omega q)} \frac{I_{0n}(\omega)}{\sqrt{\mu_n^2(\omega) - \omega^2/C^2}} \gamma_n(y, \omega) \quad (1.24)$$

$$\bar{p}_0^y(0, y, \omega) = \frac{\rho c}{\omega} \frac{1}{\cos \frac{\omega H}{c} + i q c \sin \frac{\omega H}{c}} \sin \frac{\omega(H-y)}{c} \quad (1.25)$$

$$\bar{p}_j^f(0, y, \omega) = -2\rho H \sum_{n=1}^{\infty} \frac{\mu_n^2(\omega)}{H[\mu_n^2(\omega) - (\omega q)^2] + i(\omega q)} \frac{I_{jn}(\omega)}{\sqrt{\mu_n^2(\omega) - \omega^2/C^2}} \gamma_n(y, \omega) \quad (1.26)$$

where

$$e^{2i\mu_n(\omega)H} = -\frac{\mu_n(\omega) - \omega q}{\mu_n(\omega) + \omega q} \quad (1.27a)$$

$$\gamma_n(y, \omega) = \frac{1}{2\mu_n(\omega)} \{ [\mu_n(\omega) + \omega q] e^{i\mu_n(\omega)y} + [\mu_n(\omega) - \omega q] e^{-i\mu_n(\omega)y} \} \quad (1.27b)$$

$$I_{0n}(\omega) = \frac{1}{H} \int_0^H \gamma_n(y, \omega) dy \quad (1.27c)$$

and

$$I_{jn}(\omega) = \frac{1}{H} \int_0^H \psi_j(y) \gamma_n(y, \omega) dy \quad (1.27d)$$

The vector of hydrodynamic forces acting on the upstream face of the dam \bar{R}_h^l and the reservoir bottom \bar{Q}_h could be expressed as:

$$\bar{R}_h^l(\omega) = \bar{R}_0^l(\omega) + \sum_{j=1}^J \bar{Z}_j^l(\omega) [\bar{R}_j^f(\omega) + \bar{R}_j^b(\omega)] \quad (1.28a)$$

$$\bar{Q}_h(\omega) = \bar{Q}_0^l(\omega) + \sum_{j=1}^J \bar{Z}_j^l(\omega) [\bar{Q}_j^f(\omega) + \bar{Q}_j^b(\omega)] \quad (1.28b)$$

The following equation is obtained by introducing the Equation 1.28 into Equations 1.11 and 1.12.

$$\check{S}(\omega) \bar{Z}^l(\omega) = \check{L}^l(\omega) \quad (1.29)$$

The matrix \check{S} and the vector \check{L} of Equation 1.29 are simplified by neglecting the hydrodynamic forces acting on the reservoir bottom and hydrodynamic forces resulting from the deformations at the reservoir bottom. The simplified equations for the matrix \check{S} and the vector \check{L} are as follows:

$$\begin{aligned} \check{S}_{nj}(\omega) = & [-\omega^2 + (1 + i\eta_s)\lambda_n^2] \delta_{nj} + \psi_n^T [\check{S}_f(\omega) - (1 + i\eta_s)\check{S}_f(0)] \psi_j \\ & + \omega^2 \{ \psi_n^f \}^T \bar{R}_j^f(\omega) \end{aligned} \quad (1.30a)$$

$$\check{L}_n^l = -\psi_n^T m_c \underline{1}_n^l + \{ \psi_n^f \}^T \bar{R}_0^l(\omega) \quad (1.30b)$$

The complex valued frequency response functions for the generalized coordinates \bar{Z}_j^l are determined by the solution of Equations 1.29 and 1.30. The response to arbitrary ground acceleration is obtained by the inverse Fourier transform given below.

$$Z_j^l(t) = \frac{1}{2\pi} \int_{-\infty}^{\infty} \bar{Z}_j^l(\omega) A_g^l(\omega) e^{i\omega t} d\omega \quad (1.31)$$

It should be noted that the generalized coordinates \bar{Z}_j^l are factored with the Fourier transformed ground acceleration A_g^l . The displacement response in time domain is determined by the following equation.

$$r_c(t) = \sum_{j=1}^J [Z_j^x(t) + Z_j^y(t)] \psi_j \quad (1.32)$$

The stresses in a finite element of the dam body is obtained by Equation 1.33 where σ_p is the stresses at finite element p, r_p is the displacements of the corresponding finite element and T_p is stress-transformation matrix of the element.

$$\sigma_p(t) = T_p r_p(t) \quad (1.33)$$

The general analytical procedure implemented by EAGD-84 is summarized as a flowchart in Figure 1.5.

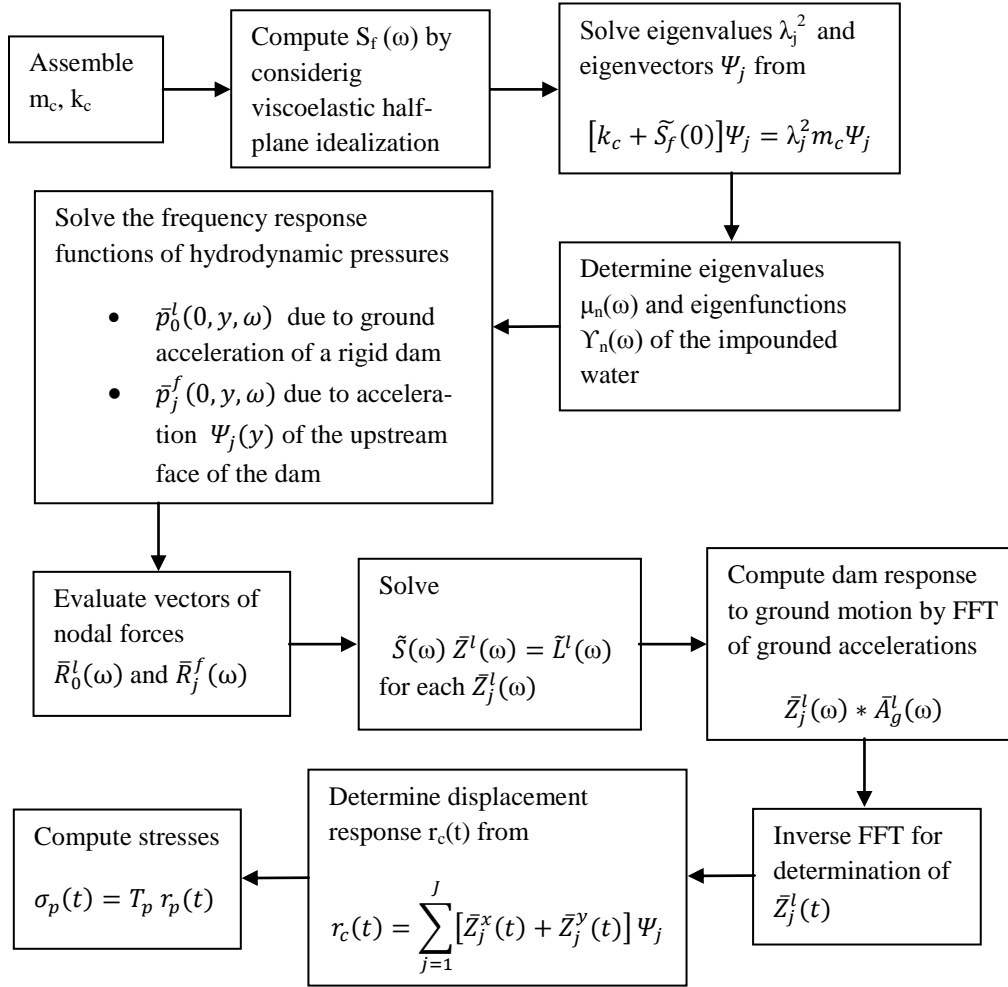


Figure 1.5 Analysis procedure of EAGD-84

1.4 Importance of Detailed Response History Analysis

This section aims to introduce the importance of conducting a detailed response history analysis for the reliable design and evaluation of concrete gravity dams. Properties of the considered dam sections are given in Table 1.1. Dam height, downstream slope and ratio of elastic modulus of dam concrete to elastic modulus of foundation rock (E_c/E_f) were selected as the main parameters of the dams. Other properties of the dam sections were kept constant. Effects of the static loads such as dead weight and hydrostatic pressures were considered in addition to the earthquake effects in the analyses. The upstream face and downstream of the crest region was taken as vertical. The cross sectional width of the crest was taken as eight meters for all considered dams. The cross sectional length of the crest region was determined by the division of the crest width to the downstream

slope of the dam. The optimum downstream slopes were computed for these dam sections by using two different approaches and results were critically evaluated.

First, the assessment method in BK guidelines was utilized for the determination of optimum downstream slopes by using response history analysis. For each section analyzed, the smallest downstream slope was found such that dam stresses remain below the limits as defined per BK guidelines. This slope is called the optimum downstream slope from response history analysis (Table 1.1). This approach, named as the response history analysis utilized the ground motion given in Chapter 3.

In order to demonstrate the importance of dynamic analysis, same dam sections were reanalyzed by using the CADAM program and the optimum downstream slopes of the dam cross sections were computed. The procedure of CADAM can be outlined as follows: First the spectrum of the ground motion was obtained for an equivalent damping considering the dam-foundation-reservoir interaction. Secondly, the spectral acceleration value at the fundamental frequency of the dam was computed and hydrodynamic and inertial forces were determined. By using these forces, dam base stresses were found by using the standard beam formulas. The principal tensile stress at the thalweg of the dam was checked to see if the dam toe was overstressed. A dynamic amplification factor of 1.50 was employed for the tensile strength of dam concrete. If the obtained principal tensile stress at the thalweg was smaller than the factored tensile strength of dam concrete (2.25 MPa for this case) the analyzed dam cross section could be accepted as sufficient. The smallest downstream slope, which provided an acceptable principal stress at the thalweg was referred as the optimum downstream slope from pseudo-static analysis (Table 1.1).

Table 1.1 Properties of dam design alternatives and optimum downstream slopes

Properties	Case-1	Case-2	Case-3	Case-4
E_c/E_f	0.10	0.50	1.00	2.00
Dam Height (in meters)	50	100	150	150
Elastic Modulus of Dam Concrete (in MPa)	15000			
Density of Dam Concrete (in kg/m ³)	2400			
Poisson's Ratio for Dam Concrete (ν_s)	0.20			
Static Tensile Strength of Dam Concrete (in MPa)	1.50			
Density of Foundation Rock (in kg/m ³)	2500			
Poisson's Ratio for Foundation Rock (ν_f)	0.33			
Hysteretic Damping Coefficient (η)	0.10			
Wave Reflection Coefficient (α)	0.90			
Optimum D/S Slope from Response History Analyses ($m_{D/S}$ H : 1.0 V)	1.00	1.00	1.00	0.80
Optimum D/S Slope from Pseudo-Static Analyses ($m_{D/S}$ H : 1.0 V)	0.80	0.80	0.80	0.70

Stress distributions along the dam base of optimum downstream slopes are given in Figure 1.6 to Figure 1.9. Normal tensile stresses observed at the thalweg are accepted as principal tensile stresses since shear stresses are found as zero at the thalweg according to the beam theory. As can be seen from these results, a satisfactory seismic performance was obtained with smaller dam cross sections for all dam design alternatives, when pseudo-static analyses were employed. In other words, it can be observed that dam cross sections which provide unacceptable seismic performances with a serious damage potential could be found safe when pseudo-static analysis was used. Unsafe results obtained by pseudo-static analyses conducted by CADAM could be explained primarily by the insufficiency of the beam analogy to estimate the stresses occurring at the base. Moreover; the inadequacy of simplified method, which is independent of excitation frequency might also result in significant differences. These observations, which may not be generalized for all possible dams, clearly layout the importance of detailed dynamic analysis in dam design.

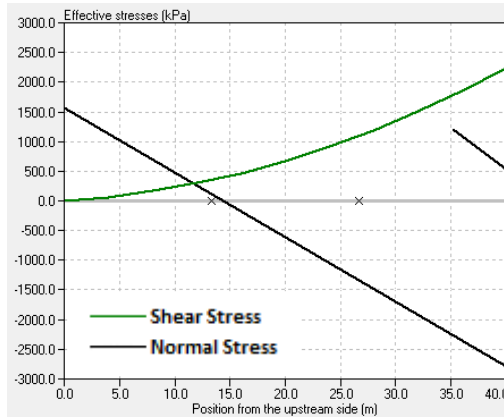


Figure 1.6 Stress distribution through dam base of case 1

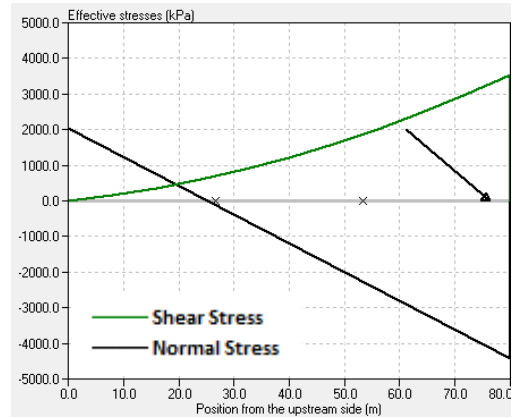


Figure 1.7 Stress distribution through dam base of case 2

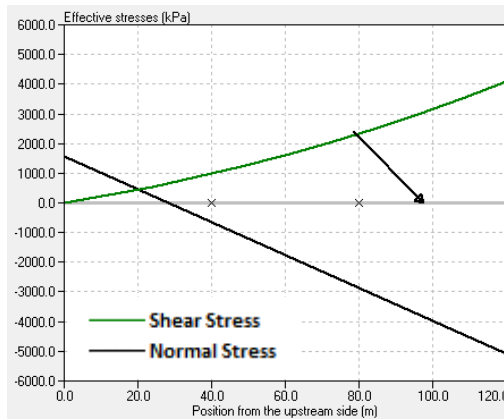


Figure 1.8 Stress distribution through dam base of case 3

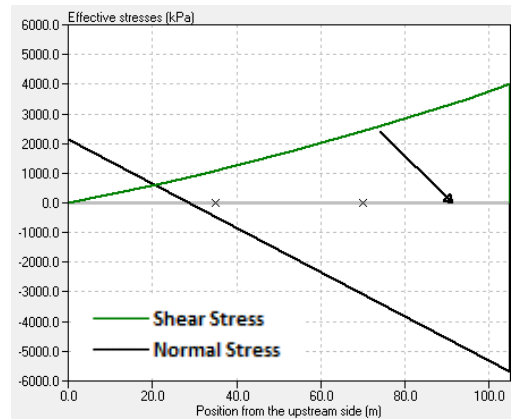


Figure 1.9 Stress distribution through dam base of case 4

1.5 Scope and Objective

An accurate evaluation of the dynamic response of a dam-reservoir-foundation rock system is essential for the design of dams in seismic prone region. Seismic response history analysis is essential for the reliable seismic design as inappropriate analysis techniques probably may result in unsafe or uneconomical designs. In order to represent the effects of dam-reservoir-foundation rock interaction accurately the foundation rock flexibility, compressibility of the reservoir water and the absorptive effect of reservoir bottom materials must be taken into consideration. The objectives of this study are

- To develop a user friendly graphical user interface to conduct seismic response history analysis of concrete gravity dams.
- To conduct parametric studies to understand effects of parameters on the seismic response.
- To investigate the most influential parameter by conducting a deterministic sensitivity analysis with tornado diagrams approach.
- To assess the structural performance of gravity dams with a probabilistic approach and determine fragility curves of a set of dams with various properties. The determination of fragility curves aims to provide a reference for both preliminary design of new dams and investigation of the structural reliability existing dams.

The development of the user interface is presented in Chapter 2. In Chapter 3 details of conducted parametric studies, deterministic sensitivity analysis and the determination of the fragility curves are discussed. The main conclusions of the conducted study are summarized and suggestions for future studies are introduced in Chapter 4.

CHAPTER 2

A USER INTERFACE FOR DAM ANALYSIS

In this chapter, the development of a user friendly interface for the analysis of earthquake response of concrete gravity dams is presented. Input parameters, pre-processing, post-processing details and results for seismic safety check are discussed. A dam analysis example is also provided for a better understanding of the capabilities of the developed interface.

2.1 General

Many of the design engineers in Turkey, unfortunately, use outdated procedures and assumptions, such as rigid foundation, rigid dam body, incompressible water etc. even for the final design of the dams. These assumptions were mainly inherited from the former approaches of earth fill dam design about four decades ago. However, the use of such outdated analysis tools may result in uneconomical designs in some cases and may result in unsafe designs for some others as demonstrated in Chapter 1. In this context, the interface tool developed in this study aims to open a window for the use of modern analysis procedures in dam design and assessment in Turkey by considering dam-reservoir-foundation rock interactions appropriately. This chapter aims to explain the key features of the developed interface along with an analysis example. The analysis engine employed in this work is based on EAGD-84 with some modifications. Although EAGD-84 is a comprehensive and widely accepted tool for seismic analysis of concrete dams within the research community, it did not find much use in practice in Turkey due to the difficulty of use. The product of this chapter is believed to overcome this limitation of EAGD-84 and introduce it to the engineering community interested in dam design and safety assessment. The execution of the interface is conducted through -m functions in Matlab. The developed Matlab scripts are compiled and converted to an executable stand-alone program to allow functioning in Matlab absent environments. The use of the interface is almost self explanatory, however key elements are described in this chapter. The interface is designed to interact with the user by pop-up notification windows in order to prevent entering improper data and other possible execution problems. It should be noted that the accuracy of the results obtained by the program is directly related with the quality and accuracy of the input data entered. Hence, it is the user's responsibility to judge the accuracy of the results.

The developed dam analysis tool uses EAGD-84 with some modifications as its analysis engine and it conducts the pre-processing and post-processing operations with a user friendly graphical user interface. This new version which is a modern processing tool is named as “EAGD ModPro”. The interface screen for EAGD ModPro is shown in Figure 2.1.

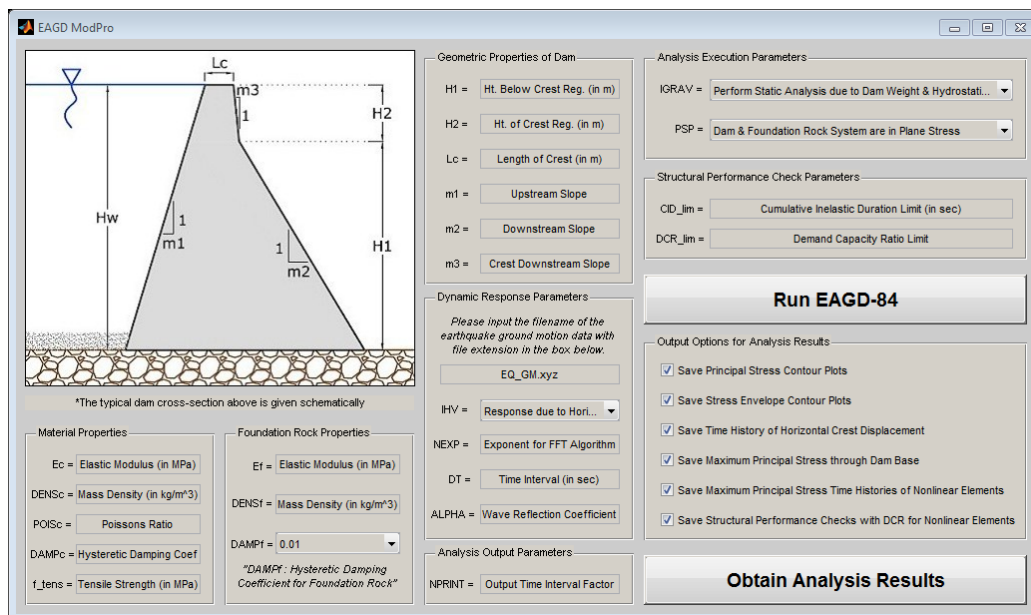


Figure 2.1 A screen capture of graphical user interface of EAGD ModPro

The use of EAGD ModPro is basically performed by executing four steps that are typical for almost all computer programs. These steps are: i-entering the input data, ii-analysis, iii- selection of post-process options and iv-obtaining the analysis results. These steps are summarized in the next sections.

2.2 Input Parameters and Pre-Processing of Input Data for Analysis

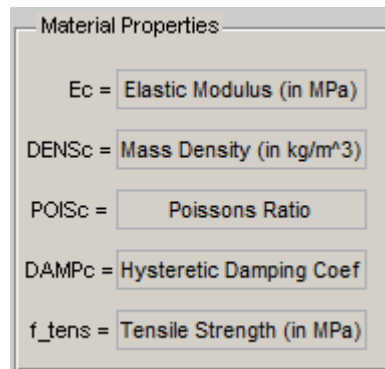
EAGD-84 requires a Fortran formatted input data file, which requires extensive care and is prone to errors. EAGD ModPro enables one to quickly prepare this input file through its user friendly graphical user interface. The software is designed to minimize the number of input parameters and possible number of errors during data entry.

The input parameters are classified into seven input sections: 1-material properties, 2-foundation rock properties, 3-geometric properties of dam, 4-dynamic response parameters, 5-analysis output parameters, 6-analysis execution parameters and 7-structural per-

formance parameters. It should be noted that EAGD-84, in its original form works in imperial unit system. EAGD ModPro is prepared to work with metric system units. Following sections brief the data for each input section.

2.2.1 Material Properties

The material properties section seeks the properties of the dam material utilized in the analysis. As it could be seen in Figure 2.2 data includes modulus of elasticity (in MPa), mass density (in kg/m^3), Poisson's ratio (ν), hysteretic damping factor (η_s) and tensile strength (in MPa) of the dam material (concrete or RCC). It should be noted that the tensile strength of the material is not essential for the execution of EAGD-84. The tensile strength of the material is stored for the structural performance check and damage assessment of the dam. The details of structural performance check and performance criteria assessment will be discussed later.



The screenshot shows a dialog box titled "Material Properties" with a light gray background. It contains five rows of input fields, each with a label and a unit description in parentheses:

- Ec = Elastic Modulus (in MPa)
- DENS = Mass Density (in kg/m^3)
- POIS = Poissons Ratio
- DAMP = Hysteretic Damping Coef
- f_tens = Tensile Strength (in MPa)

Figure 2.2 A screen capture of material properties section from GUI of EAGD ModPro

2.2.2 Foundation Rock Properties

EAGD-84 considers foundation rock flexibility within a dynamic soil structure interaction framework. Properties of the foundation rock underlying the dam are input with the help of data entry in this section. The dynamic stiffness matrix of the underlying foundation rock is generated by using the compliance data stored on a specific file named as fort.80. Elastic modulus (in MPa), mass density (in kg/m^3) and hysteretic damping factor (η_r) of the foundation rock are entered in the foundation rock properties section. The foundation rock properties section is illustrated in Figure 2.3. The hysteretic damping factor is selected from predefined values which are 0.01, 0.10, 0.25 and 0.50.

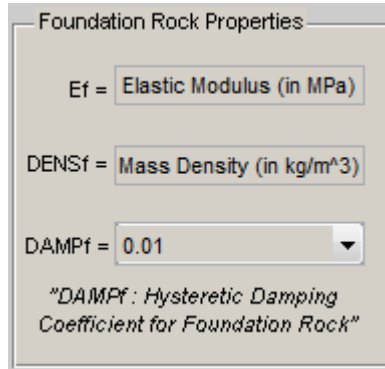


Figure 2.3 A screen capture of foundation rock properties section from GUI of EAGD ModPro

User must be aware that a functional fort.80 file must be provided for the execution of EAGD ModPro. The development of a complicated subroutine for the creation of dynamic compliance data stored on fort.80 file is beyond the scope of EAGD ModPro. Various tools developed by other researchers are available for the creation of fort.80 file (Akpınar 2013, Dasgupta 1977, 2012). EAGD ModPro focuses on conducting the pre and post processing operations in the most efficient and user friendly way as possible.

It should be reminded it is possible to conduct analysis for a rigid foundation with EAGD ModPro by choosing a sufficiently large modulus of elasticity for rock foundation. It is recommended to use the elastic modulus of foundation rock as 50 times larger than the elastic modulus of the dam material to ensure that rigid foundation behavior is ensured.

2.2.3 Geometric Properties of Dam

The geometric properties of dam section serves to create the geometry of the dam under consideration. The user enters height below the crest (in meters), height of the crest (in meters), length of the crest (in meters), upstream slope (horizontal:1), downstream slope (horizontal:1) and downstream slope of crest region (horizontal:1). Full reservoir condition is taken into consideration. Therefore height of the water table is taken as the summation of height below crest region and height of crest region in the analysis. In graphical user interface of EAGD ModPro a typical dam cross section demonstrating the input parameters is given schematically in order to explain the input of the geometric properties of dam. The typical dam cross section and a screen capture of geometric properties of dam section is given below (Figure 2.4).

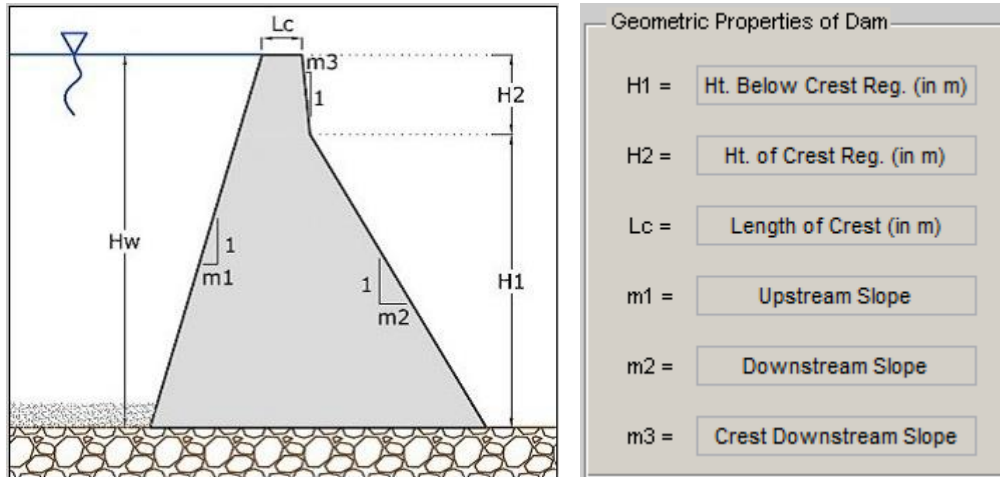


Figure 2.4 The typical dam cross section and a screen capture of geometric properties of dam section from GUI of EAGD ModPro

The finite element mesh of the dam cross section is generated by utilizing 4-node quadrilateral elements. Number of elements at the finite element mesh depends on the geometric properties of the dam. EAGD ModPro generates the meshing of the dam cross section automatically. The functions developed for the finite element mesh generation ensures the most appropriate aspect ratio of elements. In this way, it was aimed to prevent a possible error that might occur in an analysis conducted by an inexperienced engineer with finite elements. As it was stated before EAGD ModPro requires fort.80 file which contains the compliance data of the foundation rock for the execution of EAGD-84. The number of horizontal elements of the dam cross section is read from fort.80 file. In its supplied version fort.80 file contains the compliance data for 26 nodes at the dam base. In order to optimize the finite element meshing with respect to the element aspect ratios, the number of vertical elements is determined in two steps. The dam cross section is divided into two portions for this purpose. These are the part under the crest region of the dam and the crest region itself.

The number of vertical elements under the crest region is determined first. Obtaining elements with an aspect ratio approximately equal to unity at the middle of the lower region of the dam is aimed. This approach minimizes the differences in aspect ratios of the elements above and below of the element line at the middle of this portion. In other words, the minimum possible aspect ratio is satisfied at the uppermost and lowermost elements under the crest region. It should be noted that the vertical length of elements that belongs to one of the regions of dam cross section are equal. However; there might be slight difference between vertical heights of elements belonging to different regions of dam cross section. The method utilized for the determination of the number of vertical elements at the lower part of the dam is given below. The reader should note that

notations in the equations are in accordance with the typical dam cross section given above (Figure 2.4).

$$L_{Base} = (H_1 + H_2) * m_1 + L_c + (H_1 * m_2) + (H_2 * m_3) \quad (2.1)$$

$$L_{Crest Bot.} = H_2 * (m_1 + m_3) + L_c \quad (2.2)$$

$$No\ of\ Vertical\ Elem_{Lower\ Part} = \left[\frac{H_1}{\left(\frac{L_{Base} + L_{Crest\ Bot.}}{2 * No\ of\ Horizontal\ Elem.} \right)} \right] \quad (2.3)$$

The number of elements at the crest region is determined by utilizing the ratio of the height of the crest region part to the height of the part under the crest region. The equation utilized for the determination of the number of elements at the crest region is given below.

$$No\ of\ Vertical\ Elem_{Crest\ Region} = \left[\frac{H_2}{H_1} * No\ of\ Vertical\ Elem_{Lower\ Part} \right] \quad (2.4)$$

2.2.4 Dynamic Response Parameters

The parameters for the evaluation of dynamic response of the dam-reservoir-foundation rock system are specified under the dynamic response parameters section of EAGD ModPro. The dynamic response parameters section includes the earthquake ground motion data (in g), selection of the ground motion component that will be taken into consideration in computations (horizontal and/or vertical), the exponent utilized in Fast Fourier Transformation (FFT) algorithm of EAGD-84, time interval of the earthquake ground motion data (in seconds) and wave reflection coefficient representing the effect of reservoir bottom materials. The dynamic response parameters section is shown in Figure 2.5.

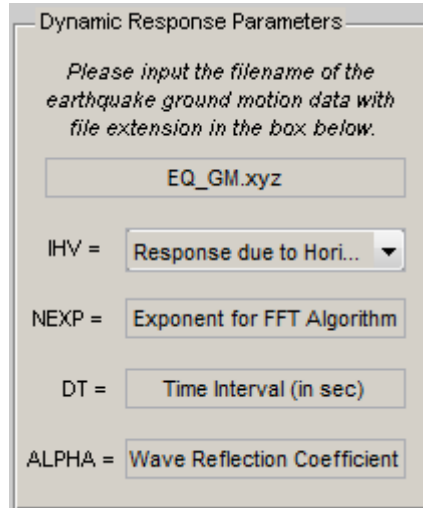


Figure 2.5 A screen capture of dynamic response parameters section from GUI of EAGD ModPro

The format of the earthquake ground motion data depends directly on the direction of ground motion considered. If the dynamic response due to only horizontal or only vertical component of the ground motion is computed the ground motion data must consist of one column. If the dynamic response due to both horizontal and vertical components of ground motion will be computed the ground motion data must consist of two columns in one ground motion data file. The first column must include the horizontal component of the ground motion data and the second column must include the vertical component of the ground motion data. It should be noted that both columns must be the same in length, thereby requiring zero padding for the shorter data. Time interval for both horizontal and vertical components of the ground motion must also be same.

The selection of the time interval of earthquake ground motion data and the exponent utilized in the FFT algorithm of EAGD-84 is directly related with the accuracy of the analysis results. The other response parameters involved in the computation of the frequency response functions and dynamic response of dam-reservoir-foundation rock system with the use of the Fast Fourier Transform algorithm are selected in this selection. The equations for the determination of the other response parameters utilized in the computations are summarized below. In these equations time interval of earthquake ground motion and the exponent utilized in the Fast Fourier Transform algorithm are denoted by DT and NEXP respectively.

$$\begin{array}{l} \text{Number of excitation frequencies /} \\ \text{Number of time intervals:} \end{array} \quad N = 2^{NEXP} \quad (2.5)$$

$$\text{Duration of response history:} \quad T = N * DT \quad (2.6)$$

$$\text{Frequency increment:} \quad \Delta f = \frac{1}{2T} \quad (2.7)$$

$$\text{Maximum frequency represented:} \quad F = N * \Delta f \quad (2.8)$$

The following conditions must be satisfied with the selection of the DT and NEXP values for the reliability of the analysis results (Fenves and Chopra, 1984):

i-The maximum excitation frequency must be greater than the frequencies of the considerable harmonics resulting from the earthquake ground motion data. Therefore it is suggested that the maximum excitation frequency must be greater than 25 Hz. In order to satisfy this condition DT value must be selected less than or equal to 0.02 seconds. EAGD ModPro enforces this condition while entering DT value with the help of a pop-up notification window opened on the graphical user interface.

ii-The maximum vibration frequency must be greater than the frequency of the highest vibration mode taken into account in the analysis. The analysis is conducted by considering ten generalized coordinates since the foundation rock flexibility is included. At the end of each analysis EAGD ModPro prints the maximum excitation frequency and the frequency of the highest vibration mode in a text file named as Natural Vibration Frequencies.txt, which can be used to ensure the satisfaction of the above criterion.

iii-The number of excitation frequencies must be greater than the number of ground accelerations read from the earthquake ground motion data. This condition must be fulfilled by the selection of NEXP value. EAGD ModPro ensures the fulfillment of this condition with the help of a pop-up notification window.

The frequency increment must be small enough to compute the frequency response functions accurately. Moreover the aliasing error resulting from the FFT algorithm must be minimized. In order to fulfill these requirements the maximum excitation frequency must satisfy the following criterion. EAGD ModPro prints whether the criterion below is satisfied or not into the text file stated above. One must also check the fulfillment of the requirements with the help of this text file.

$$DT * 2^{NEXP} \geq \frac{1}{f_1} \max \left\{ 25, \frac{1.5}{\eta_s} \right\} \quad (2.9)$$

EAGD ModPro utilizes compliance data stored in fort.80 file in order to determine the dynamic stiffness matrix for the flexible foundation rock. The dynamic stiffness matrix of the foundation rock is computed up to a certain maximum excitation frequency (Equation 2.10). Therefore the maximum excitation frequency must be less than the limit excitation frequency which the dynamic stiffness matrix is defined. The fulfillment of this requirement depends on the satisfaction of the following criterion. EAGD ModPro secures meeting this criterion with the help of its graphical user interface.

$$F \leq \frac{5}{2} \sqrt{\frac{G_f / \rho_f}{\pi b}} \quad (2.10)$$

It should be noted that G_f is the elastic shear modulus of the foundation rock (in k/ft²), ρ_f is the density of the foundation rock (in k.sec²/ft⁴) and b is the distance between the nodal points at the base of dam cross section (in ft) for the criterion stated above.

EAGD-84 considers the presence of reservoir-sediment interaction during the computation of the frequency response functions. The interaction between the sediment and reservoir is taken into account by the wave reflection coefficient defined under dynamic response parameters section. The reservoir bottom materials have an absorbing effect due to a one dimensional damper like response during earthquake motions. The wave reflection coefficient is simply as the ratio of the unabsorbed hydrodynamic pressure waves reflected from the reservoir bottom. The wave reflection coefficient is recommended as 0.9 to 1.0 for new dams, whereas it might be selected as 0.75 or 0.90 for the analysis of older dams (Fenves and Chopra, 1986). It should be noted that usage of higher values of wave reflection coefficient is a more conservative approach. Therefore; in the case of the absence of reliable data, it is recommended to utilize higher values the for wave reflection coefficient.

2.2.5 Analysis Output Parameters

The analysis output parameters section allows the selection of the time intervals to print analysis results. The number of time intervals selected to print the analysis output has a significant effect on the post-processing time of the raw analysis results. Moreover, the size of raw output file depends on the number of time intervals. The previous experiences show that printing the analysis output at every five time intervals is an appropriate way for manageable data size. It should also be kept in mind that usage of too long time intervals endanger the accuracy of the analysis outputs.

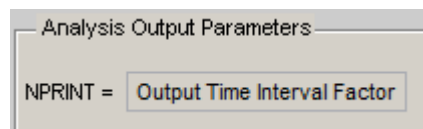


Figure 2.6 A screen capture of analysis output parameters section from GUI of EAGD ModPro

2.2.6 Analysis Execution Parameters

The analysis execution parameters section controls the type of the analyses i.e. whether the effects of static loads such as dam weight and hydrostatic pressure are included and the assumption made for two dimensional finite element analysis (plane stress or strain). The dialogue box for this section is shown in Figure 2.7.

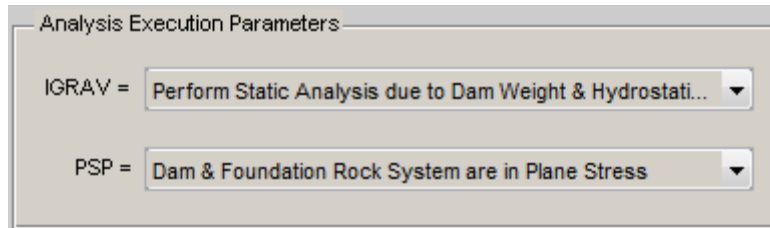


Figure 2.7 A screen capture of analysis execution parameters section from GUI of EAGD ModPro

The effects of static loads on the dynamic response might be considered or ignored depending on the user's selection. The combination of the dynamic response with the response due to static loads such as dam weight or hydrostatic pressure represents the actual behavior of the dam-reservoir-foundation rock system. Printing only the dynamic response option, on the other hand, gives the opportunity to investigate the absolute effect of the strong ground motion on dam-reservoir-foundation rock system behavior.

The selection between plane stress and plane strain assumptions depends on the construction methodology of the dam under investigation. If the keyed contraction joints (or no transverse joints) are utilized during the construction, the monoliths of the dam may be assumed to be behaving as a single unit under the strong ground motion. The use of plane strain assumption is appropriate for this case. When the dam is designed with vertical contraction joints, the monoliths of the dam may vibrate independently under the strong ground motion. The plane stress assumption should be used for the representation of dams designed with vertical contraction joints. It should be noted that plane stress and plane strain assumptions are valid for gravity dams which are located in wide valleys. Three dimensional analyses are required for gravity dams which are located in narrow valleys and arch dams.

2.2.7 Structural Performance Check Parameters

EAGD ModPro is capable of performing the structural performance check and damage criteria assessment of the dam analyzed according to BK Guidelines. The structural

performance check parameters section stores the parameters necessary for the structural performance check and damage assessment. The cumulative inelastic duration limit (in seconds) and the demand capacity ratio limit for the elements experiencing nonlinear behavior is entered in this section (Figure 2.8). The execution of EAGD-84 is independent from these parameters, even the raw analysis results data could be obtained without entering any input at this section. However, it is essential to enter the parameters to operate EAGD ModPro and to obtain the post-processed analysis results.

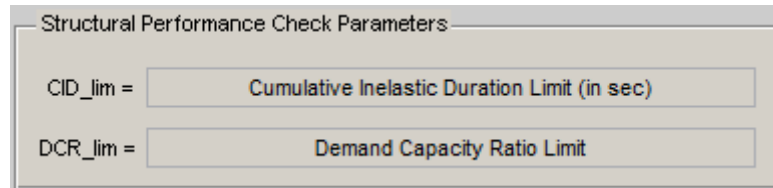


Figure 2.8 A screen capture of structural performance check parameters section from GUI of EAGD ModPro

2.3 Analysis Results and Post-Processing of Raw Output Data

The procedure of the obtaining post-processed analysis results could be summarized by the following four steps: i-the input variables, ii-execution of EAGD-84, iii-selection of the appropriate output to be obtained after post-processing of raw analysis iv- execution of EAGD ModPro to conduct post-processing operations. In EAGD ModPro the execution of EAGD-84 and the post-processing operations are conducted separately due to the fact that post-processing operations consumes a considerable amount of time. In this way it is intended to gain the opportunity of controlling the raw data results before conducting lengthy post-processing operations. As it could be seen from Figure 2.9, the execution of EAGD-84 and obtaining the post-processed analysis results are controlled by different push buttons labeled as “Run EAGD-84” and “Obtain Analysis Results”.



Figure 2.9 Screen captures of the push buttons that control execution of EAGD-84 and post-processing operations from GUI of EAGD ModPro

The results that will be produced at the end of the execution of EAGD ModPro are selected by the output options for analysis results section which could be seen in Figure 2.10. Since the output file obtained at the end of the analysis conducted by EAGD-84 is impractical for the professional purposes, EAGD ModPro produces post-processed results which are user friendly and suitable for the professional purposes.

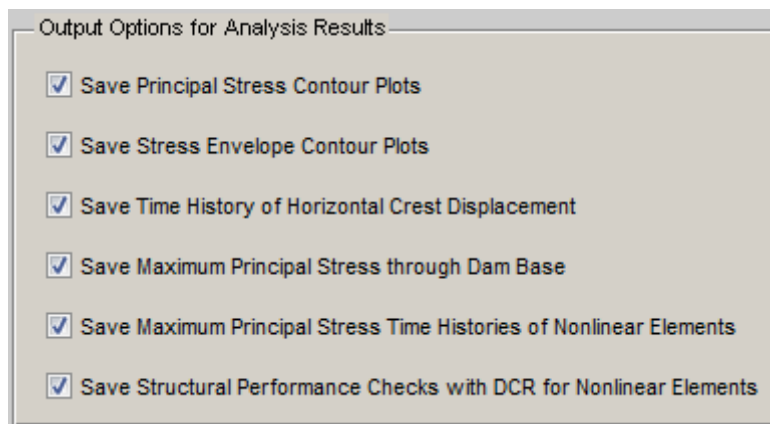


Figure 2.10 A screen capture of output options for analysis results section from GUI of EAGD ModPro

EAGD ModPro produce contour plots for principal stresses and stress envelopes, time history of horizontal crest displacement and maximum principal stress through dam base. It should be noted that EAGD ModPro defines tensile stresses as positive. Therefore; the term "maximum" for stress labels the highest tensile stress (or the smallest compressive stress). In addition EAGD ModPro is also capable of conducting the structural performance check and damage criteria assessment of the dam analyzed according to BK Guidelines.

The structural performance check and damage criteria assessment of the dam is conducted in accordance with the methodology described in the design guideline published by Concrete Dams Committee of DSÍ (2012). The methodology described in the design guideline is similar to the design and assessment approach recommended by US Army Corps of Engineers (USACE, 2003). The sufficiency of the linear time history analysis in deciding dam safety is conducted by EAGD ModPro by using this methodology. The structural performance check and assessment of the damage is constituted on the demand capacity ratio and cumulative inelastic stress duration terms. Demand capacity ratio (DCR) represents the ratio of the tensile stress to the tensile strength of the concrete. In other words, nonlinear behavior is expected to initiate when the demand capacity ratio exceeds one. The cumulative duration of the stress levels above the tensile

strength of concrete is taken as a measure of the damage estimation. As a damage indicator the advantage of the cumulative inelastic stress duration over the classic number of stress cycles approach is that it considers both magnitude and duration of the inelastic stresses. For gravity dams, the acceptable limits for demand capacity ratio and cumulative inelastic duration are 2 and 0.4 seconds respectively. As it is demonstrated in Figure 2.12, cumulative inelastic duration limit decreases linearly and reaches to zero when demand capacity ratio is equal to 2. The validity of the assessment with linear time history analysis is determined by the cumulative inelastic duration curve for permitted demand capacity ratio range (Figure 2.11). If the cumulative inelastic duration curve falls below this performance limit curve, the expected performance of the dam is considered as acceptable. Otherwise, nonlinear time history analysis is required for a more precise damage assessment as the results from elastic analysis indicate the occurrence of visible/significant damage, which may or may not jeopardize dam safety. In addition to the demand capacity ratio and cumulative inelastic duration limits, the cracked cross sectional area should also be limited for the sufficiency of the assessment with linear time history analysis. If the ratio of the cracked area to the cross section of the dam exceeds 15 percent nonlinear time history analysis is required (Ghanaat, 2004). This methodology is implemented in EAGD ModPro for accurate and fast assessment of dam safety.

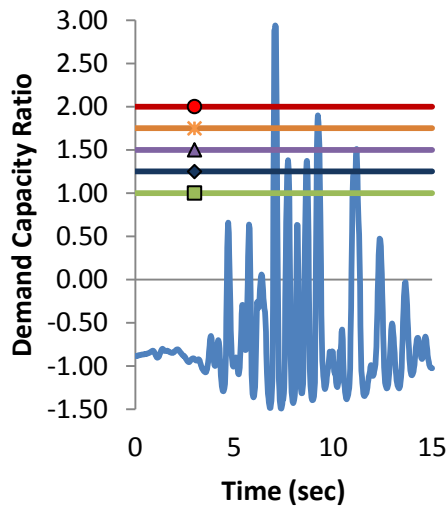


Figure 2.11 Computation of the cumulative inelastic durations for acceptable DCR levels

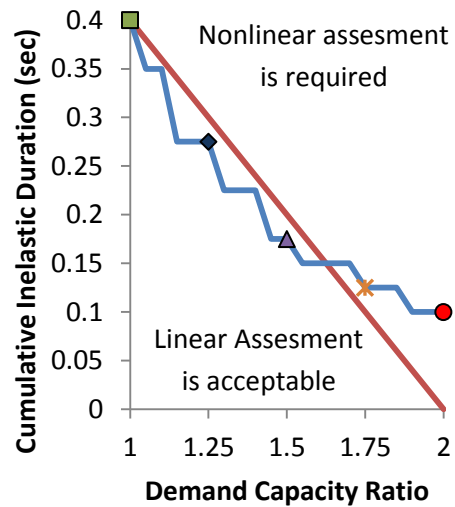


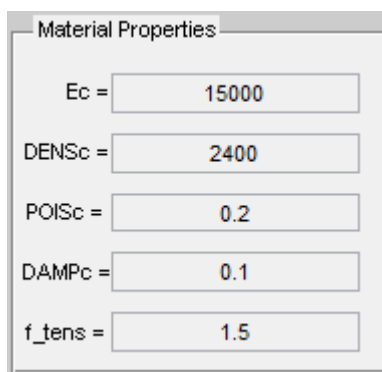
Figure 2.12 Structural performance check and damage criteria assesment curve

2.4 A Dam Analysis Example Conducted with EAGD ModPro

The characteristics and capabilities of EAGD ModPro are discussed in detail in the previous sections. In order to better demonstrate the use of EAGD ModPro a dam analysis example is presented in this section.

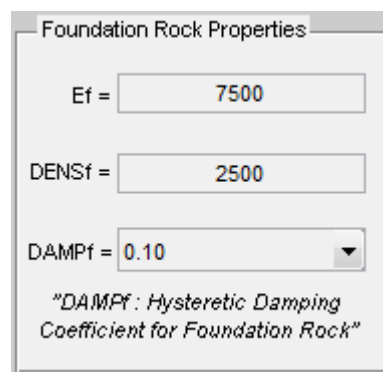
2.4.1 Modeling

The parameters for the dam material and foundation rock properties section are input as shown in Figure 2.13 and Figure 2.14.



Property	Value
Ec	15000
DENS c	2400
POIS c	0.2
DAMP c	0.1
f_tens	1.5

Figure 2.13 Input data entered under material properties section



Property	Value
Ef	7500
DENS f	2500
DAMP f	0.10

"DAMP f: Hysteretic Damping Coefficient for Foundation Rock"

Figure 2.14 Input data entered under foundation rock properties section

The geometric dimensions of the dam are input following the self explanatory notation given in Figure 2.15. As it stated previously, the finite element mesh is generated automatically by EAGD ModPro without needing any interaction with the user. The number of finite elements used at the dam base is selected as 25 in this version and it depends on the compliance data file (fort.80) utilized for the analysis.

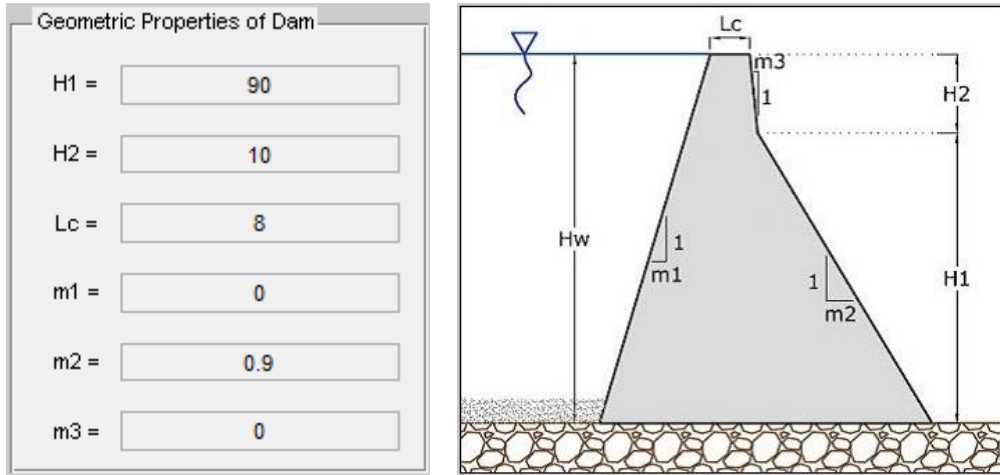


Figure 2.15 Input data entered under geometric properties of dam section and the typical dam cross section

After the input of material properties and dam geometry, ground motion data is loaded as shown in Figure 2.16. Only the horizontal component of the ground motion is taken into consideration in this demonstration. As it is recommended for the case of the absence of reliable reservoir bottom information, the wave reflection coefficient is entered as 0.9. The remaining dynamic response parameters are entered in accordance with the limitations of EAGD-84 which are discussed previously. The data entered under dynamic response parameters section is shown in Figure 2.17.

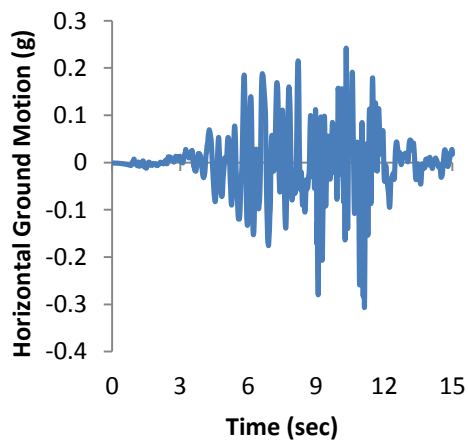


Figure 2.16 Horizontal earthquake ground motion utilized for dam analysis example

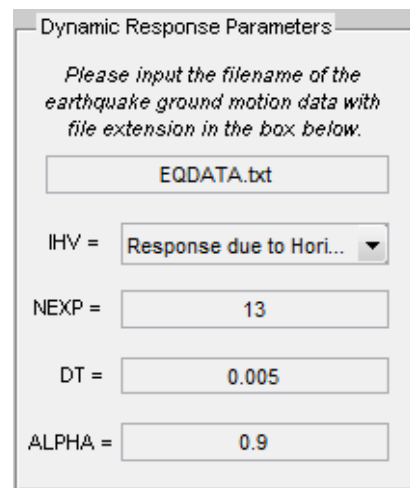


Figure 2.17 Input data entered under dynamic response parameters section

For this dam analysis example, the number of time intervals to print the analysis output is selected as five to obtain an output file with a manageable data size (Figure 2.18). As it could be seen from Figure 2.17 time interval of the earthquake ground motion data is 0.005 seconds; hence EAGD-84 will print the analysis result for every 0.025 seconds. The selected number of time intervals to print the analysis output is recommended for the acceptable time consumption during post processing operations.

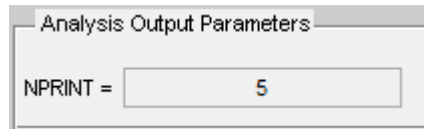


Figure 2.18 Input data entered under analysis output parameters section

The effects of static loads such as dam weight and hydrostatic pressure are included in the analysis results. The finite element analysis is conducted with the plane stress assumption. The selected analysis execution options are shown in Figure 2.19.

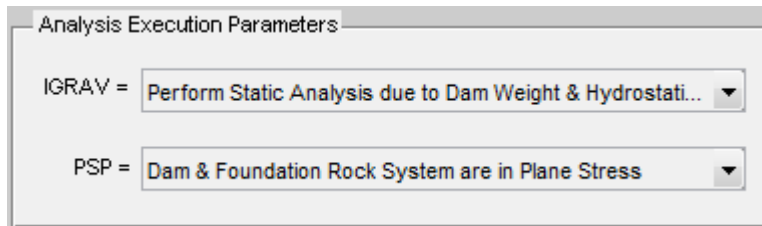


Figure 2.19 Selected analysis execution options under analysis execution parameters section

The dam analysis example includes the structural performance check and damage criteria assessment of the dam. The structural performance check and damage assessment parameters are selected in accordance with the recommendations for gravity dam assessment (BK Guidelines, 2012). The cumulative inelastic duration limit is selected as 0.40 seconds and demand capacity ratio limit is selected as 2 (Figure 2.20). Tensile strength of the dam concrete is taken as 1.5 MPa for this dam analysis example (Figure 2.13)

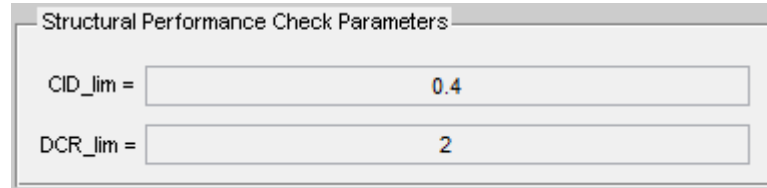


Figure 2.20 Input data entered under structural performance check parameters section

Execution of EAGD ModPro is conducted by clicking the push button labeled as “Run EAGD-84” (Figure 2.9). The post processed analysis results and outputs produced by EAGD ModPro will be discussed in the following section.

2.4.2 Results

The raw data for the analysis results of the dam analysis example are stored in an output file produced by the execution of EAGD ModPro, which post processes the results stored on the output file and produces results which are in a suitable graphical format. EAGD ModPro allows user to select the type of output for post processing operations. In order to familiarize with the all output from EAGD ModPro, all the available output options are selected for the dam analysis example (Figure 2.21).

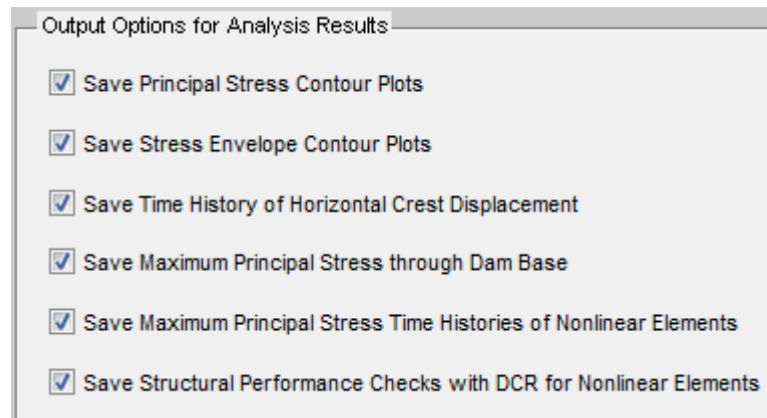


Figure 2.21 Selected output options for the dam analysis example

EAGD ModPro produces outputs to give information about the utilized finite element model for every conducted analysis. The details of the finite element model are printed to a text file in order to better understand the numbering of the finite elements and ele-

ment nodes. The text file which gives the details of the finite element meshing properties is shown at Figure 2.22. In addition to printing the details of the finite element meshing properties in a text file, the finite element mesh and node/element numbering of the dam cross section is also illustrated with as in Figure 2.23.

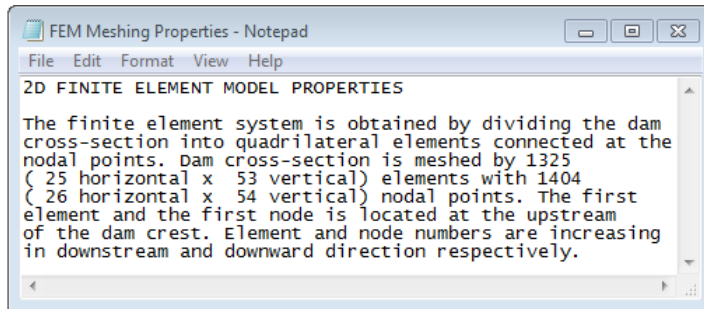


Figure 2.22 A screen capture from the text file which includes the details of the finite element meshing properties

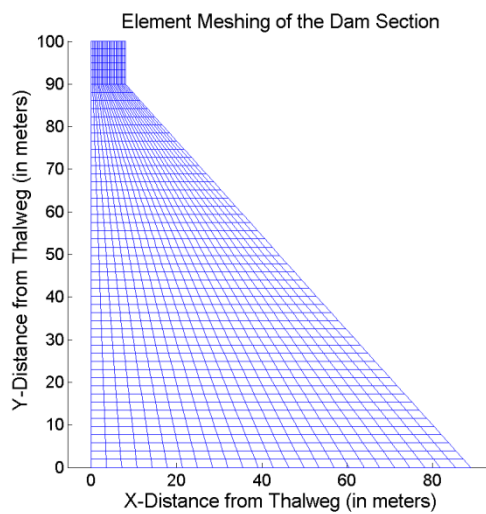


Figure 2.23 The finite element meshing of the dam cross section

The natural vibration frequencies of the first ten vibration modes are printed for the dam on an elastic foundation with empty reservoir case. As discussed in the dynamic response parameters section, earthquake ground motion time interval (DT) and selected exponent for the FFT algorithm (NEXP) must satisfy certain conditions in order to en-

sure the accuracy of the dynamic analysis conducted. The verification of DT and NEXP values are also included in the text file. The user must control the verification of DT and NEXP values before utilizing the analysis results obtained from EAGD ModPro. The text file which includes natural vibration frequencies and verification of DT and NEXP values for the dam analysis example is shown in Figure 2.24.

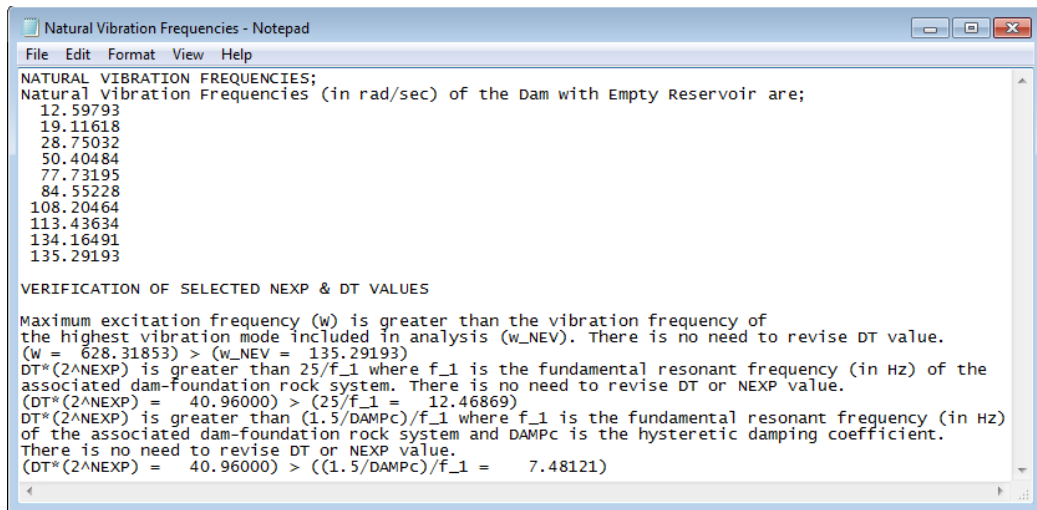


Figure 2.24 A screen capture from the text file which includes natural vibration frequencies and verification of selected NEXP and DT values

After post processing operations all the tiff files containing the finite element meshing, contour plots, crest displacement history, maximum principal stress through dam base and structural performance check plots are stored in a folder named as “Analysis Results” which is created in the same directory with EAGD ModPro. The maximum and minimum principal stress contour plots produced by EAGD ModPro are shown in Figure 2.25 and Figure 2.26. In order to examine the stress level of elements easily, EAGD ModPro plots the finite element meshing of the dam cross section on the contour plots. In addition to principal stress contour plots, the contour plots which illustrate the axial and shear stress envelopes of the elements are also produced (Figure 2.27 to Figure 2.32). All of the contour plots include color bars at the right hand side in order to demonstrate the magnitude of the stress levels of elements.

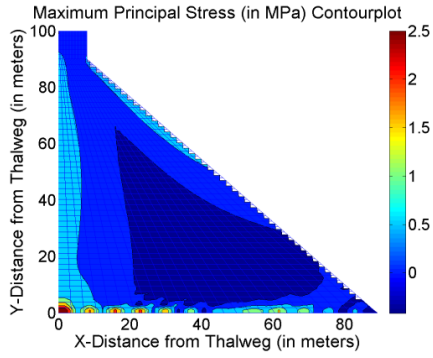


Figure 2.25 Maximum principal stress contour plot

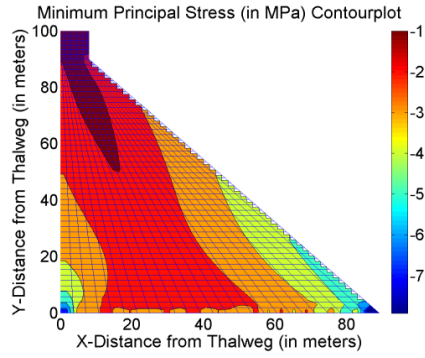


Figure 2.26 Minimum principal stress contour plot

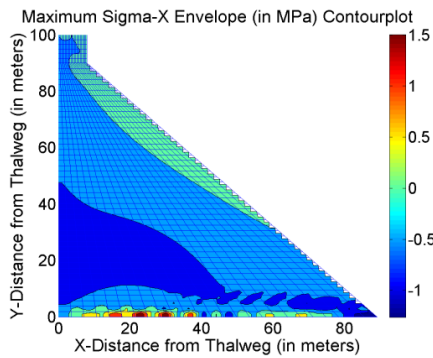


Figure 2.27 Maximum sigma-x envelope contour plot

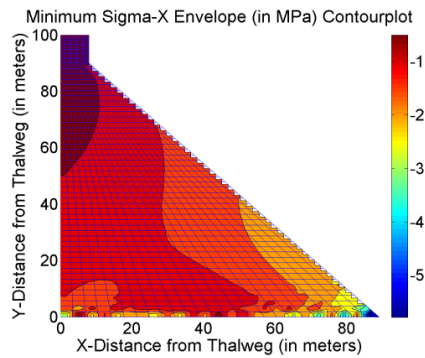


Figure 2.28 Minimum sigma-x envelope contour plot

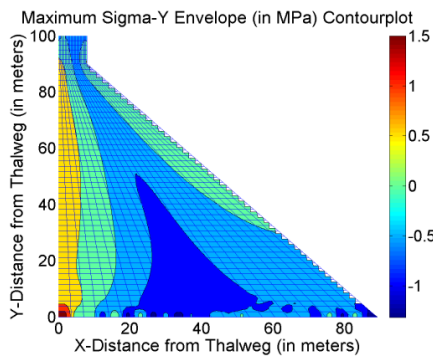


Figure 2.29 Maximum sigma-y envelope contour plot

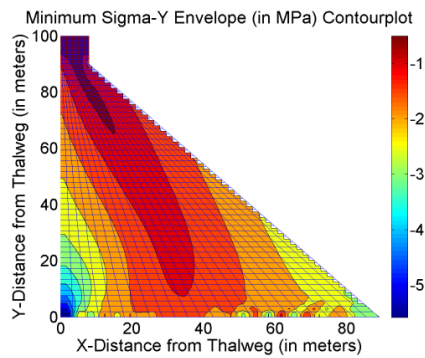


Figure 2.30 Minimum sigma-y envelope contour plot

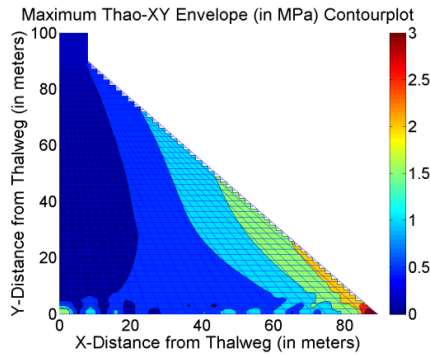


Figure 2.31 Maximum thao-xy envelope contour plot

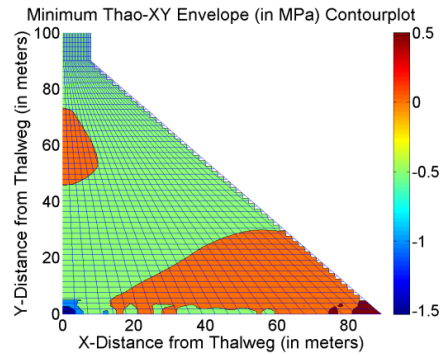


Figure 2.32 Minimum thao-xy envelope contour plot

In addition to the stress contour plots, time history of the horizontal crest displacement and maximum principal stress through dam base are also produced and stored as image files. Time history of the horizontal displacement displays the maximum upstream and downstream displacements of the crest. The maximum principal stress envelope through dam base provides information on the resulting stresses experienced at the dam foundation. Time history of the horizontal crest displacement and maximum principal stress through dam base are shown in Figure 2.33 and Figure 2.34.

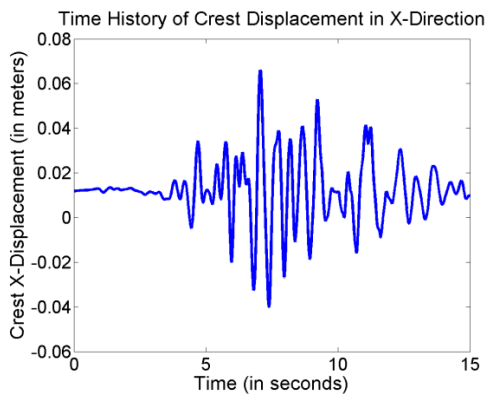


Figure 2.33 Time history of horizontal crest displacement

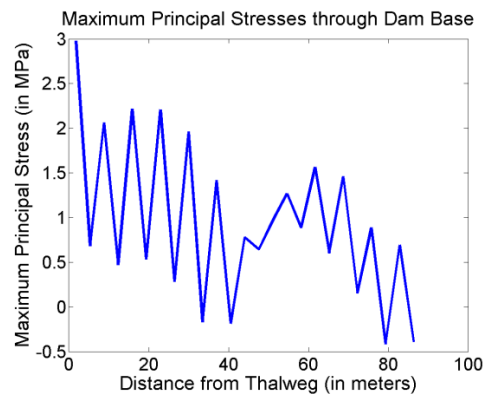


Figure 2.34 Maximum principal stress through dam base

The structural performance check and damage criteria assessment is also conducted as a part the dam analysis example. EAGD ModPro produces and stores the results of structural performance check and damage assessment as tiff files. As a result of the

structural performance check and damage assessment time history of the maximum principal stress and cumulative inelastic duration curves are produced for each element which experiences nonlinear behavior. Sufficiency of the assessment with linear time history analysis is verified with these outputs. At the end of the dam analysis seven elements exceeded the tensile strength of the concrete for the example under consideration. The most critical damage generally appears at the thalweg region of the dam, whose results are shown in Figure 2.35 and Figure 2.36.

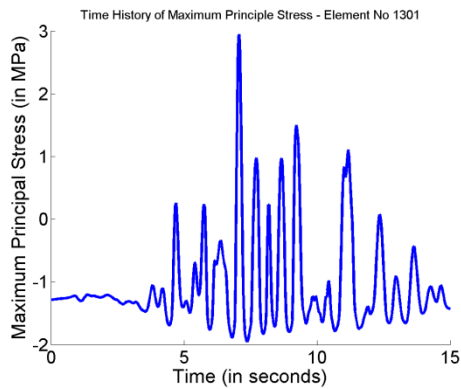


Figure 2.35 Maximum principal stress time history of the thalweg element

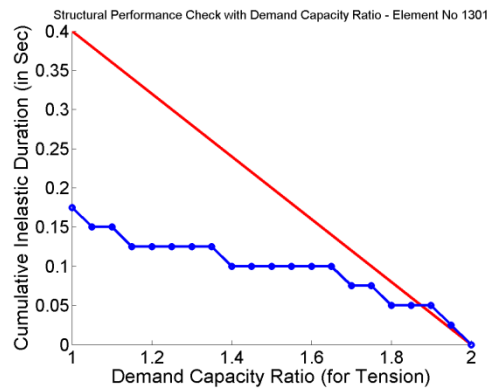


Figure 2.36 Cumulative inelastic duration curve of the thalweg element

At the end of every analysis EAGD ModPro displays a message window which shows the ratio of the cracked cross sectional area to the dam cross section. For the sufficiency of the structural performance check and damage criteria assessment user should also be careful about whether the cracked area ratio exceeds the 15 percent limit or not. The message window which is displayed at the end of the dam analysis example is given in Figure 2.37.



Figure 2.37 Message window which shows the ratio of the cracked area to the dam cross section

CHAPTER 3

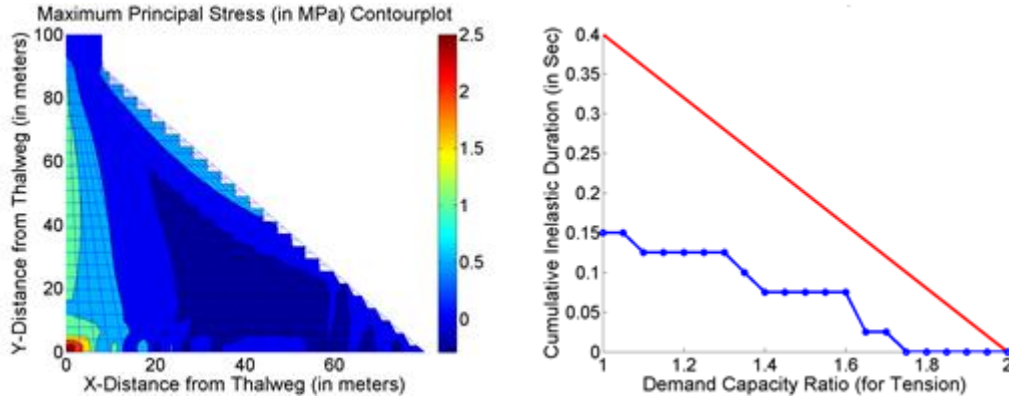
VULNERABILITY OF CONCRETE GRAVITY DAMS

Parametric studies performed to better understand the parameters affecting the seismic response of concrete gravity dams are presented in this chapter. A deterministic sensitivity analysis was also conducted to display the most influential parameters. Afterwards, fragility curves for gravity dams with typical sections were determined by using the linear elastic procedures of seismic analysis and damage assessment.

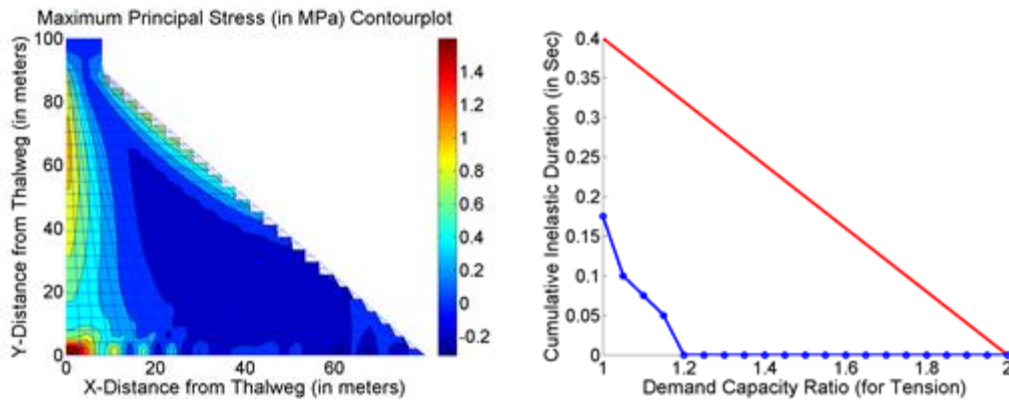
3.1 Parametric Studies

This section presents the results of the analyses conducted to investigate the effects of the material and dam geometry parameters on the performance of typical dam monoliths. In order to examine the effects of these parameters the optimum of the cross sections which provide an acceptable seismic performance is determined for dams with various properties. The cross sectional area minimization which reduces the cost is considered as the objective of the optimization in this study. Therefore the cross section which provides a satisfactory assessment result with the minimum cross sectional downstream slope is referred as the optimum dam cross section. For this purpose numerous analyses were conducted for dams with various heights and properties. The conducted analyses focus on the examination of effects of the variation of cross sectional downstream slope and ratio of elastic modulus of dam concrete to elastic modulus of foundation rock (E_c/E_f).

A specific ratio of elastic modulus of dam concrete to elastic modulus of foundation rock could be obtained by various values of elastic moduli of dam concrete and foundation rock. Although all other parameters are kept same the selection of these values varies the obtained principal stresses and performance curves (Figure 3.1). This variation is resulting from the dominance of the effect of variation of the elastic modulus of foundation rock on the seismic analysis results (see Chapter 3.2). However; the utilization of E_c/E_f ratio aims to investigate the effect of stiffening and softening of the foundation rock on a specific dam case. For this purpose a specific value is selected for the elastic modulus of dam concrete and elastic modulus of foundation rock values are determined with the help of this value in the conducted analyses.



a) $E_c/E_f = 15000 \text{ MPa}/7500 \text{ MPa}$



b) $E_c/E_f = 10000 \text{ MPa}/5000 \text{ MPa}$

Figure 3.1 Maximum principal stress contourplots and structural performance curves of dams with the same E_c/E_f ratio (with different values of elastic moduli)

The parametric study was conducted for five dam heights with five cross sectional downstream slope alternatives. Four ratios of elastic modulus of dam concrete to elastic modulus of foundation rock were also included in the analyses. The values of dam height, downstream slope and ratio of elastic modulus of dam concrete to elastic modulus of foundation rock alternatives are shown in Table 3.1. In order to better distinguish the effects of varying parameters on the seismic performance all other analysis parameters are kept constant in the analyses. The constant values of the dam concrete and foundation rock properties employed in the course of the analyses are given in Table 3.2. The wave reflection coefficient utilized in the analyses is selected as 0.9 as shown in Table 3.2.

Table 3.1 Values of the parameters utilized in parametric study

Parameters	Values
Dam Height (in meters)	50, 75, 100, 125, 150
Downstream Slope ($m_{D/S} H : 1.0 V$)	0.60, 0.70, 0.80, 0.90, 1.00
E_c/E_f	0.10, 0.50, 1.00, 2.00

Akkar (2010) conducted a site specific seismic hazard analysis for the Melen Dam location and proposed a spectrum with a 2% probability of being exceeded in 50 years, i.e. 2475 years of return period (Figure 3.2). Then a synthetic ground motion was fitted to the deaggregated spectrum (Figure 3.2). Only the horizontal component of the ground motion data was proposed in that study.

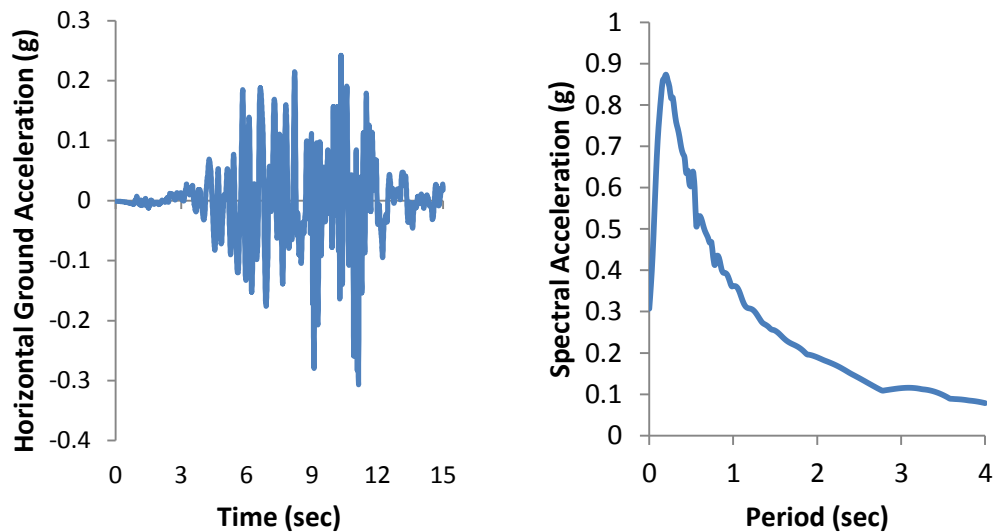


Figure 3.2 Acceleration time history and acceleration response spectrum of the proposed synthetic ground motion

Table 3.2 Values of the dam concrete properties and foundation rock properties utilized in parametric study

Properties	Values
Elastic Modulus of Dam Concrete (in MPa)	15000
Density of Dam Concrete (in kg/m ³)	2400
Poisson's Ratio for Dam Concrete (ν_s)	0.20
Static Tensile Strength of Dam Concrete (in MPa)	1.50
Density of Foundation Rock (in kg/m ³)	2500
Poisson's Ratio for Foundation Rock (ν_f)	0.33
Hysteretic Damping Coefficient (η)	0.10
Wave Reflection Coefficient (α)	0.90

The plane stress assumption is utilized for the conducted analyses. Influences of the static loads such as dam weight and hydrostatic pressure are included in the analyses results. The analyses are conducted with the full reservoir assumption which represents the most critical situation. Foundation rock flexibility is taken into account with the generated dynamic stiffness matrices for flexible foundation rock. The compliance data which is stored in a file named as fort.80 is utilized for the determination of the dynamic stiffness matrix of the flexible foundation. The same compliance data file is utilized for all analyses. Since the foundation flexibility is taken into account, the analyses are conducted by considering ten generalized coordinates (Fenves and Chopra, 1984).

The parametric study includes the analyses of numerous dams with different heights and downstream slopes. The upstream faces of all dams are taken as vertical. The downstream of the crest region of all dams are also considered as vertical as well (Figure 3.3). The cross sectional width of the dam crest is taken constant as eight meters for each section. The cross section length of the crest region is determined by the division of the crest width to the downstream slopes of dams. The finite element meshing of the dam cross section is produced by 4-node quadrilateral finite elements. The number of finite elements utilized for the meshing of the dam cross section is taken constant for all analyses. The restriction of the number of finite elements aims to ease the comparison of the analyses results of dams with different geometric properties and prevent possible discrepancies resulting from inconsistent finite element meshing. The dam cross section is divided into 25 elements in horizontal direction. In vertical direction dam section is divided into a total of 25 elements. The crest region is divided into two elements and the length below the crest region is divided into 23 elements. All of the dam alternatives are analyzed with a finite element model with 625 elements. The typical finite element meshing of the dam cross section is given in Figure 3.3.

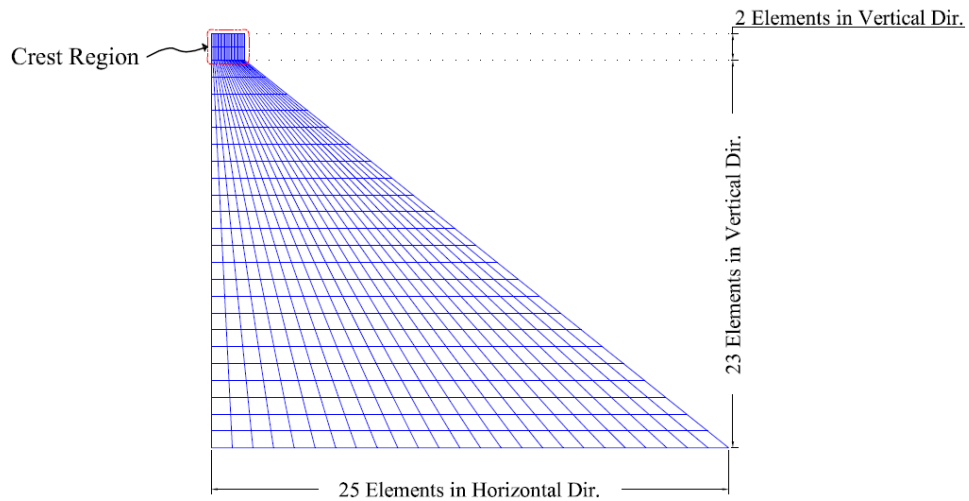


Figure 3.3 Typical dam meshing utilized in the parametric study

The accuracy of the stress distribution obtained with a finite element model containing 625 elements was verified by conducting analyses with different number of elements. These analyses were conducted by considering static forces such as dead weight and hydrostatic pressures and rigid foundation assumption. A typical dam section with a height of 100 meters and a downstream slope of 0.80 was considered. All other analysis parameters are taken same with the conducted parametric study. Finite element analyses with 625 elements, 2500 elements and 5625 elements were conducted. Maximum principal tensile stress distributions through the dam base obtained by using these finite element models are compared (Figure 3.4). Although the obtained tensile stresses vary for the first finite element at the thalweg, the stress distributions obtained by finite element models with different number of elements are similar. It should be noted that mesh refinement at a corner can always produce erroneous stresses. Hence checking the stresses at some distance away from the corner provides some averaging and provides more reliable stress estimations. Results indicate the stress error at the center of the first base element for 625 elements has an error of about 19% compared to the stress at the same location in the model with 5625 elements. This error is deemed as acceptable for the purposes of this study.

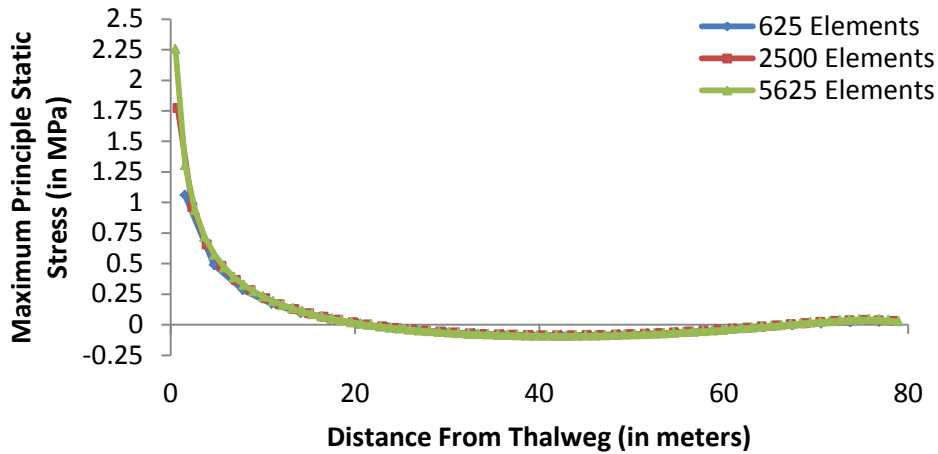


Figure 3.4 Maximum principal stresses through dam base obtained by different finite element models

The area under the performance limit curve and the region of the structural performance curve exceeding the performance limit curve (named hereafter as the Exceeded Area) is computed for all dam alternatives of the parametric study. Computation of the Exceeded Area is shown schematically in Figure 3.5. The magnitude of this area can be thought as a measure of inelastic action expected. Analysis results for the exceeded area as a function of downstream slope for different E_c/E_f ratios and dam heights are shown in Figure 3.6.

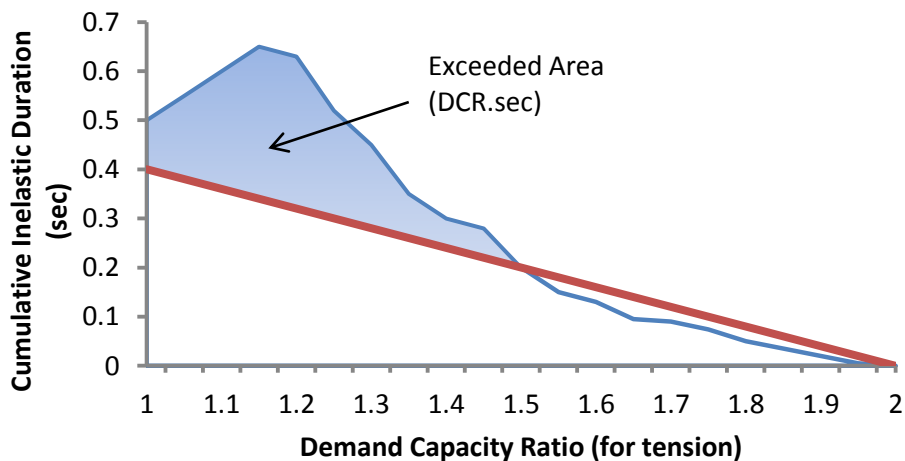


Figure 3.5 Schematic illustration of the exceeded area

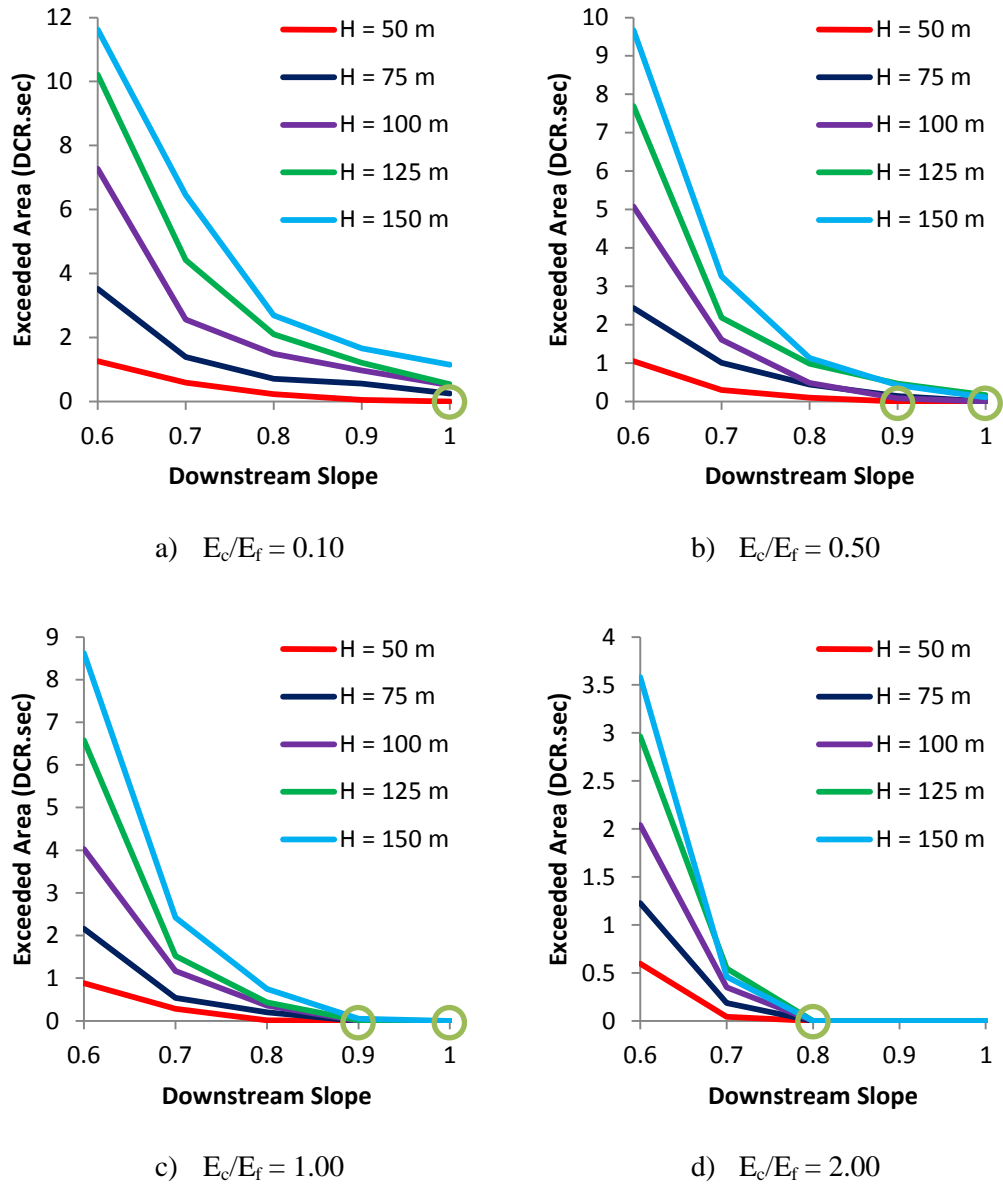


Figure 3.6 The parametric study results for the thalweg elements of analyzed dams

The parametric study results clearly show that the increase of the ratio of elastic modulus of dam concrete to elastic modulus of foundation rock decreases the stress levels of the dam. The consideration of E_c/E_f results in more economical designs with smaller downstream slopes. When the ratio of elastic modulus of dam concrete to elastic modulus of foundation rock is 0.10 only the dam section which has 50 meters of height with a downstream slope of 1.0 satisfies the design criterion. When the ratio of elastic modulus of dam concrete to elastic modulus of foundation rock is increased to 0.50 the dam with a height of 50 meters and a downstream slope of 0.90 appeared as the optimum cross

section alternative. Dams with heights of 75 and 100 meters and the highest considered downstream slope also exhibit acceptable seismic performance. When the ratio of elastic modulus of dam concrete to elastic modulus of foundation rock is increased to 1.0 the dams which have 50, 75 and 100 meters of height and a downstream slope of 0.90 satisfy the design criterion. Seismic performance of dams with heights of 125 and 150 and the highest considered downstream slope are also satisfactory. When the ratio of elastic modulus of dam concrete to elastic modulus of foundation rock is 2.0 the seismic performance of all dams with a downstream slope of 0.80 are found as acceptable. These observations underline the importance of taking the foundation rock flexibility into consideration in the analyses. Softening of the foundation rock significantly decreases the seismic stress demands which results in more economical designs. However when the flexibility of the foundation rock is taken into account the bearing capacity of the foundation rock must always be taken into consideration, which is excluded in this study. The results of the parametric study show that the stress levels increase with the increase of the dam height. This is an expected result since the hydrodynamic pressures and effects of the higher modes increases with the increase of dam height and reservoir depth.

The effects of the material and dam geometry parameters on the maximum horizontal crest displacement (relative to the dam base) response which is an indicator of the seismic performance are also investigated. Similar to the exceeded areas, the maximum horizontal crest displacements are plotted as a function of downstream slope for different E_c/E_f values (Figure 3.7). The results show that the maximum horizontal crest displacements increase with the increase of the dam height. On the other hand as the cross sectional downstream slope increases the obtained maximum horizontal crest displacements decrease. The increase of the maximum crest displacement could be explained by the increase of the slenderness of the dam cross section. Interestingly a significant variation of the maximum crest displacements could not be observed with the change of E_c/E_f ratio. Although it might be expected that the total horizontal crest displacements increase with the increase of the flexibility of foundation rock, relative horizontal crest displacements with respect to the dam base are not affected by changes in E_c/E_f . It should be reminded that these results may not be generalized for every possible ground motion.

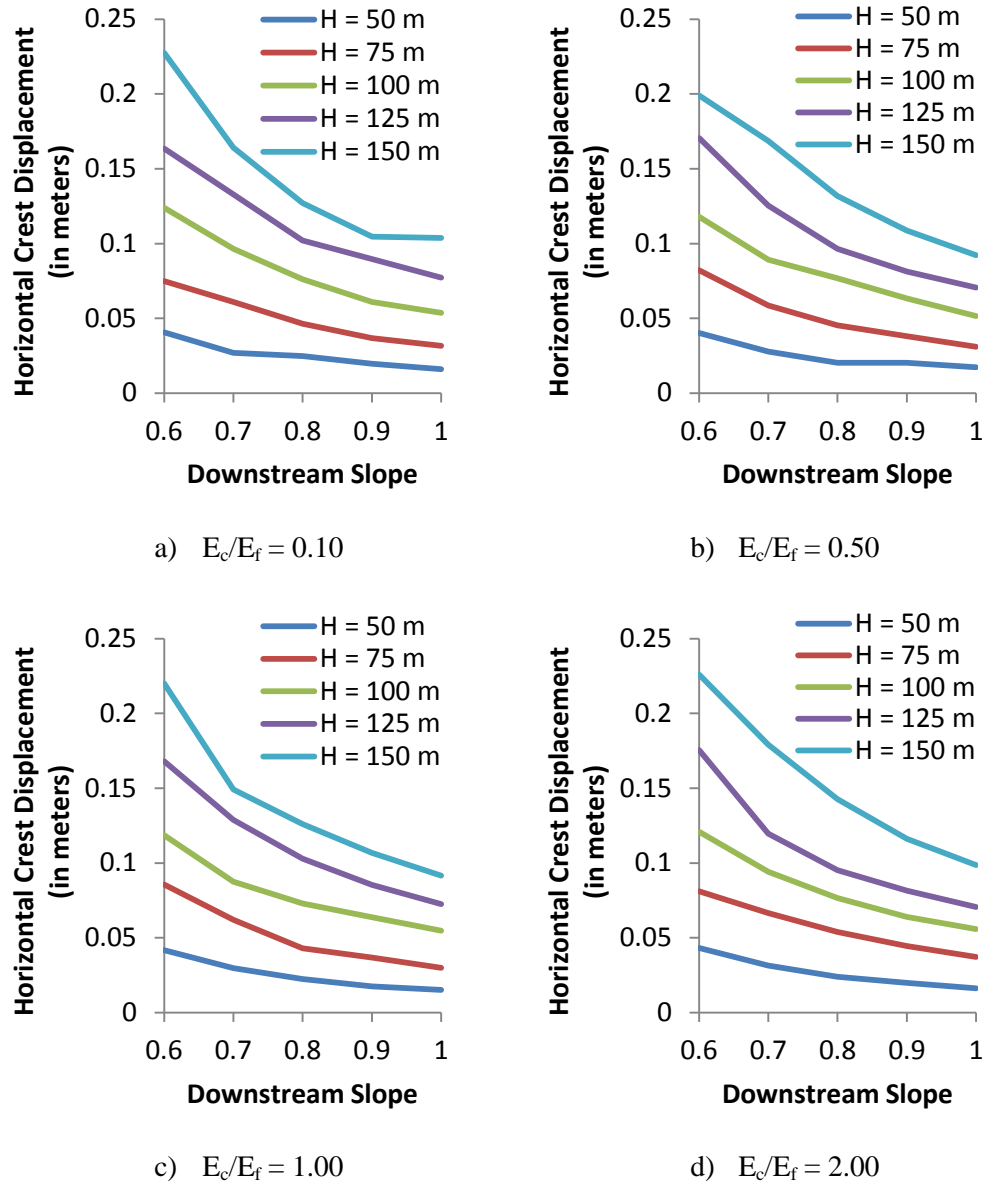


Figure 3.7 Maximum horizontal crest displacements

It should be noted that all of these observations are valid only for gravity dams with specific properties. Since the analyses are conducted with the plane stress assumption, the parametric study results may not reflect the dams located in narrow valleys. However; the conducted parametric study gives notable indications about the effects of parameter selections on the behavior of the wide gravity dams.

3.2 Deterministic Sensitivity Analysis (Tornado Diagrams)

Deterministic sensitivity analysis which is conducted for the investigation of the effects of the random variables on the seismic response of a gravity dam is introduced in this section. Tornado diagram method is utilized for the illustration of the effect of each parameter independently. Tornado diagram arrays the investigated parameters with a descending order in which the most influencing parameter at the top and the least influencing one at the bottom. In order to obtain the tornado diagram, parameters to be considered are determined and several analyses are conducted by changing only one parameter at each case. When investigating the effect of a parameter a maximum and a minimum value are considered as upper and lower boundaries. Other parameters are taken in their median values in order to highlight the effect of the investigated parameter. The difference of the results obtained for upper and lower boundaries of a parameter is defined as swing. The length of swing indicates the effect of the random variable by demonstrating the variability of the results. Tornado diagram is obtained by the arrangement of the swings of each parameter in a descending order in which the largest swing is located at the top. The production of the tornado diagram is shown in Figure 3.8.

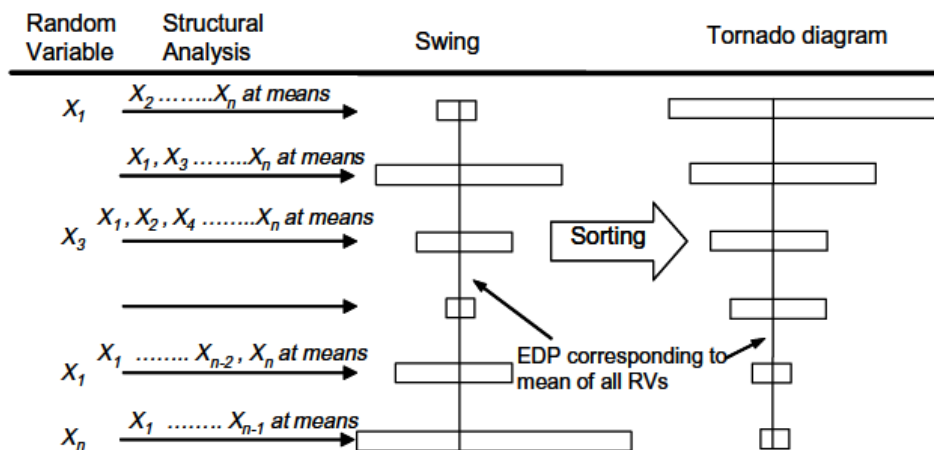


Figure 3.8 Tornado diagram production process (Binici and Mosalam, 2007)

The influence of random variables are investigated by considering three engineering demand parameters which are maximum principal tensile stress, maximum crest displacement and the maximum value of the cumulative inelastic duration obtained by the assessment with linear elastic analysis.

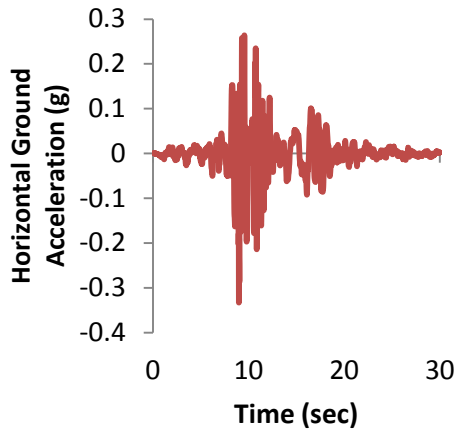
The following parameters are selected as random variables to be investigated:

- Elastic modulus of dam concrete (E_c)
- Elastic modulus of foundation rock (E_f)
- Hysteretic damping coefficient for dam concrete (η_c)
- Hysteretic damping coefficient for foundation rock (η_f)
- Ground motion data type (EQ Type)
- Wave reflection coefficient (α)

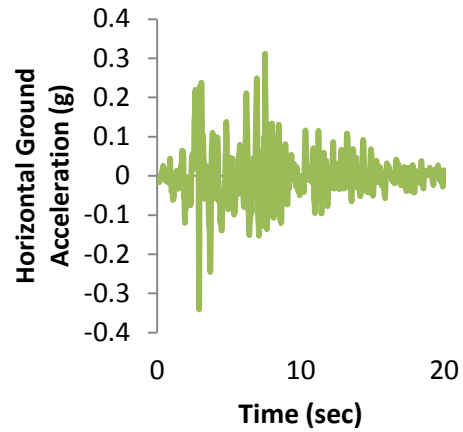
Median, maximum and minimum values of the investigated parameters are given in Table 3.3. The upper and lower boundaries and the variation of the parameters are selected by considering a realistic representation of the extreme values appeared in real life cases. A site specific seismic hazard analysis for the Melen Dam location was conducted and a spectrum with a 2% probability of being exceeded in 50 years i.e. 2475 years of return period was proposed by Akkar in 2010. Three synthetic ground motions which were fitted to the deaggregated spectrum were utilized as median, minimum and maximum ground motions in the conducted deterministic sensitivity analysis. Only the horizontal components of the ground motions are taken into consideration. Time histories and acceleration spectra of the ground motions are given in Figure 3.9.

Table 3.3 Input parameters utilized in deterministic sensitivity analysis

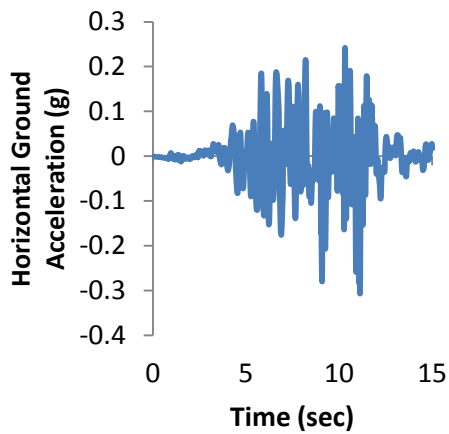
Parameters	Median	Minimum	Maximum
E_c (in MPa)	20000	15000	25000
E_f (in MPa)	20000	5000	35000
η_c	0.10	0.05	0.15
η_f	0.10	0.01	0.25
α	0.90	0.80	1.00



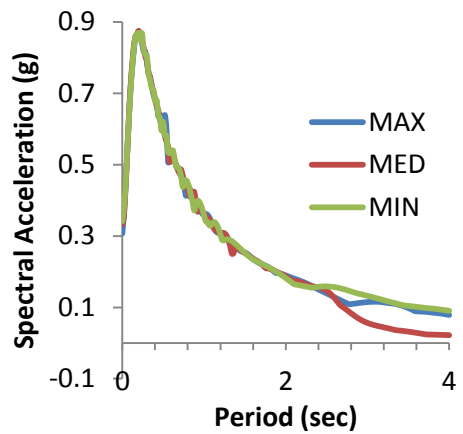
(a) Time history of the median ground motion



(b) Time history of the minimum ground motion



(c) Time history of the maximum ground motion



(d) Acceleration response spectra of the ground motions

Figure 3.9 Acceleration time histories and elastic response spectra of the proposed synthetic ground motions

The other analysis parameters which affect the seismic response are kept constant in all analyses. The properties of the dam concrete and foundation rock which are kept constant during the analyses are given in Table 3.4. The assumptions utilized in analyses are same with the assumptions made for the analyses conducted for parametric studies. The plane stress assumption is utilized. Influences of the static loads are taken into account. Full reservoir case is considered. Foundation rock flexibility is taken into consideration with the same approach. Geometric idealizations and meshing properties of the finite element model also identical with the ones employed in parametric studies.

Table 3.4 Values of the dam concrete properties and foundation rock properties utilized in deterministic sensitivity analysis

Properties	Values
Dam Height (in meters)	100
Downstream Slope ($m_{D/S} H : 1.0 V$)	1.00
Density of Dam Concrete (in kg/m^3)	2400
Poisson's Ratio for Dam Concrete (ν_s)	0.20
Static Tensile Strength of Dam Concrete (in MPa)	1.50
Density of Foundation Rock (in kg/m^3)	2500
Poisson's Ratio for Foundation Rock (ν_f)	0.33

The median results obtained from the analysis of the median model are given Table 3.5. The engineering demand parameters obtained by the median model were utilized for the normalization of the results of conducted analyses. The analysis results are normalized to 1 by dividing to the median model results. The normalized analyses results indicate the ratio of variation, which is defined as swing, by the change of control parameter. The tornado diagrams were obtained by the arrangement of the calculated swings.

Table 3.5 Median model results for engineering demand parameters

Demand Parameters	Median Results
Maximum Principal Tensile Stress (in MPa)	2.715
Maximum Crest Displacement (in meters)	0.0405
Maximum Cumulative Inelastic Duration (in sec)	0.225

The results for maximum principal tensile stresses, maximum crest displacements and maximum cumulative inelastic durations are given in Table 3.6 to Table 3.8. As it could be seen from the results the increase of the ratio of elastic modulus of dam concrete to elastic modulus of foundation rock increases the observed tensile stresses and inelastic durations. This observation is parallel to the results of the parametric studies. The increase of damping and reservoir bottom absorptions eases the responses as it is expected.

Table 3.6 Maximum principal tensile stress results (in MPa)

Parameters	Minimum Stress (in MPa)	Maximum Stress (in MPa)
Elastic Modulus of Dam Concrete (E_c)	3.128	2.343
Elastic Modulus of Foundation Rock (E_f)	0.372	2.920
Hysteretic Damping Coefficient for Dam Concrete (η_c)	2.874	2.562
Hysteretic Damping Coefficient for Foundation Rock (η_f)	3.152	2.100
Ground Motion Data Type (EQ Type)	2.435	2.792
Wave Reflection Coefficient (α)	2.650	2.775

The increase of elastic modulus of foundation rock decreased the observed maximum crest displacement. This could be explained by the decrease of rigid body motion as a result of the stiffening of the foundation rock. The stiffening of the dam body decreased the obtained maximum crest displacement as it is expected.

Table 3.7 Maximum crest displacement results (in meters)

Parameters	Minimum Crest Displacement (in meters)	Maximum Crest Displacement (in meters)
Elastic Modulus of Dam Concrete (E_c)	0.0547	0.0323
Elastic Modulus of Foundation Rock (E_f)	0.0479	0.0380
Hysteretic Damping Coefficient for Dam Concrete (η_c)	0.0417	0.0393
Hysteretic Damping Coefficient for Foundation Rock (η_f)	0.0433	0.0365
Ground Motion Data Type (EQ Type)	0.0375	0.0408
Wave Reflection Coefficient (α)	0.0400	0.0407

Table 3.8 Maximum cumulative inelastic duration results (in sec)

Parameters	Minimum Cumulative Inelastic Duration (in sec)	Maximum Cumulative Inelastic Duration (in sec)
Elastic Modulus of Dam Concrete (E_c)	0.25	0.1
Elastic Modulus of Foundation Rock (E_f)	0	0.7
Hysteretic Damping Coefficient for Dam Concrete (η_c)	0.25	0.175
Hysteretic Damping Coefficient for Foundation Rock (η_f)	0.3	0.1
Ground Motion Data Type (EQ Type)	0.1875	0.225
Wave Reflection Coefficient (α)	0.175	0.25

Tornado diagrams obtained by the arrangement of the swings of random variables are given in Figure 3.10 to Figure 3.12. The elastic modulus of foundation rock appears to be the most influencing parameter for the maximum principal tensile stress and maximum cumulative inelastic duration. The second most influential parameter for these responses is the hysteretic damping coefficient of the foundation. The minimum value selected for the foundation rock damping is considerably low. Therefore such a significant effect resulting from the lower bound of hysteretic foundation rock damping is pronounceable. The selection of such a value is a result of the restrictions due to available compliance data and EAGD-84. It is observed that the elastic moduli of dam concrete and foundation rock are most and second most important parameters that affect the maximum crest displacement. Ground motion type, hysteretic damping of the dam concrete and reservoir bottom absorption ratio are found as the least influencing parameters. The obtained tornado diagrams demonstrate that the foundation rock properties such as elastic modulus of foundation rock and hysteretic damping coefficient of foundation rock have a significant influence on the engineering demand parameters. Therefore an extensive care is required for the accurate determination of these parameters. It highlights the importance of rigorous site investigations, surveys and in-situ testing which are essential for the correct estimation of the geological and geotechnical properties of the dam site.

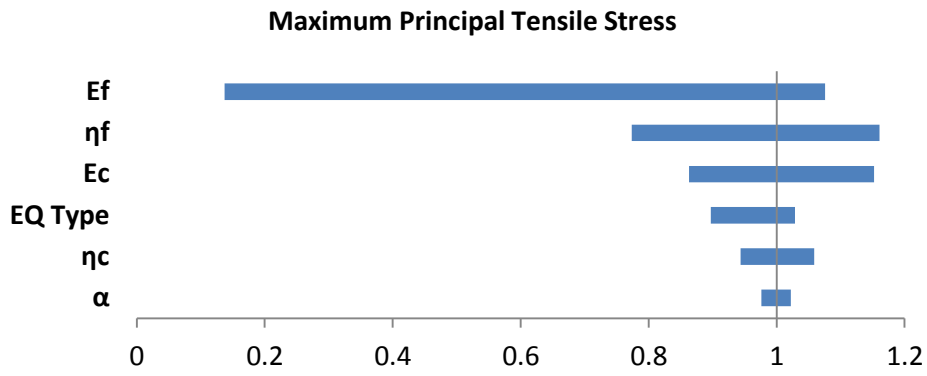


Figure 3.10 Tornado diagram for maximum principal tensile stress

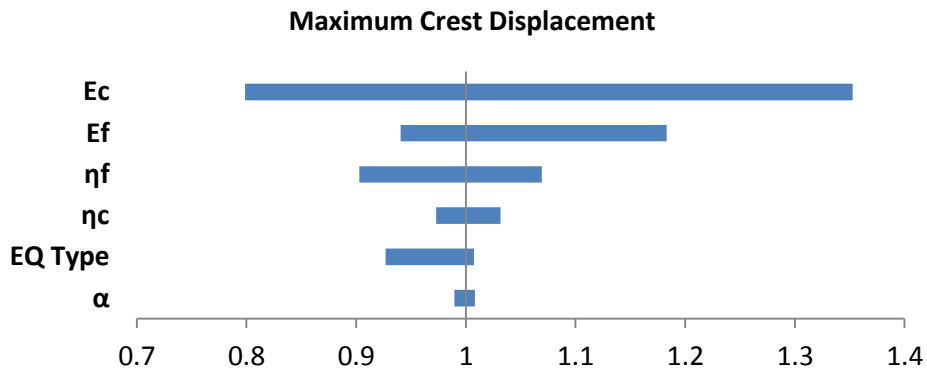


Figure 3.11 Tornado diagram for maximum crest displacement

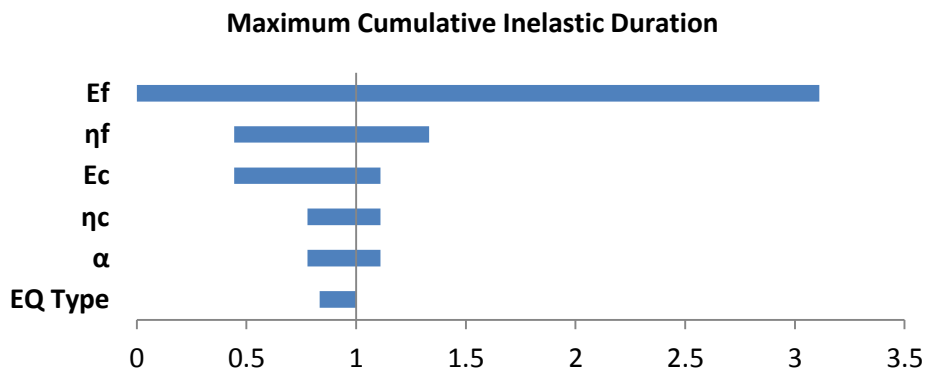


Figure 3.12 Tornado diagram for maximum cumulative inelastic duration

3.3 Fragility Curves

This section aims to assess the structural performance of the gravity dams with a probabilistic approach. For this purpose fragility curves of various dam alternatives are determined. Since it is intended to produce a reference for both the preliminary design phase of the new dams and the investigation of the structural reliability of existing dams a wide range of dam alternatives are assessed. It should be reminded that the term fragility in the context used herein refers to the possibility of having visible damage as a result of significantly exceeding the linear response limits. In other words, fragility is not meant to denote a probability of collapse for the purposes of this study.

Fragility analysis aims to evaluate the structural performance in probabilistic terms. Fragility could be summarized as the conditional probability of failure of the structure. The probabilistic structural performance evaluation and damage assessment of a structure is conducted with the determination of the fragility curves. Fragility curves exhibit the probability of the exceeding a structural limit state as a function of the engineering demand parameter. In this study, the sufficiency of the linear time history analysis for the structural performance check and damage criteria assessment is taken as the limit state for the dam which is subjected to strong ground motion. The methodology presented in the design guideline published by Concrete Dams Committee of DSİ (2012) is taken as the basis for the damage criteria assessment. The details of the methodology and the determination of the sufficiency of the linear time history analysis for the damage assessment and structural performance check are discussed previously. The spectral acceleration at the fundamental mode of the dam is the engineering demand parameter of the determined fragility curves.

Determination of the seismic fragility curve of a dam section requires the consideration of the performances under a set of ground motions. The necessity of the consideration of a set of ground motions is a direct result of the probabilistic approach of fragility analysis. Determination of the acceleration response spectra of the considered ground motions is the first step of the determination of the fragility curves. The acceleration response spectra of ground motions were obtained by a computer program named as Utility Software for Data Processing developed by Akkar et al. (personal communication, 2011). The fundamental period of the dam with the full reservoir case is determined next. For this purpose the dam with a full reservoir was subjected to a unit impulse which has a magnitude of 1 m/s^2 . Effects of the static loads were excluded in the analysis. Fast Fourier transformation of the horizontal crest displacement history of the analyzed dam was performed and displacement results were obtained in the angular frequency domain. Obtained displacement results are in a discrete form, thereby crest acceleration response in the angular frequency domains was obtained by Equation 3.1. The fundamental angular frequency of the dam was determined by the investigation of the frequency which corresponds to the first peak of the acceleration response. The fundamental angular frequency is transformed to fundamental period by Equation 3.2.

$$\ddot{u} = \omega^2 u \quad (3.1)$$

$$T = \frac{2\pi}{\omega} \quad (3.2)$$

In Equation 3.1 and Equation 3.2 angular frequency, period, displacement response and acceleration response in frequency domain are represented by ω , T , u and \ddot{u} respectively.

The spectral acceleration demands for the fundamental period of the dam with a full reservoir were determined from the obtained acceleration response spectra of the earthquake set. Seismic fragility curve of a dam basically demonstrates the probabilities of observing unacceptable damage for a scale of spectral acceleration demand. For this purpose dynamic analyses of a dam under a set of scaled ground motions must be conducted. Scaling of the ground motion aims to obtain a spectral acceleration value which is equal to the spectral acceleration demand at the fundamental period of the dam with a full reservoir. Since performance evaluation of the dam is conducted by linear elastic analysis, the scaling of the ground motion could be achieved by simply scaling the response analysis results of the dam. Therefore, dynamic analyses of the dam under the set of considered ground motions were conducted only once and the principal stress time histories were scaled for the specific spectral acceleration demand. The factor utilized for the scaling of the response results was obtained by the division of the spectral acceleration demand to the spectral acceleration for the fundamental period of a dam with a full reservoir. Fragility analysis was conducted for a scale of spectral accelerations which starts with zero and ends with 3.0 g. Spectral acceleration demands were increased with an increment of 0.1 g. The initial fragility curve of the dam was obtained by conducting a set of assessments for all spectral acceleration demands and determining the probabilities of observing visible damage.

The initial fragility curve obtained for the considered scale of spectral acceleration demands was in a scatter data form. In order to determine a smooth fragility curve which is suitable to cover all possible spectral acceleration demand values an exponential function of spectral accelerations was fitted to determined fragility data. The selected exponential function is:

$$f(S_a) = 1 - e^{-\left(\frac{S_a}{a}\right)^b} \quad (3.3)$$

where S_a is the spectral acceleration demand and a and b are the constants for the regulation of the form of fragility curve. The selection of an exponential function aims to represent the nature of the seismic fragility behavior of the concrete gravity dams. In order to minimize the error while fitting fragility curves to fragility data the least squares method is utilized for the determination of the values of constants a and b . The procedure of the determination of a fragility curve is summarized in Figure 3.13.

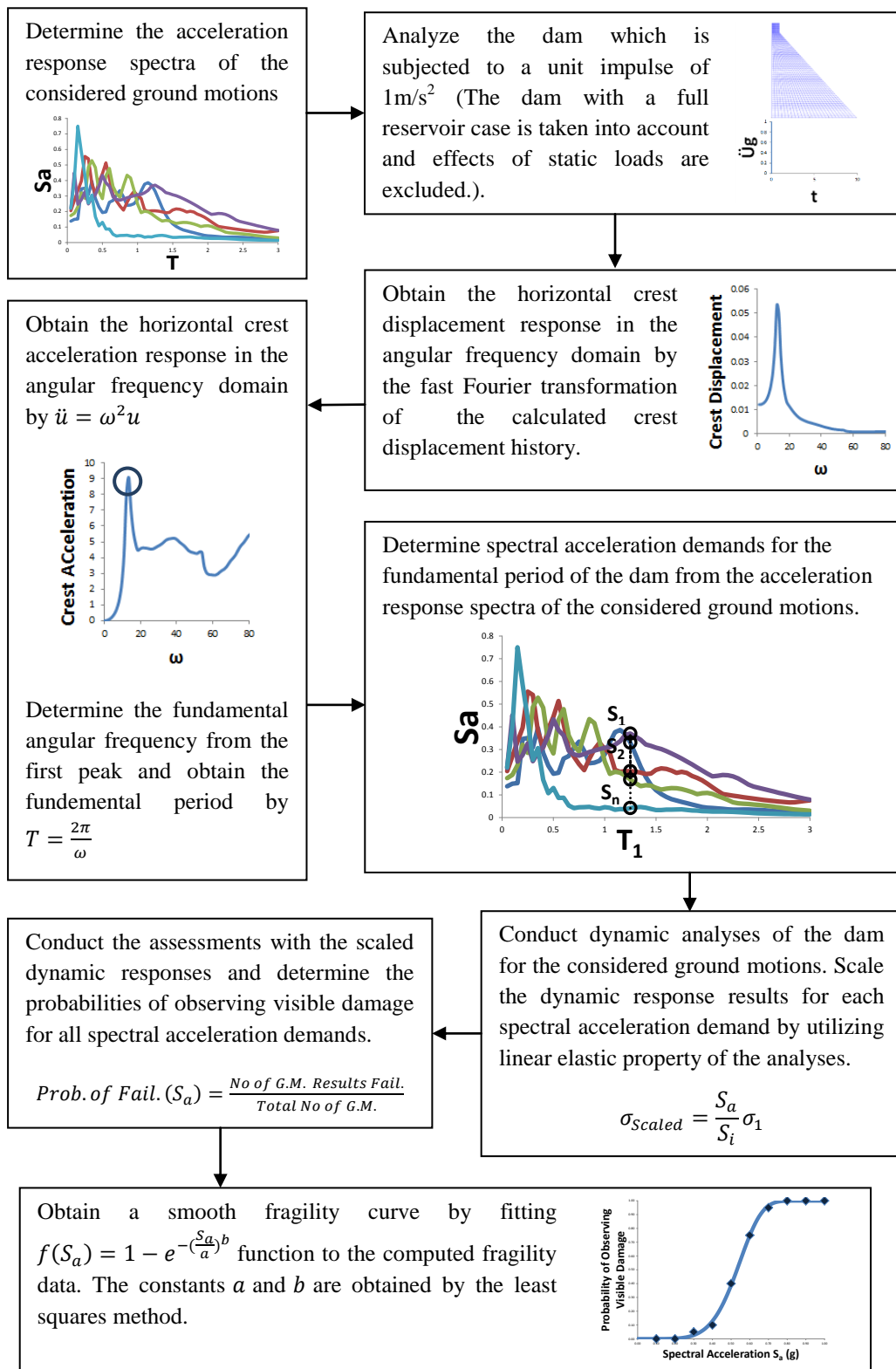


Figure 3.13 The procedure of the determination of a fragility curve

The determination of a set of fragility curves aims to produce a general reference for concrete gravity dams. For this reason fragility analyses were conducted for dams with various parameters. Five dam heights and three cross sectional downstream slopes alternatives were taken into consideration. Three ratios of elastic modulus of dam concrete to elastic modulus of foundation rock (E_c/E_f) and static tensile strength of dam concrete (f_{tens}) alternatives were included. In order to reflect the analysis with rigid foundation rock assumption one of the ratios of elastic modulus of dam concrete to elastic modulus of foundation rock was selected as 0.02. The purpose of production a general reference for both the preliminary design phase and the investigation of the structural reliability is taken as the basis for the selection of these parameters. The values of considered dam height, downstream slope, ratio of elastic modulus of dam concrete to elastic modulus of foundation rock and tensile strength of dam concrete alternatives are given in Table 3.9.

Table 3.9 Values of the parameters utilized in fragility analysis

Parameters	Values
Dam Height (in meters)	50, 75, 100, 125, 150
Downstream Slope ($m_{D/S} H : 1.0 V$)	0.70, 0.85, 1.00
E_c/E_f	0.02, 1.00, 2.00
f_{tens} (in MPa)	1.00, 1.50, 2.00

All other analysis parameters were kept constant in all analyses and these parameters are selected in accordance with the general properties of the existing gravity dams. Since the ratio of the elastic modulus of dam concrete to elastic modulus of foundation rock is a parameter in fragility analysis, the elastic modulus of foundation rock is computed from the assigned ratio and the selected elastic modulus of dam concrete. The elastic modulus of the dam concrete is kept constant at the conducted analyses. Same hysteretic damping coefficient is selected for both dam concrete and foundation rock. The values of the properties of dam concrete and foundation rock are given in Table 3.10. The wave reflection coefficient is selected as 0.9 as could be seen in Table 3.10.

Table 3.10 Values of the dam concrete properties and foundation rock properties utilized in fragility analysis

Properties	Values
Elastic Modulus of Dam Concrete (in MPa)	20000
Density of Dam Concrete (in kg/m ³)	2400
Poisson's Ratio for Dam Concrete (ν_s)	0.20
Density of Foundation Rock (in kg/m ³)	2500
Poisson's Ratio for Foundation Rock (ν_f)	0.33
Hysteretic Damping Coefficient (η)	0.10
Wave Reflection Coefficient (α)	0.90

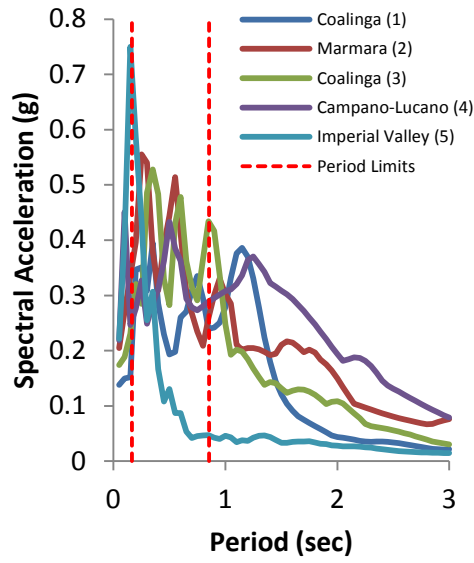
Fragility curves were determined by using two dimensional analyses conducted with plane stress assumption suitable for dam monoliths. The effects of the static loads which are dam weight and hydrostatic pressure were included. Full reservoir condition was taken into consideration. The effect of the foundation rock flexibility was included by the generation of dynamic stiffness matrix of flexible foundation. The dynamic stiffness matrix of the flexible foundation was determined with the compliance data stored in fort.80 file. The same compliance data was utilized for all analyses performed for the fragility curves. As a result of the consideration of the foundation rock flexibility ten generalized coordinates were taken into account at the conducted analyses (Fenves and Chopra, 1984). The results of the analyses were printed for every five ground motion time interval to conserve time and data space.

The cross sectional width of the crest region is kept constant as eight meters. Both the upstream faces and the downstream of the crest region of all dams are considered as vertical. The cross sectional lengths of the crest region is determined by the division of the constant crest width to the cross sectional downstream slopes. All dam cross sections are meshed with 4-node quadrilateral finite elements. The same number of finite elements is utilized for the meshing of the dam cross section in all analyses. The number of finite elements is restricted to prevent potential discrepancies resulting from inconsistent finite element meshing. Dam cross section is divided into 25 elements in both horizontal and vertical direction. The crest region is divided into two elements and the length below crest region is divided into 23 elements in vertical direction. A total of 625 elements are utilized for the meshing of the dam cross section. Geometric and finite element meshing properties of the dam cross sections are parallel with the properties of the sections utilized at the conducted parametric studies. Since the typical finite element meshing of dam cross section utilized for parametric study is already given in Figure 3.3 another figure is not given in this section.

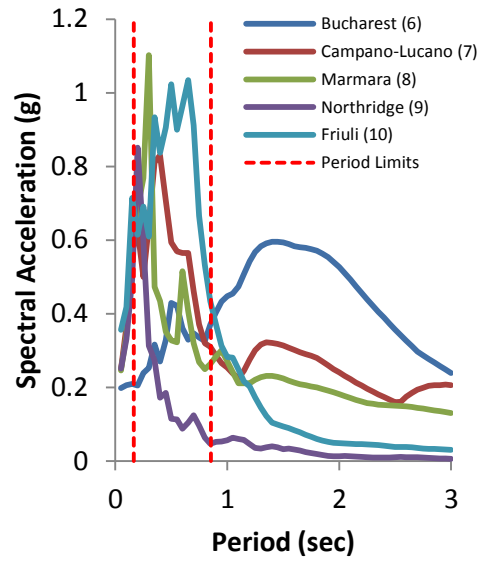
A set of earthquakes which includes data of 20 ground motions was utilized for the determination of the fragility curves of the dam alternatives. Since the number of earthquakes utilized in fragility analysis is greater than the previous studies only acceleration response spectra of ground motions and general information about the earthquakes are given (Figure 3.14, Table 3.11).

Table 3.11 General information about the ground motions utilized in fragility analysis

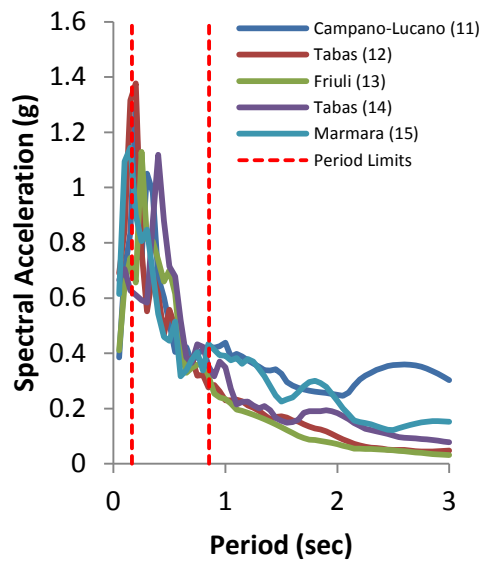
EQ No.	Name	Location	Date	Soil Type	Magnitude	PGA
1	Coalinga	USA	1983	Granite	6.5	0.136
2	Marmara	Turkey	1999	Rock	7.4	0.167
3	Coalinga	USA	1983	Granite	6.5	0.172
4	Campano-Lucano	Italy	1980	Rock	6.5	0.181
5	Imperial Valley	USA	1979	Granite	6.5	0.186
6	Bucharest	Romania	1977	Rock	6.4*	0.194
7	Campano-Lucano	Italy	1980	Rock	6.5	0.216
8	Marmara	Turkey	1999	Rock	7.4	0.227
9	Northridge	USA	1994	Rock	6.7	0.233
10	Friuli	Italy	1976	Rock	6.3	0.316
11	Campano-Lucano	Italy	1980	Rock	6.5	0.323
12	Tabas	Iran	1978	Rock	6.4*	0.338
13	Friuli	Italy	1976	Rock	6.3	0.357
14	Tabas	Iran	1978	Rock	6.4*	0.385
15	Marmara	Turkey	1999	Rock	7.4	0.407
16	Loma Prieta	USA	1989	Rock	7	0.435
17	Loma Prieta	USA	1989	Rock	7	0.442
18	North P. Springs	USA	1986	USGS (A)	6.2	0.492
19	North P. Springs	USA	1986	USGS (A)	6.2	0.612
20	Morgan Hill	USA	1984	Rock	6.1	0.711



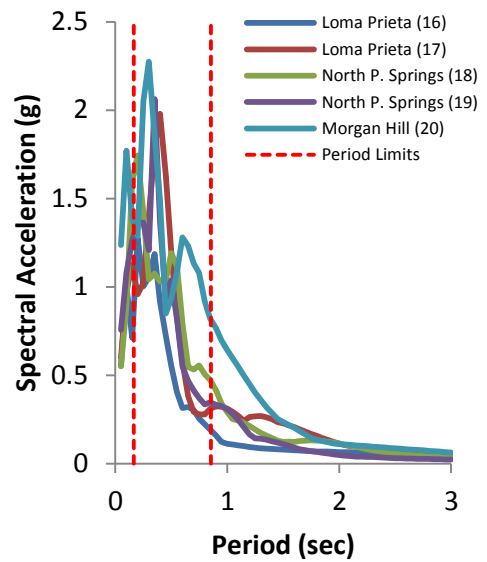
(a) Earthquakes 1-5



(b) Earthquakes 6-10



(c) Earthquakes 11-15



(d) Earthquakes 16-20

Figure 3.14 Acceleration response spectra of the ground motions utilized in fragility analyses

Fragility curves were grouped by taking the sectional geometry properties into consideration. A group of fragility curves includes the fragility curves of a dam with a specific height and cross sectional downstream slope. There are nine curves at each group for

every ratio of elastic modulus of dam concrete to elastic modulus of foundation rock and tensile strength of dam concrete alternatives. In order to prevent confusion fragility curves of dams with similar ratio of elastic modulus of dam concrete to elastic modulus of foundation rock were plotted by the same color and marked with the same type of token. On the other hand fragility curves of dams with the same tensile strength of dam concrete were plotted by utilizing the same line style. There are fifteen groups of fragility curves since five dam height and three cross sectional downstream slope alternatives are included in fragility analysis. Fragility curves are given in Figure 3.15 to Figure 3.29.

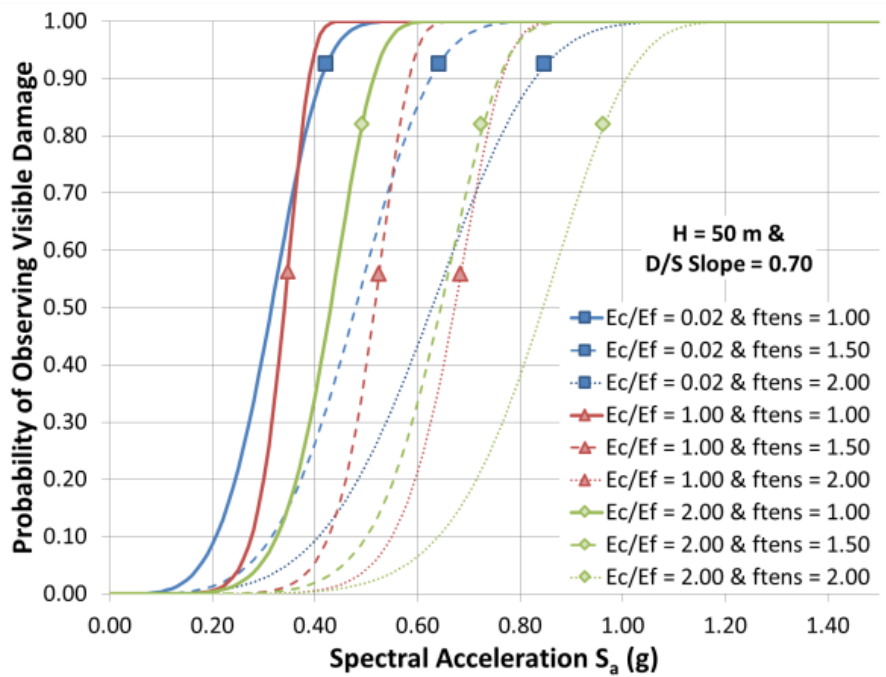


Figure 3.15 Fragility curves of dams with a height of 50 meters and a downstream slope of 0.70

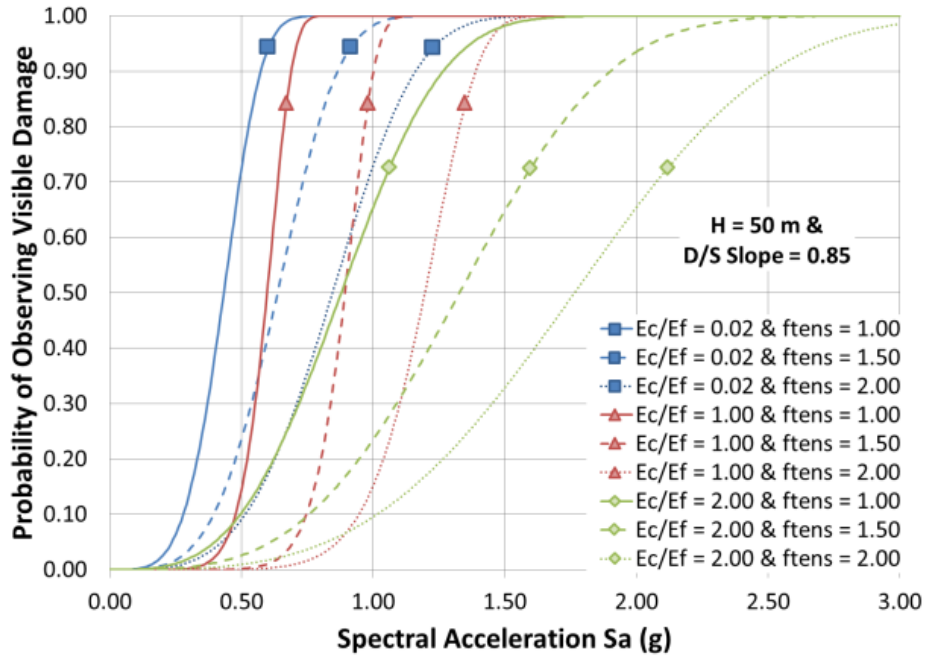


Figure 3.16 Fragility curves of dams with a height of 50 meters and a downstream slope of 0.85

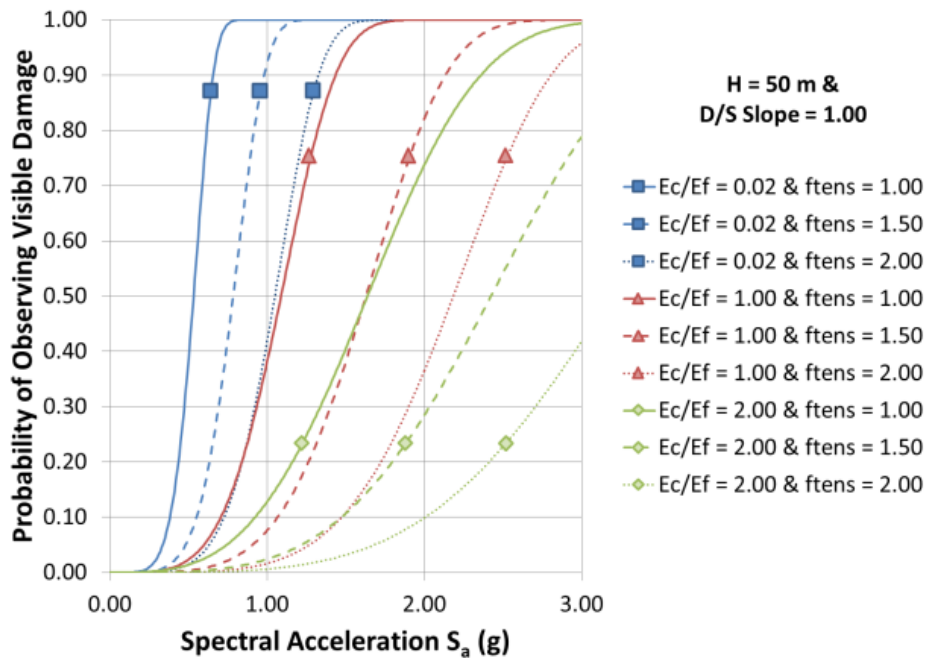


Figure 3.17 Fragility curves of dams with a height of 50 meters and a downstream slope of 1.00

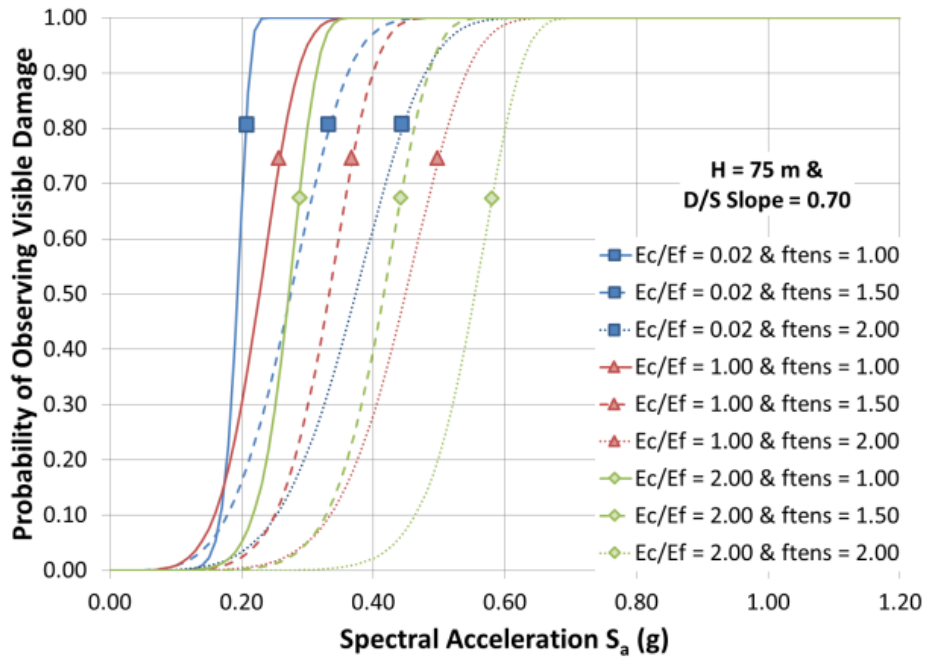


Figure 3.18 Fragility curves of dams with a height of 75 meters and a downstream slope of 0.70

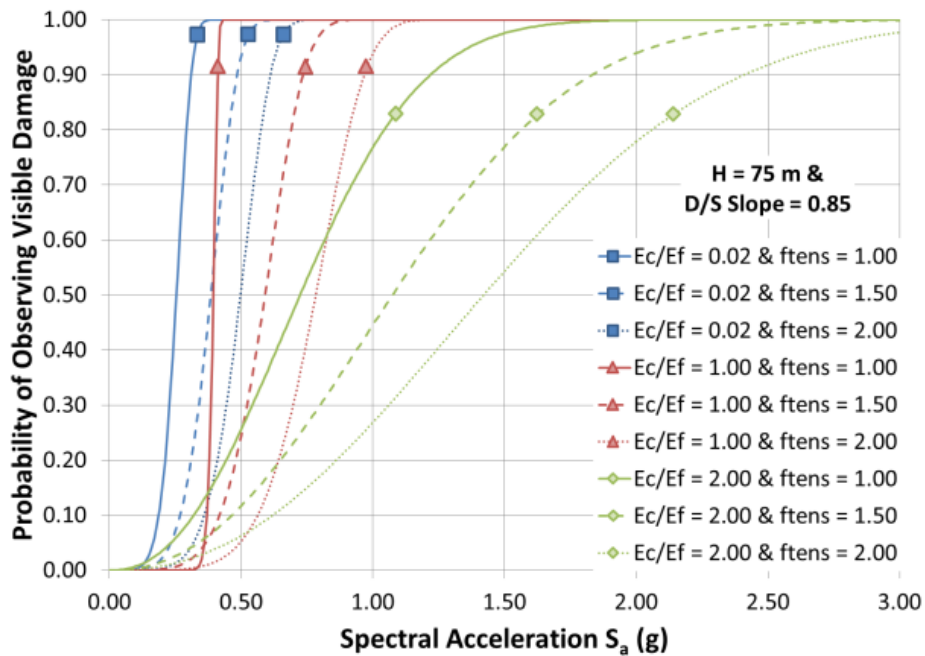


Figure 3.19 Fragility curves of dams with a height of 75 meters and a downstream slope of 0.85

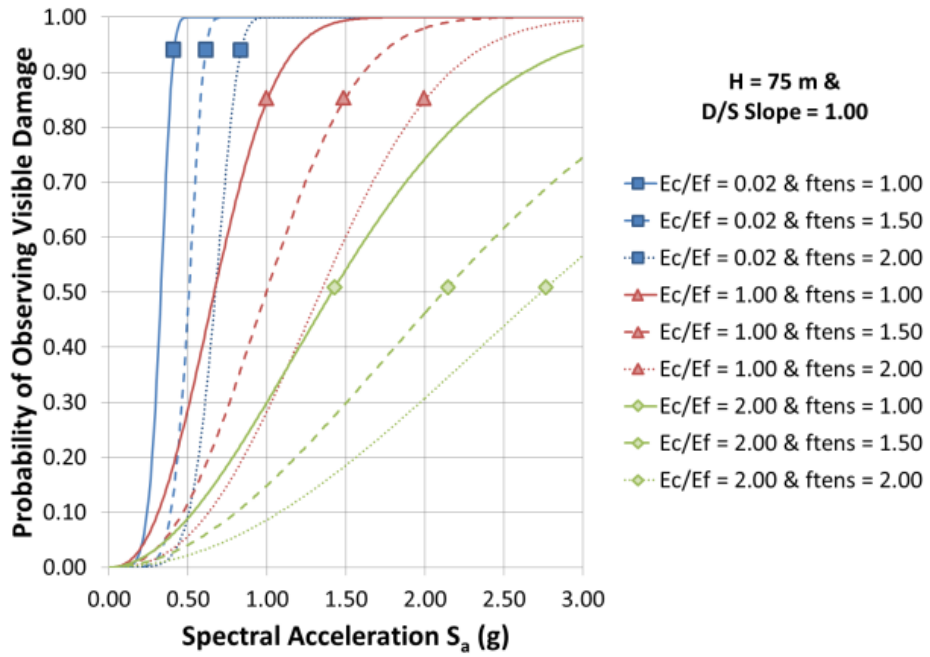


Figure 3.20 Fragility curves of dams with a height of 75 meters and a downstream slope of 1.00

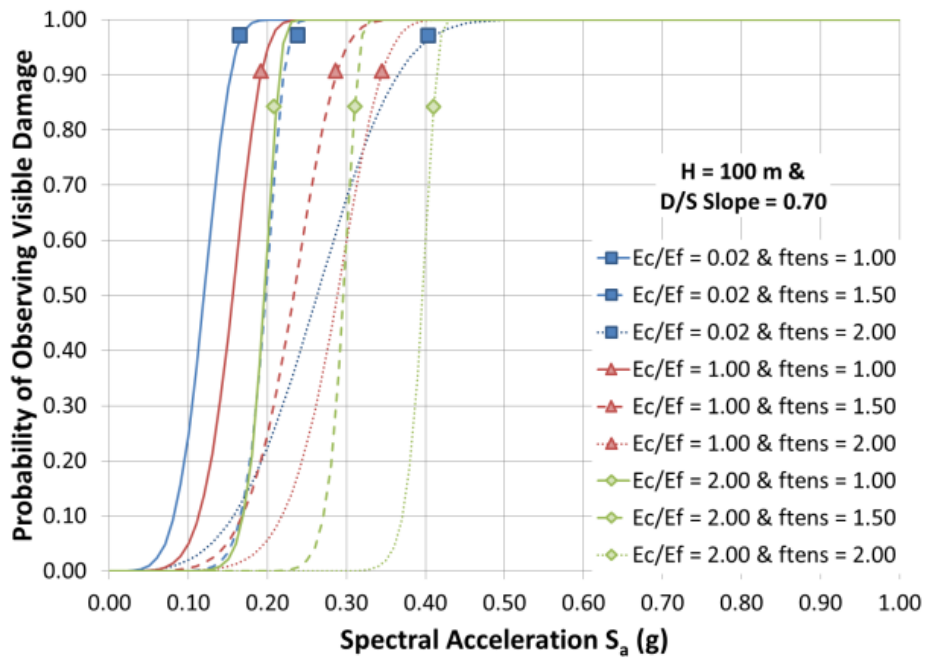


Figure 3.21 Fragility curves of dams with a height of 100 meters and a downstream slope of 0.70

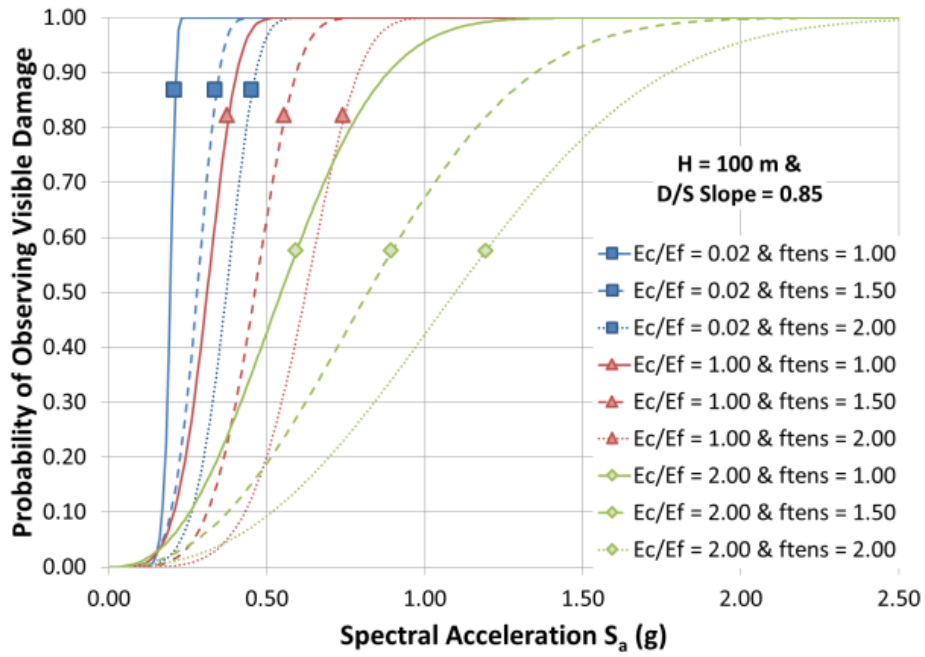


Figure 3.22 Fragility curves of dams with a height of 100 meters and a downstream slope of 0.85

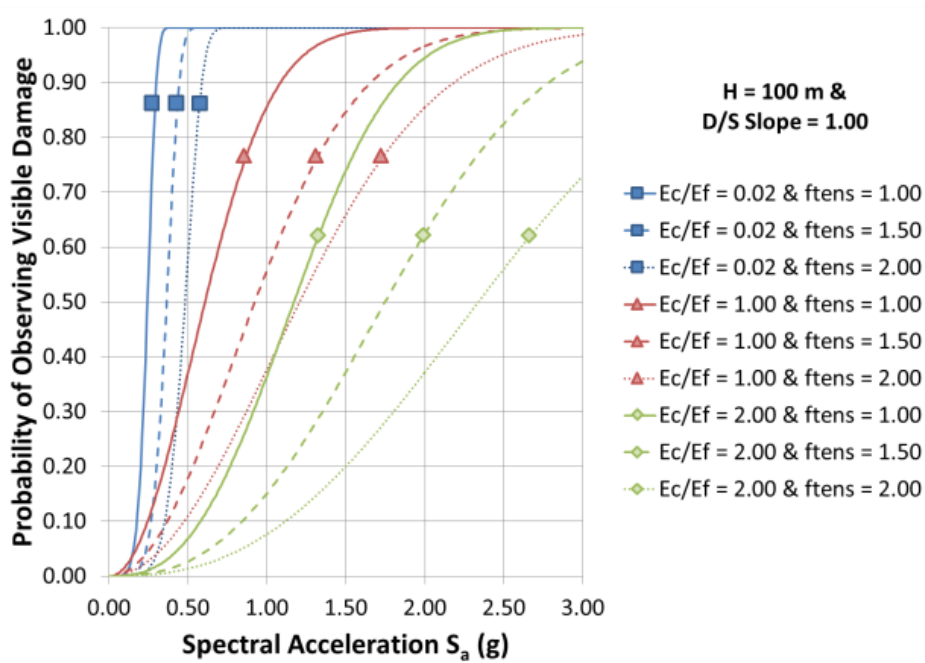


Figure 3.23 Fragility curves of dams with a height of 100 meters and a downstream slope of 1.00

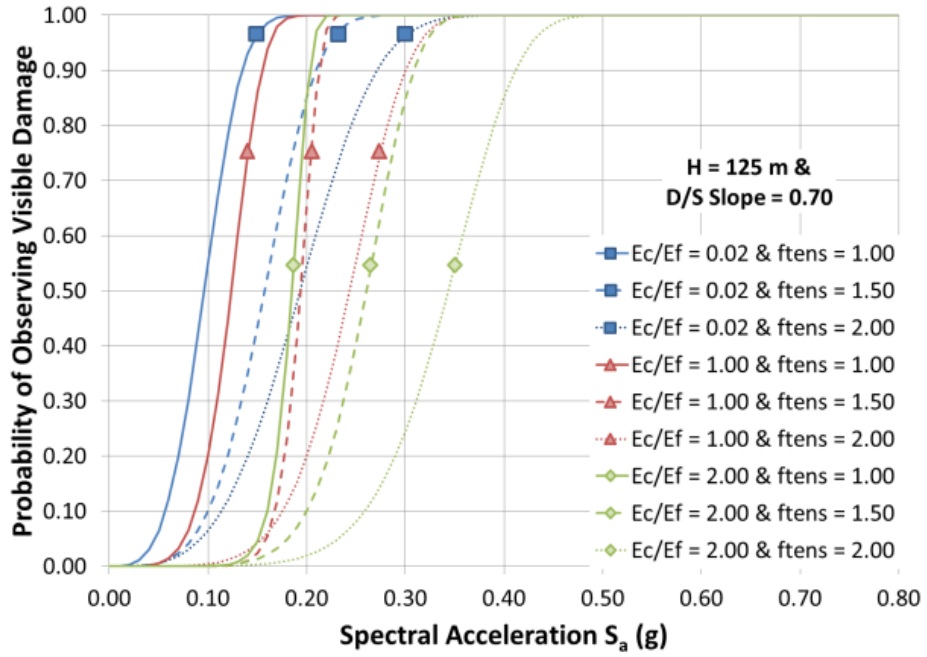


Figure 3.24 Fragility curves of dams with a height of 125 meters and a downstream slope of 0.70

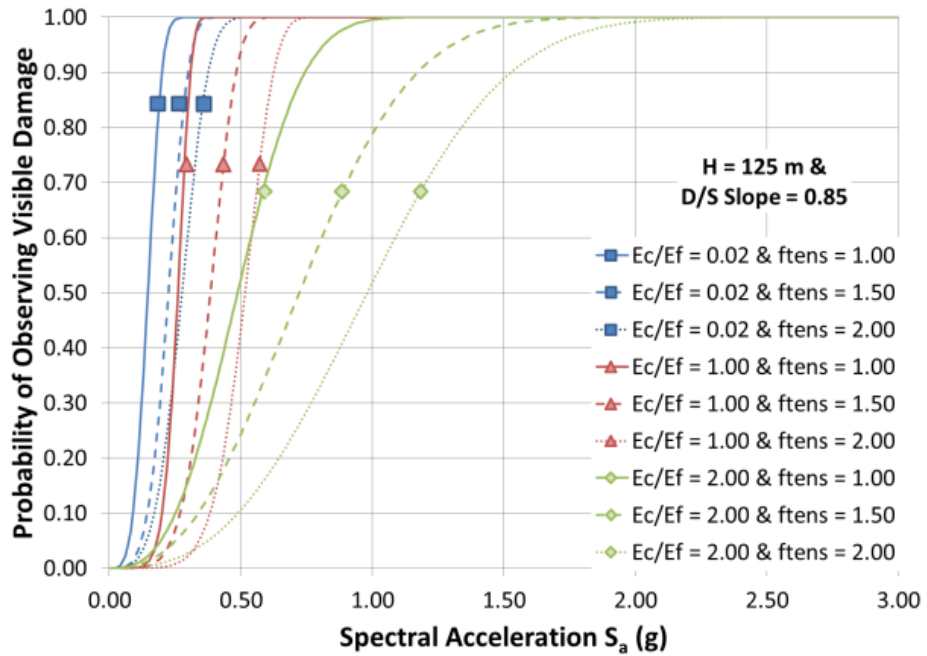


Figure 3.25 Fragility curves of dams with a height of 125 meters and a downstream slope of 0.85

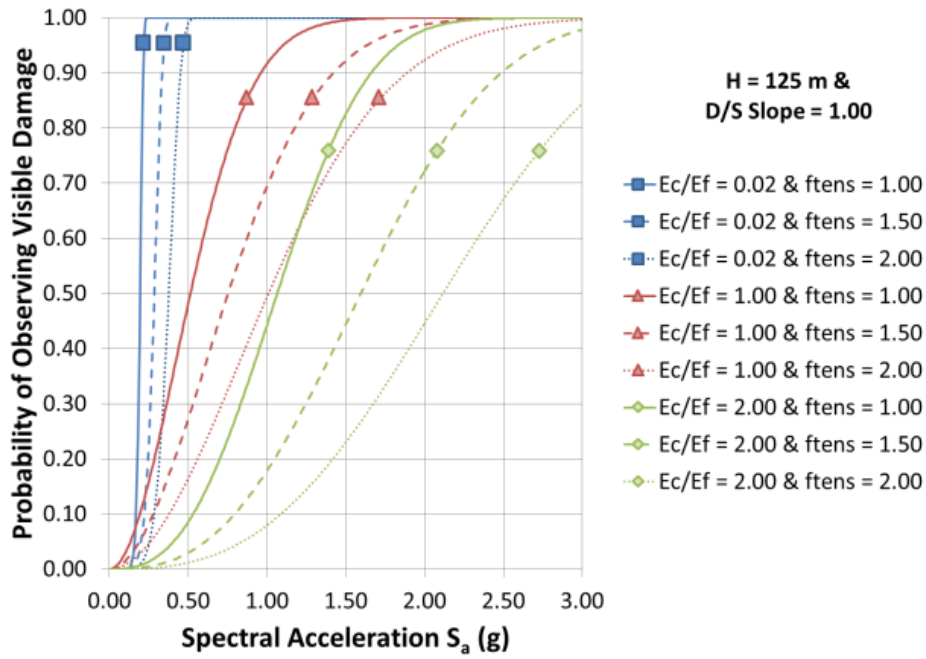


Figure 3.26 Fragility curves of dams with a height of 125 meters and a downstream slope of 1.00

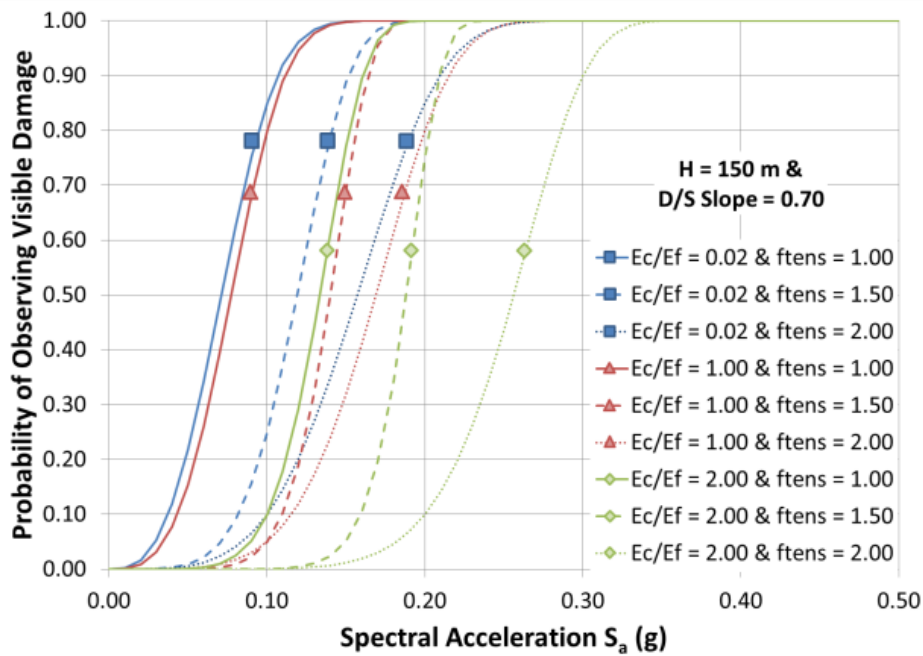


Figure 3.27 Fragility curves of dams with a height of 150 meters and a downstream slope of 0.70

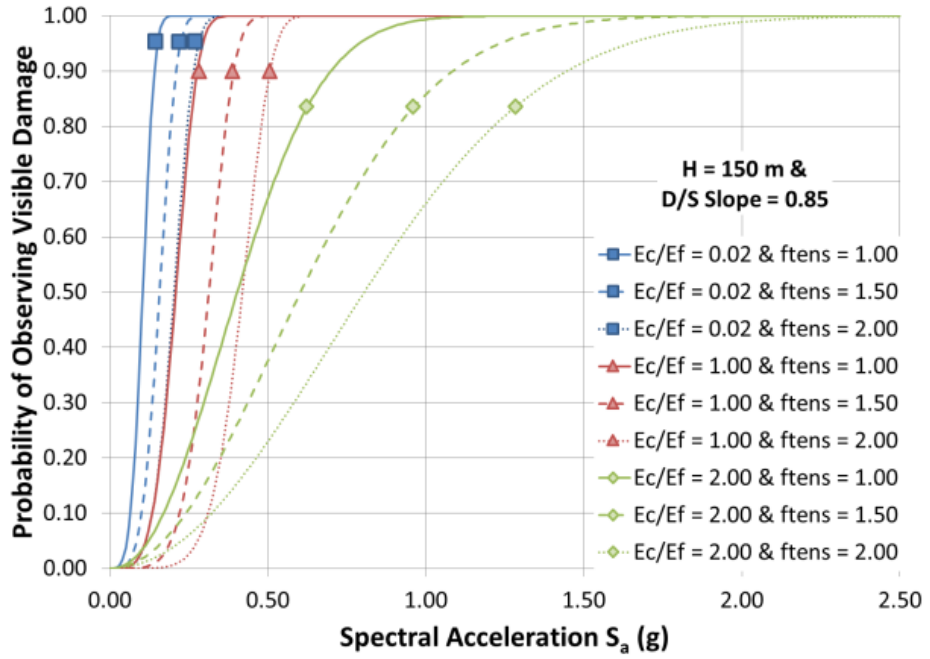


Figure 3.28 Fragility curves of dams with a height of 150 meters and a downstream slope of 0.85

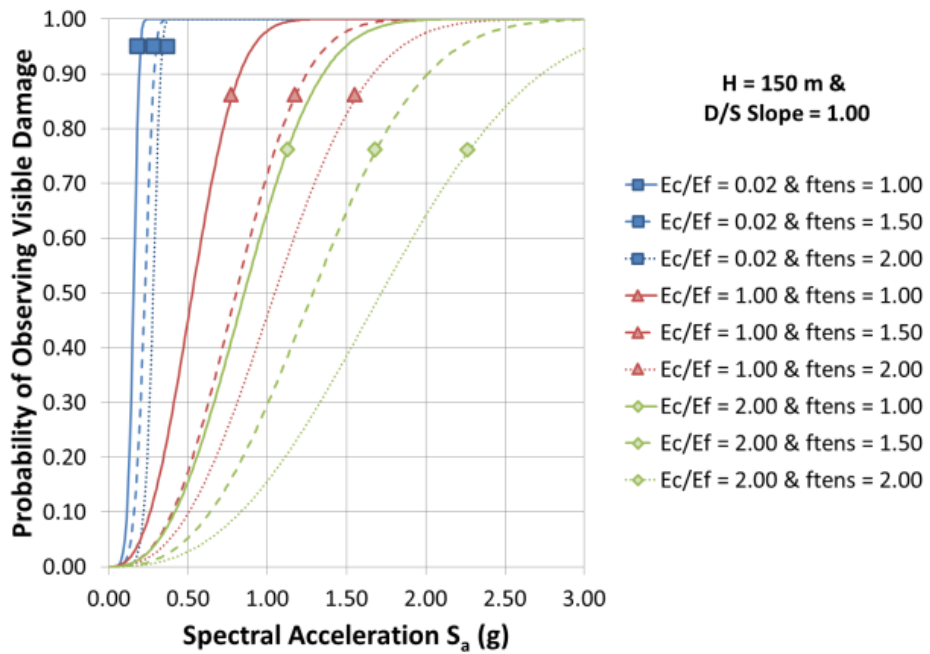


Figure 3.29 Fragility curves of dams with a height of 150 meters and a downstream slope of 1.00

The fragility curves illustrated above exhibit consistency with the observations from the parametric study. The increase of the ratio of elastic modulus of dam concrete to elastic modulus of foundation rock decreases the probability of a visible damage in dam body for a given specific spectral acceleration demand. Hydrodynamic pressures and the effects of the higher vibration modes increase with the increase of dam height. For a specific spectral acceleration demand as the dam height increases the probability of observing unacceptable seismic performance increases. As expected the probability of observing of serious damage decreases with the increase of the tensile strength of dam concrete. The cross sectional downstream slope of dam also has a significant effect on the probability of the observing a nonlinear behavior. The enlargement of dam cross section obviously decreases the probability of observing a visible damage at the end of the strong ground motion. It should be noted that these conclusions are made by considering other variable parameters as constant.

Spectral acceleration demands for specific probabilities of the observing visible damage are also presented. 50 percent and 90 percent probabilities of observing serious damage are considered. Spectral acceleration demand values were determined by the iterative solution of the exponential equations which are fitted to fragility data to obtain a smooth fragility curve. Spectral acceleration curves were grouped by considering ratio of elastic modulus of dam concrete to elastic modulus of foundation rock. Each group includes nine curves for the design parameter which are the D/S slope and tensile strength of dam concrete. Spectral acceleration demands were plotted against dam heights. Spectral acceleration demands curves are given in Figure 3.30 to Figure 3.35.

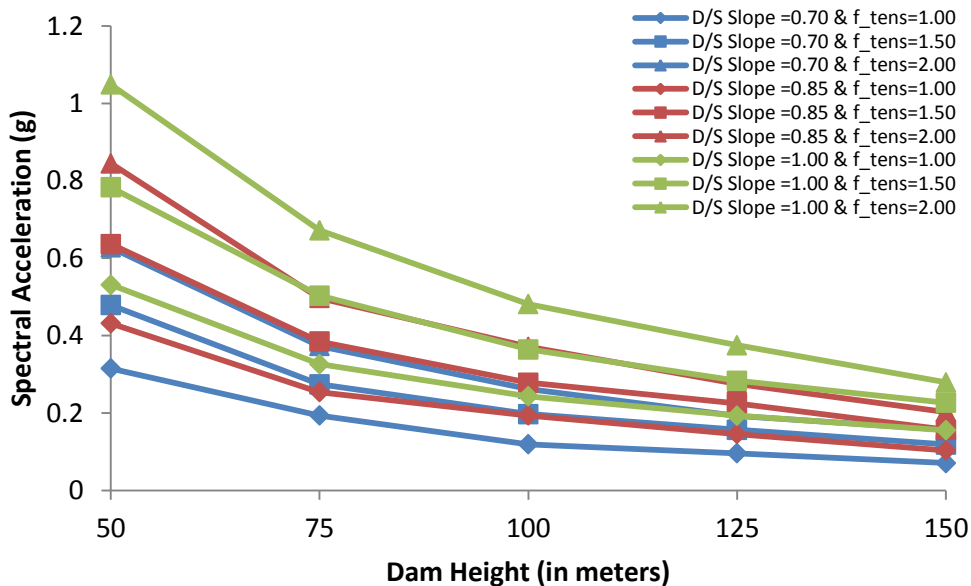


Figure 3.30 Spectral acceleration demands for 50% probability of observing visible damage ($E_c/E_f = 0.02$)

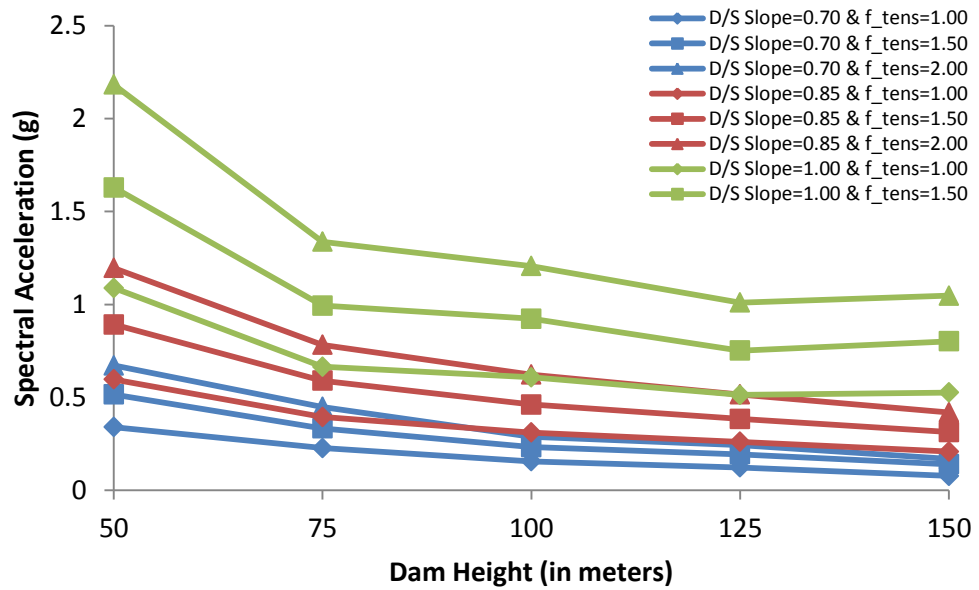


Figure 3.31 Spectral acceleration demands for 50% probability of observing visible damage ($E_c/E_f = 1.00$)

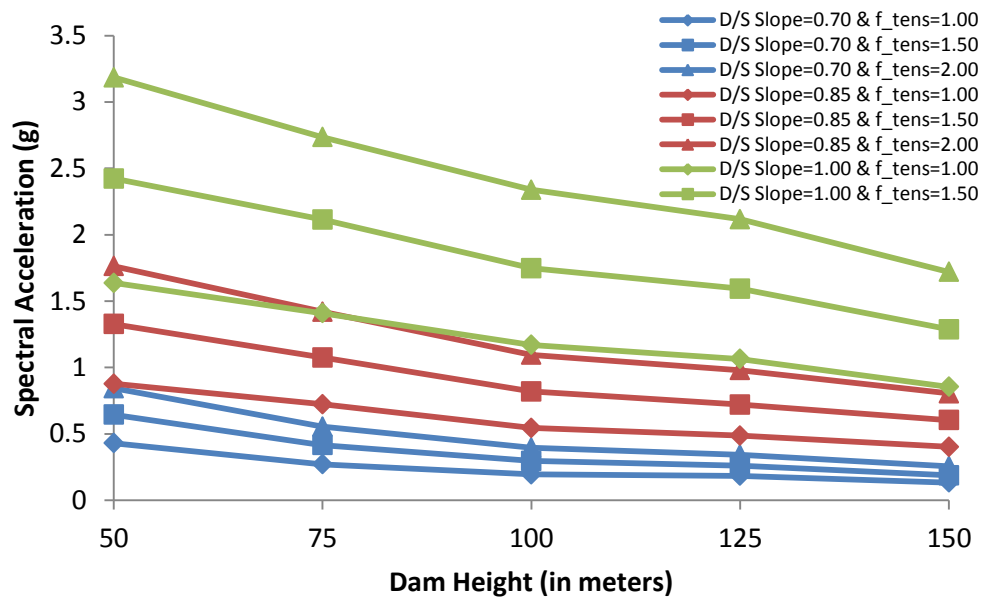


Figure 3.32 Spectral acceleration demands for 50% probability of observing visible damage ($E_c/E_f = 2.00$)

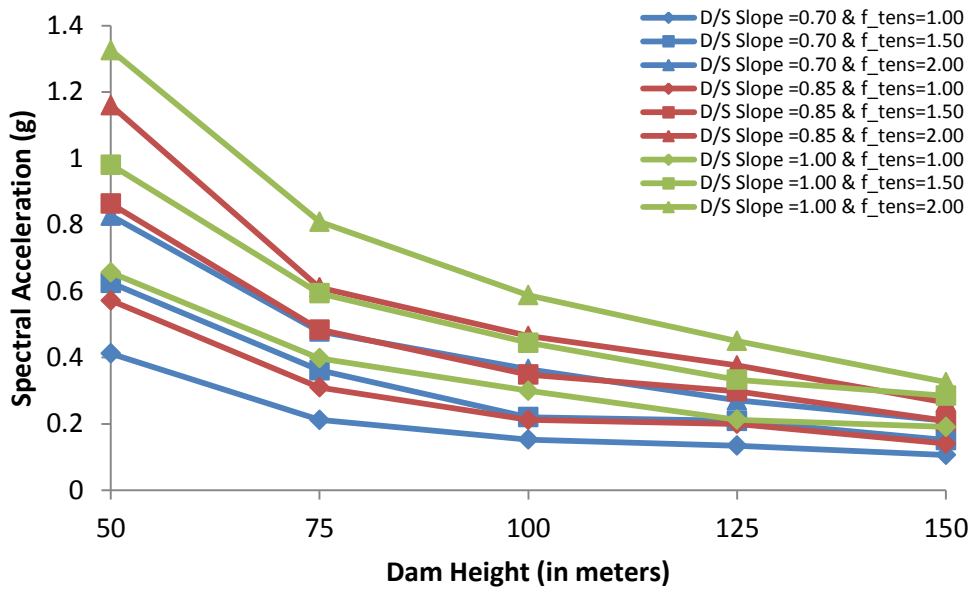


Figure 3.33 Spectral acceleration demands for 90% probability of observing visible damage ($E_c/E_f = 0.02$)

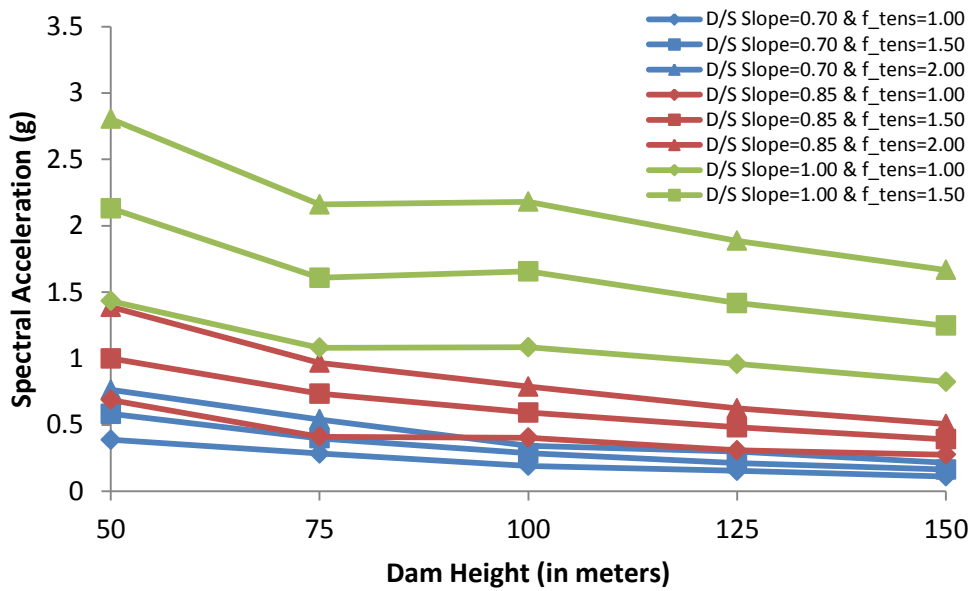


Figure 3.34 Spectral acceleration demands for 90% probability of observing visible damage ($E_c/E_f = 1.00$)

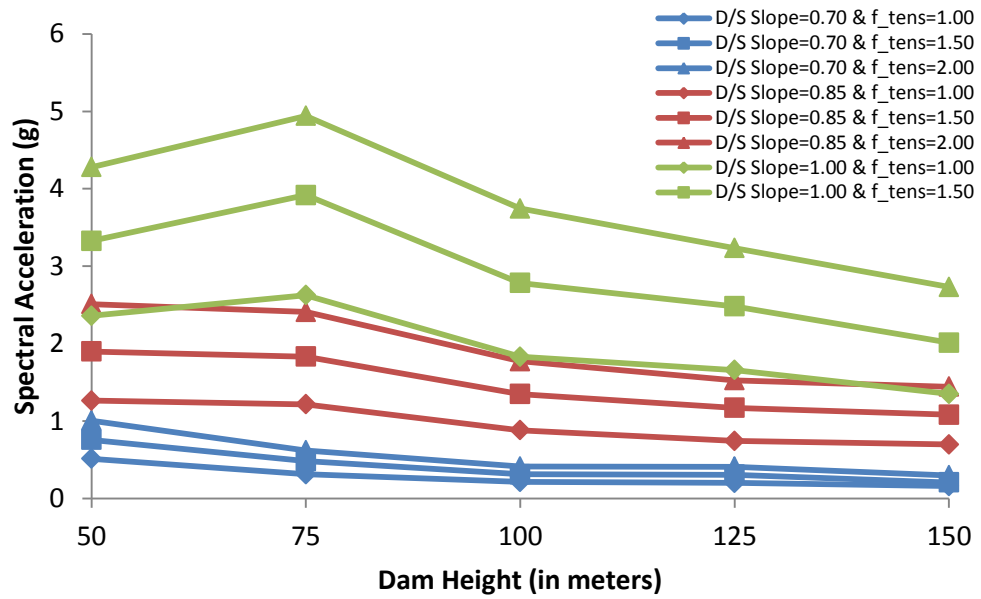


Figure 3.35 Spectral acceleration demands for 90% probability of observing visible damage ($E_c/E_f = 2.00$)

Spectral acceleration demands for a specific probability of observing visible damage varies with a pattern consistent with the discussions made for fragility curves. Spectral acceleration demand increases with the increase of the ratio of elastic modulus of dam concrete to elastic modulus of foundation rock. A lower spectral acceleration demand is required for the same probability of observing a serious damage as the dam height increases. The increase of tensile strength of dam concrete and cross sectional downstream slope results in the requirement of a higher spectral acceleration demand. However, an exact conclusion could not be made for whether tensile strength of dam concrete or cross sectional downstream slope is more effective. Spectral acceleration demand for the dam with same properties increases with the increase of the probability of occurrence nonlinear damage as it is expected. Some spectral acceleration demands which are not consistent with the general fashion of the curves are also obtained. These demands could be explained imperfections of the fitted exponential function.

Dam sections with a high risk of observing serious damage for a spectral acceleration demand of 1.0 g can be summarized as follows. Almost all dam sections are under the risk of unsatisfactory seismic performance when the ratio of elastic modulus of dam concrete to elastic modulus of foundation rock is 0.02. When the ratio of elastic modulus of dam concrete to elastic modulus of foundation rock is increased to 1.00, dam sections with heights of 100 meters or higher and downstream slopes of 0.85 or smaller exhibits a high risk of observing serious damage. When the ratio of elastic modulus of dam concrete to elastic modulus of foundation rock is increased to 2.00, only the dam sections

which have a downstream slope of less than 0.85 are under the risk of unacceptable seismic performance.

The determination of the fragility data utilized for the fragility curves and obtained spectral acceleration demand curves were conducted by plane stress assumption. Therefore the obtained results are valid only for the dams which behave in accordance with the plane stress assumption under a strong ground motion. In other words conducted analyses do not give accurate estimations for gravity dams which are located in narrow valleys or arch dams. Moreover it should also be reminded that fragility curves are determined with analyses under several regulations. The determined fragility curves aims to be utilized as a reference for the preliminary design phase of the new dams and the investigation of the structural reliability of existing dams. In order to obtain results with an acceptable accuracy it is required to perform detailed analyses.

CHAPTER 4

CONCLUSION

4.1 General

In this study, a user friendly interface for the dynamic analysis of concrete gravity dams was presented and seismic response of concrete gravity dams was investigated. A computer program named as EAGD-84 was utilized for the analyses conducted in this study. EAGD-84 was employed as the analysis engine of the developed user interface.

Parametric studies were conducted to better understand the effects of parameters on the seismic response of concrete gravity dams. The pseudo-static analyses of several dam alternatives were conducted by utilizing a computer program named as CADAM. The results of pseudo-static analyses were compared with the results of parametric studies to underline the importance of the detailed response history analysis for the reliable design of concrete gravity dams. A deterministic sensitivity analysis was conducted for the determination of the most influential parameters. Moreover; the structural performance of dams with typical sections and various properties was evaluated with a probabilistic approach. Fragility curves of the dams were determined by assessments with linear elastic analyses. The conclusions of these studies can be summarized as followings:

- The stress levels are directly related with the ratio of elastic modulus of dam concrete to elastic modulus of foundation rock. As the ratio increases the stress level of the dam decreases. Therefore the consideration of foundation flexibility might result in more economical designs with smaller downstream slopes. It should be noted that the bearing capacity of the foundation rock must always be taken into consideration when the foundation rock flexibility is taken into account.
- The increase of the dam height results in increase at the stress level. The increase of the stress levels could be explained by the increase of both hydrostatic and hydrodynamic pressures and higher mode effects.
- Elastic modulus of the foundation rock appears as the most influencing parameter of the maximum principal tensile stress and the maximum cumulative inelastic duration responses. On the other hand, the maximum crest displacement response is mostly affected by the change of elastic modulus of dam concrete.

- The probability of observing visible damage is inversely proportional with the tensile strength of concrete.
- Increase of the cross sectional downstream slope decreases the probability of unacceptable damage occurrence.
- Investigations conducted by the plane stress and plane stress assumptions are not valid for gravity dams located in narrow valleys or arch dams.

This study takes only the linear elastic behavior of dam-reservoir-foundation rock system into consideration. The foundation rock was idealized as an isotropic, viscoelastic half plane. The further studies might investigate the effect of nonlinear behavior on the seismic response. The foundation rock idealization might also be improved by taking the effect of layered foundations into consideration. A user friendly interface might be developed for the generation of compliance data for the flexible foundation. A study might be conducted for the investigation of the reliability of gravity dams through the country. Moreover; the shortcomings of two dimensional analyses might be investigated by utilizing three dimensional results. Development of reliable procedures for the calibration of two dimensional analyses results for the dams located in narrow valleys or arch dams might also be practical for the professional purposes.

REFERENCES

- Akkar, S. (2010). *Melen Barajı İçin Tasarım Spektrumunun Olasılık Hesaplarına Dayalı Sismik Tehlike Analizi*. Ankara: METU.
- Arabshahi, H., & Lotfi, V. (2008). Earthquake Response of Concrete Gravity Dams Including Dam-Foundation Interface Nonlinearities. *Engineering Structures*, Vol. 30, 3065-3073.
- Bhattacharjee, S. S., & Leger, P. (1994). Application of NFLM Models to Predict Cracking in Concrete Gravity Dams. *Journal of Structural Engineering*, Vol. 120, No. 4, 1255-1271.
- Bhattacharjee, S. S., & Leger, P. (1995). Fracture Response of Gravity Dams due to Rise of Reservoir Elevation. *Journal of Structural Engineering*, Vol. 121, No. 9, 1298-1305.
- Binici, B., & Mosalam, K. M. (2007). Analysis of Reinforced Concrete Columns Retrofitted with Fiber Reinforced Polymer Lamina. *Composites: Part B*, Vol. 38, 265-276.
- BK. (2012). Beton Barajlar Tasarım İlkeleri Rehberi. 1. *Barajlar Kongresi (Rehber: 004)*. Ankara: DSİ.
- Bougacha, S., Tassoulas, J. L., & Roesset, J. M. (1993). Analysis of Foundations on Fluid-Filled Poroelastic Stratum. *Journal of Structural Engineering Mechanics*, Vol. 119, No. 8, 1632-1648.
- Bougacha, S., Tassoulas, J. L., & Roesset, J. M. (1993). Dynamic Stiffness of Foundations on Fluid-Filled Poroelastic Stratum. *Journal of Structural Engineering Mechanics*, Vol. 119, No. 8, 1649-1662.
- Chopra, A. K. (1966). *Hydrodynamic Pressures on Dams During Earthquakes*. Berkeley, California: Structures and Materials Research, 66-2.
- Dagupta, G., & Chopra, A. K. (1977). *Dynamic Stiffness Matrices for Homogenous Viscoelastic Halfplanes*. California, Berkeley: Earthquake Engineering Research Center, UCB/EERC-77/26.
- Fenves, G., & Chopra, A. K. (1984). *EAGD-84 A Computer Program for Earthquake Analysis of Concrete Gravity Dams*. Berkeley, California: Earthquake Engineering Research Center, UCB/EERC-84/11.
- Fenves, G., & Chopra, A. K. (1984). *Earthquake Analysis and Response of Concrete Gravity Dams*. Berkeley, California: Earthquake Engineering Research Center, UCB/EERC-84/10.

Fenves, G., & Chopra, A. K. (1986). *Simplified Analysis for Earthquake Resistant Design of Concrete Gravity Dams*. Berkeley, California: Earthquake Engineering Research Center, UCB/EERC-85/10.

Ghanaat, Y. (2004). Failure Modes Approach to Safety Evaluation of Dams. *13th World Conference on Earthquake Engineering*. Vancouver, B.C., Canada.

Javanmardi, F., Leger, P., & Tinawi, R. (2005). Seismic Structural Stability of Concrete Gravity Dams Considering Transient Uplift Pressures in Cracks. *Engineering Structures*, Vol. 27, 616-628.

Lotfi, V., Roesset, J. M., & Tassoulas, J. L. (1987). A Technique for the Analysis of the Response of Dams to Earthquakes. *Earthquake Engineering and Structural Dynamics*, Vol. 15, 463-490.

Medina, F., Dominguez, J., & Tassoulas, J. L. (1990). Response of Dams to Earthquakes Including Effects of Sediments. *Journal of Structural Engineering*, Vol. 116, No. 11, 3108-3121.

Öziş, Ü., & Alsan, M. (1990, July). Beton Baraj İnşaatının Türkiye'de Gelişmesi. *İMO Teknik Dergi*, pp. 147-158.

US Army Corps of Engineers. (2003). *Time-History Dynamic Analysis of Concrete Hydraulic Structures*. Washington, DC: Engineering and Design, EP 1110-2-6051.

Westergaard, H. M. (1933). Water Pressures on Dams During Earthquakes. *American Society of Civil Engineers*, 419-472.

World Energy Council Turkish National Committee. (2012). *Enerji Raporu 2012*. Ankara.

Yakut, A., & Erduran, E. (2004). Drift Based Damage Functions for Reinforced Concrete Columns. *Computers and Structures*, Vol. 82, 121-130.